JOURNAL OF MATHEMATICAL SCIENCES AND MODELLING

ISSN: 2636-8692

VOLUME V
ISSUE III

VOLUME V ISSUE III
ISSN 2636-8692

December 2022
http://dergipark.gov.tr/jmsm

JOURNAL OF MATHEMATICAL SCIENCES AND MODELLING

Editors

Editorial Board of Journal of Mathematical Sciences and Modelling

Contents

Journal of Mathematical Sciences and Modelling, 5 (3) (2022) 80-91
Research Article

Journal of Mathematical Sciences and Modelling

Journal Homepage: www.dergipark.gov.tr/jmsm
ISSN 2636-8692
DOI: http://dx.doi.org/10.33187/jmsm.972781

Boolean Hypercubes, Classification of Natural Numbers, and the Collatz Conjecture

Ramon Carbó-Dorca[1*] and Carlos Castro Perelman[2]

[1] *Institut de Química Computacional i Catàlisi / Universitat de Girona/ Girona Spain and Ronin Institute/ Montclair, New Jersey, USA*
[2] *Center for Theoretical Studies of Physical Systems/ Clark Atlanta University, Atlanta, GA. and Ronin Institute/ Montclair, New Jersey, USA*
[*] *Corresponding author*

Article Info

Keywords: *Collatz conjecture, Collatz operator, Collatz vector spaces, Natural hypercubes, Recursive generation of natural numbers, Classification of natural numbers*
2010 AMS: *03E10, 11Z05*
Received: *17 July 2021*
Accepted: *16 September 2022*
Available online: *18 November 2022*

Abstract

Using simple arguments derived from the Boolean hypercube configuration, the structure of natural spaces, and the recursive exponential generation of the set of natural numbers, a linear classification of the natural numbers is presented. The definition of a pseudolinear Collatz operator, the description of the set of powers of 2, and the construction of the natural numbers via this power set might heuristically prove the Collatz conjecture from an empirical point of view.

1. Introduction

The Collatz conjecture, associated with a simple computational algorithm over the natural set $\mathbb{N}$, remains unsolved as far as the authors know, despite having attracted the interest of many researchers; see reference [1] for literature on the subject and references [2]–[21] for recent studies and more literature. Recently, a preprint claimed to have reached the solution, but the file still is not posted [22]. More recently, a paper [23] indicates the intractable nature of the conjecture.

1.1. Preliminary considerations

Reference [1] reported that a good deal of computations was performed on $\mathbb{N}$ subsets with the assistance of a Python 3.0 program. Some calculations were related to large Mersenne numbers, and others with numerical series of similar structures of natural numbers. Despite the significant quantity of tested numbers in reference [1], no natural number studied was found *Collatz **not** compliant*. Any tested natural number submitted to the Collatz algorithm, see the **Appendix** for more details, seems to yield unity.

The largest Mersenne number[1] tested recently in this laboratory is number 39 on the list of Mersenne primes; see the web page in reference [24]: $\mu_2(13466917) \approx 3 \cdot 10^{21}$, which has 4053946 digits and has taken 51440634 steps of the Collatz algorithmic path to yield 1. Such a calculation has expended a considerable time, even running on a ten-core i9 CPU.

One can be confident in the previous computational experience, see reference [1]. Also, while writing the present paper, we performed a large set of additional tests. In this way, we observed more information about the behavior of the Collatz algorithm. All tests keep yielding no natural number Collatz compliant exception.

Considering this, the present authors have carried on a previous discussion, connecting the quantum mechanical harmonic oscillator with the Collatz conjecture [19]. The present study corresponds to another point of view of the problem based on numerical and algebraic empirical considerations.

[1] A Mersenne number can be described as: $\mu_2(N) = 2^N - 1$.

Email addresses and ORCID numbers: **ramoncarbodorca@gmail.com, 0000-0002-9219-0686 (R. Carbó-Dorca), perelmanc@hotmail.com, 0000-0002-7276-9957 (C. C. Perelman),**

1.2. Empirical computational proof of Collatz conjecture frontiers

In the opinion of the present authors, outside of the strictly computational area, some action has to be done to prove empirically that all the elements of the set of natural numbers $\mathbb{N}$ are Collatz compliant. Such an aim is based, apart from the previously mentioned computations, on two points consisting in that:

First, Gödel-like reasoning can be easily applied [25] to the solution of the Collatz conjecture by computational means. As in this case will be no a priori limit to testing a natural number if, for instance, it is chosen as a Mersenne number $\mu_2(N)$, with N growing indefinitely. But also, one can consider that at some step S of the Collatz path, see the **Appendix** for more information, which can be represented as: $C_S[\mu_2(N)] = M$, a resultant natural number M might grow larger than $\mu_2(N)$, making any attempt to use an induction reasoning useless.

Second, the application of the Erdös discrepancy conjecture [26] permits us to admit that there will be, in any dimension, some Boolean vector $\langle \mathbf{h}_M|$ present, which might be the binary representation of a more significant decimal number. Note that the index M means that it can be any binary representation of the natural numbers in the interval: $\left\{2^N; \mu_2[M]\right\}$

Due to all of these previous ideas, continuing to try to understand the Collatz problem by following a different way than the previous experience, the present paper seeks to empirically demonstrate that the set of natural numbers $\mathbb{N}$ is heuristically Collatz compliant.

1.3. Structure of this study on Collatz conjecture

To achieve this objective, the current analysis will be developed as follows.

Initially, we set as a starting point the description of how the Collatz algorithm and the definition of a Collatz operator work. Essentially, this corresponds to describing the operator action on the set of powers of 2 and the possibility of considering the Collatz operator (pseudo-)distributive concerning the sum of two natural numbers.

Next appears the discussion of an essential part of this work: the structure of Boolean hypercubes and the possibility of describing a recursive building of the natural number set. Such construct permits to devise of an empirical-heuristic demonstration of the Collatz algorithm convergence for all elements of the natural number set.

The following section studies the formalism of natural and Collatz vector spaces, shown to correspond to an extension of the application of the Collatz algorithm to N-tuples constructed with natural numbers.

After these preliminaries, the discussion studies the expression of any natural number, taking the set of natural powers of 2: $2^{\mathbb{N}}$, as a basis. That opens the door to analyzing the action of the Collatz operator, defined in reference [1] over *any* natural number.

Afterward, the line of work directs to the description of the classification of natural numbers using what can be named (one)classes.

Finally, such a previous step allows empirically studying the Collatz compliance of both natural numbers and natural classes. Such a view of the natural numbers proves $\mathbb{N}$ is heuristically Collatz compliant.

2. Collatz Algorithm and Collatz Operator

2.1. Introduction: Collatz algorithm and operator, Collatz algorithm path and steps, and Collatz compliance

Although an algorithm variant leads to a shorter number of Collatz algorithm steps, namely the Syracuse algorithm, the original Collatz algorithm is easily described for the present paper using pseudocode, presented in the **Appendix**. As already explained in reference [1], we performed many computations within both algorithmic paths, the original and the Syracuse. The previous results yield no exception of Collatz compliance in any of the substantial natural number set tested.

Also, the Collatz algorithm can be formally defined using:

$$\forall n \neq m \wedge S \in \mathbb{N} : C_S[n] = m \in \mathbb{N}, \tag{2.1}$$

where the subindex S means the Collatz heuristic operator $C[\circ]$ has been applied S-th times over an initial natural number n yielding the natural number m.

Such an operator, described in the equation (2.1) applied over a natural number, corresponds to arriving, after a sequence of S steps, at one location on the Collatz n-path as defined by the **Appendix** algorithm, while the resultant natural number m might appear greater than 1.

In the case that the Collatz algorithm applied to the number n reaches in his n-path the ending number 1 after S steps, that is:

$$n \in \mathbb{N} : C_S[n] = 1, \tag{2.2}$$

we can denominate the natural number n as Collatz compliant.

Nonetheless, the number of times the operator is applied to a given natural number in the path to reach the number 1, is relatively irrelevant when one tries only to see if a given natural number is Collatz compliant. If this is the case, we can simplify the notation and write the end of the Collatz algorithm applied on any number using the operator $C[\circ]$ without a subindex, like:

$$n \in N : C[n] = 1, \tag{2.3}$$

or with some explicit subindex symbol, like in the equation (2.2), meaning that for the natural number n, the Collatz algorithm has ended. Thus, indicating that n is Collatz compliant following a corresponding n-path. That is: a sequence of natural numbers starting at n and ending at 1 after following several n-path steps S.

It is interesting to note that, according to the Collatz algorithm shown in the **Appendix**, the equalities: $C[0] = 1$ and $C[1] = 1$ hold in any case.

When the Collatz algorithm path ends with unit 1, the Collatz operator, if the Collatz conjecture is true, can be considered as a transformation of each element of the whole natural number set $\mathbb{N}$ into 1. That is, one can suppose the following equality involving all the natural number set:

$$C[\mathbb{N}] = (1,1,1,\ldots 1,\ldots) = \langle \mathbf{1}|$$

will hold, and thus symbolically represents the so-called Collatz conjecture.

2.2. The behavior of the Collatz operator and stopping Collatz algorithm before the end

A remark about the application of the Collatz operator (2.1) is due here. Any Collatz n-path sequence of a given number n, if converging to 1, implies that at some n-path step, one shall necessarily arrive at a number that has to be *lesser than the initial tested number*.

It must be kept in mind now that there is no problem in supposing that, when applying the Collatz operator to a number n, all the previous numbers $m < n$ tested are Collatz compliant: $C[m] = 1$.

That is, supposing that the application of the operator depicted in the equation (2.1) to a number n is performed after using, previously and systematically, the Collatz operator on an increasing sequence of natural numbers like:

$$\mathbb{M}_n = \{0,1,2,\ldots,m,\ldots,(n-1)\} \tag{2.4}$$

and we can hypothesize that we previously found it Collatz compliant fulfilling:

$$C[\mathbb{M}_n] = \langle \mathbf{1}_n| . \tag{2.5}$$

If at some step S of the n-path the Collatz algorithm arrives at some number $m \in \mathbb{M}_n$, being $m < n$, then at this moment the Collatz algorithm does not need to continue, whenever one can suppose that the m-path is known and converges:

$$if \quad C_S[n] = m \wedge m < n \wedge C[m] = 1 \Rightarrow C[n] = 1.$$

Such a possibility might shorten the number of steps dramatically in the Collatz algorithm in some cases, at the expense of compulsorily implementing a comparison between the initial number and the number resulting at each Collatz algorithmic step. Nevertheless, such a modification could slow the Collatz algorithm application computational speed in cases where the lesser number lies far from the algorithmic beginning within many steps of the Collatz path.

Looking for this feature, we tested many Collatz compliant numbers.

2.2.1. Testing Collatz compliance of even natural numbers

In this sense, *even* natural numbers present a Collatz compliant condition at the first iteration. The result of the Collatz algorithm will transform the number into half of the initial value. Therefore, the set of even natural numbers can be considered Collatz compliant, a consequence already described in the reference [1].

One can easily prove even natural numbers Collatz compliance. Just consider the sequence of the equation (2.4) submitted to the property of being Collatz compliant with the equation (2.5). We can write the even numbers associated with the sequence (2.4) as:

$$\mathbb{E}_n = 2 \otimes \mathbb{M}_n = \{0,2,4,\ldots,2m,\ldots,2(n-1)\},$$

where the symbol $2\otimes$ means that every element of the set $\mathbb{M}_n$ is multiplied by 2. Then, the application of the Collatz algorithm first step to the even set $\mathbb{E}_n$ can be symbolized by:

$$C_{\langle \mathbf{1}|}[\mathbb{E}_n] = \mathbb{M}_n$$

thus, in the following steps, one can suppose that the Collatz compliance expressed in the equation (2.5) holds for the set $\mathbb{M}_n$; therefore, this is the same to say $\mathbb{E}_n$ being Collatz compliant, that is:

$$C_{\langle \mathbf{S}|}[\mathbb{E}_n] = C_{(\langle \mathbf{S}| - \langle \mathbf{1}|)}[\mathbb{M}_n] = \langle \mathbf{1}| .$$

Empirically, odd natural numbers possess a similar property to even numbers at other positions of the Collatz path.

2.3. Third step concerning Collatz compliance

For several odd numbers, it has been computationally found within this research that the Collatz path for them provides lesser natural elements than the initial tested number, just at the algorithm's *third* step.

For the set of Mersenne twins, defined as $\nu_2(N) = \mu_2(N) + 2 = 2^N + 1$, we already found such an occurrence, see reference [1]. Whatever the attached Boolean hypercube dimension N, one obtains: $C_3[\nu_2(N)] < \nu_2(N)$, meaning that the Mersenne twins are heuristically Collatz compliant.

On the contrary, the Collatz operator applied on Mersenne numbers yields, after some indefinite number of steps S, a value less than the starting Mersenne number: $C_S[\mu_2(N)] = m < \mu_2(N)$.

2.3.1. Example about a Collatz algorithm third step concerning a lesser number

Another interesting example of the Collatz algorithm yielding a lesser number at the third step corresponds to the sequence of pairs of the powers of odd natural numbers, using prime numbers in both the basis B and the power P:

$$\left\{ Z(B,P) = B^P \pm (B-1) \,|B; P = 3,5,7,... \right\} \Rightarrow C_3[Z] < Z; \tag{2.6}$$

which corresponds to a sequence associated with some generalization of Mersenne numbers and his twins. For example, the pair:

$$Z(11,7) = 11^7 \pm 10 \equiv \{19487161; 19487181\},$$

submitted to the Collatz Algorithm produces at the third step, two numbers less than the $Z(11,7)$ pair:

$$C_3[Z] = \{14615371; 14615386\}.$$

Finally, meaning that these numbers might be empirically considered Collatz compliant or that the following property holds for the whole set $Z(B,P)$ defined in the equation (2.6):

$$\forall Z : C_3[Z] = 1$$

Noting that using composite numbers as a basis B, the finding of a lesser number is apparent in the Z-path, but the path position of this occurrence fluctuates. However, some cases keep the 3-step trend in one of the pairs, for example:

$$\left(6^7 - 5\right) > C_{13}\left[6^7 - 5\right] \wedge \left(6^7 + 5\right) > C_3\left[6^7 + 5\right].$$

The third step rule, though, does not disappear whenever the composite number used as a basis is a product of prime numbers. Also, if the basis is a composite of products of primes, we can choose the power as an even number without losing the third step property somehow. For example:

$$\left(20^6 - 19\right) > C_3\left[20^6 - 19\right] \wedge \left(20^6 + 19\right) > C_6\left[20^6 + 19\right],$$

those results indicate that a systematic search of this kind of extended numbers could be interesting from the point of view of the Collatz algorithm properties.

The whole situation is interesting because it opens a heuristic Collatz compliance landscape to a large set of natural numbers represented not only by the Mersenne twins but by the extended $Z(B,P)$ set.

2.4. Powers of two and the Collatz operator action on them

When applied over the natural number set, the tree's central trunk generated by the Collatz algorithm or operator appears as the set of the powers of 2.

First of all, considering this, we can write the set of all powers of two as:

$$\mathbf{2}^{\mathbb{N}} = \left\{2^0, 2^1, 2^2, ..., 2^N, ...\right\} = \left\{1, 2, 4, ..., 2^N, ...\right\} \equiv \left\langle \mathbf{2}^{\mathbb{N}} \right|, \tag{2.7}$$

one can see that it possesses as many elements as the natural number set:

$$\mathbb{N} = \{0, 1, 2, ..., N, ...\} \equiv \langle \mathbb{N}|, \tag{2.8}$$

yet one has to write:

$$2^{\mathbb{N}} \subset \mathbb{N}$$

Anyway, when applying the Collatz operator over any power of 2 using the number of Collatz operator 2^N- path steps explicitly, one can describe that the following relation holds:

$$\forall N \in \mathbb{N} : C_N\left[2^N\right] = 1 \equiv C\left[2^N\right] = 1, \tag{2.9}$$

according to equations (2.7) and (2.8), a general application result of the Collatz operator over the whole set of powers of 2 is easy to write as:

$$C_{\langle N|}\left[2^N\right] = \langle \mathbf{1}| \tag{2.10}$$

It must be repeated that, in general, the Collatz operator might be applied to any natural number for a certain number of steps until it yields 1. Then this number could be considered Collatz compliant. In this sense, all the elements of the even number set $2^{\mathbb{N}}$ are Collatz compliant with certainty.

Compared with the set $2^{\mathbb{N}}$, the numbers, $Z(B,P)$ defined in the equation (2.6) possess another kind of Collatz compliance, empirically obtained.

2.5. When loops might be present in the Collatz algorithm

Now we must say that in the case at some step S in a Collatz path, the following circumstance is found:

$$C_S[n] = n, \tag{2.11}$$

then an infinite loop will be present in the Collatz algorithm application. Therefore, if the whole set of natural numbers has to be Collatz compliant, the equality in the equation (2.11) *cannot* be present in any natural number Collatz path.

3. The Collatz Operator over a Sum of Natural Numbers

3.1. Introduction: On the possibility of defining a pseudolinear Collatz operator

Let us denote by $C_{S_a}[a]$ the symbolic implementation of the full Collatz operation-algorithm acting on the natural number a and ending on 1, with S_a being the number of Collatz algorithm steps associated with a. Moreover, $C_{S_b}[b]$ is the symbolic implementation of the full Collatz operation-algorithm acting on the natural number b and ending on 1, S_b meaning the number of Collatz algorithm steps associated with it.

Then $C_{S_{(a+b)}}[a+b]$ is the symbolic implementation of the full Collatz algorithm action on the sum $a+b$ and ending on 1, with $S_{(a+b)}$ being the number of steps associated with $a+b$, and which *do not* need to be equal to $S_a + S_b$.

With these definitions, from now on, the present work is based on one, and only one heuristic assumption:

If, and only if, the Collatz symbolic operation satisfies the following relation for any pair of natural numbers $\{a,b\}$:

$$C_{S_{(a+b)}}[a+b] \equiv C_{S_a}[a] + C_{S_b}[b], \tag{3.1}$$

we will be able to show that the Collatz conjecture is true, at least in an empirical-heuristic manner.

In other words, the Collatz conjecture can be recast in the pseudolinear or pseudo distributive forms of the Collatz operator displayed by the equation (3.1).

Strictly speaking, the equation (3.1) is **not** linear because when $a \neq b$ the three symbolic operations: $C_{S_a}[a]$, $C_{S_b}[b]$, and $C_{S_{(a+b)}}[a+b]$ represent three **different** Collatz operator path results.

To obtain this new perspective, and without considering relevant the number of steps needed to arrive at the Collatz algorithm completion, but the completion of the algorithm by itself, one can heuristically write for the sum of two Collatz compliant natural numbers:

$$\begin{aligned} if \quad & \{a,b\} \in \mathbb{N} \wedge \{C[a] = 1 \wedge C[b] = 1\} \\ & \rightarrow C^{[2]}[a+b] = C[C[a]+C[b]] = C[1+1] = C[2] = 1. \end{aligned} \tag{3.2}$$

Note that the operator $C^{[2]}[+]$ has to be *strictly* applied to the sum of two Collatz compliant numbers. It is equivalent to using the Collatz algorithm in two steps: first, as a pseudolinear operator over the two terms of the sum, and second, as the Collatz operator over the sum of the two final units yielded by the previous application.

3.2. Some examples

To have a particular view of what represents the equation (3.2) above, one could talk about a Collatz n-path for all the steps obtained when applying the Collatz algorithm to a natural number n.

For instance, the Collatz 3-path possesses 7 elements or steps:

$$3:10:5:16:8:4:2:1$$

while the Collatz 7-path possesses 16 steps:

$$7:22:11:34:17:52:26:13:40:20: \mathit{10: 5: 16: 8: 4: 2: 1}.$$

As a curiosity, the Collatz 3-path coincides with the last 7 steps of the Collatz 7-path. This fact is signaled by writing the coincident steps in *cursive*. Moreover, it seems that this is a property of the Mersenne numbers, which have in common these 7 last steps, at least for several of the continuing elements of the Mersenne sequence, for instance: 15, 31, and 63.

The significant situation in 3- and 7-path cases is that both are Collatz compliant; thus, we can write: $C[3]=1$ and $C[7]=1$. Therefore, according to the previous considerations, we can also write:

$$C[10] \equiv C^{[2]}[3+7] = C[C[3]+C[7]] = C[2] = 1,$$

noting the equivalence but not the equality between $C[10]$ and $C^{[2]}[3+7]$.

To stress the need for the twofold application of the Collatz operator, we can alternatively write more compactly:

$$C^{[2]}[3+7] = C[C[3+7]] = C[2] = 1.$$

That proves that the number 10 is Collatz compliant whenever the numbers 3 and 7 are Collatz compliant. It is a prominent property of the number 10, as this number, as commented, appears in both the Collatz 3-path and Collatz 7-path and the three successive Mersenne numbers Collatz paths.

Also, one must consider that number 10 is even, and thus in the first iteration yielding 5, a number less than 10. As commented before, this will be sufficient to consider the number 10 as Collatz compliant.

3.3. Collatz algorithm on particular sums of natural numbers

These last considerations allow us to observe that if a natural number $n \in \mathbb{N}$ is Collatz compliant: $C[n]=1$, then according to the definition of the Collatz operator acting on a sum of natural numbers, the following equalities for even natural numbers hold:

$$\begin{aligned} C^{[2]}[n+n] &= C[C[n]+C[n]] = C[2] = 1 \\ &\rightarrow C^{[2]}[n+n] = 1 \rightarrow C[2n] = 1. \end{aligned} \tag{3.3}$$

This last result constitutes a coherent outcome concerning the previously discussed behavior of even natural numbers.

The addition of the number 1 to any Mersenne number $\mu(N)$ provides the corresponding power of 2: $\mu(N)+1 = 2^N$, therefore one can write:

$$C[\mu(N)+1] = C\left[2^N\right] = 1,$$

but according to the previous considerations about the pseudolinearity of the Collatz operator, one can also write:

$$C^{[2]}[\mu(N)+1] = C[C[\mu(N)]+C[1]] = C[2] = 1.$$

Also, one must be aware that the odd numbers, derived from natural numbers which are Collatz compliant, can be considered as being Collatz compliant too because one can write:

$$\begin{aligned} &C[n] = 1 \wedge C[2n] = 1 \Rightarrow \\ &\quad C^{[2]}[2n+1] = C[C[2n]+C[1]] = C[2] = 1 \rightarrow C^{[2]}[2n+1] = 1. \end{aligned} \tag{3.4}$$

Alternatively, this can also be written in an extended way, involving the sum of three, instead of two, natural numbers:

$$\begin{aligned} &C[n] = 1 \Rightarrow \\ &\quad C^{[2]}[2n+1] = C[C[n]+C[n]+C[1]] = C[3] = 1 \\ &\quad \rightarrow C^{[2]}[2n+1] = 1. \end{aligned} \tag{3.5}$$

Therefore, one can deduce that if any natural number $n \in \mathbb{N}$ is Collatz compliant, that is: $C[n]=1$, then the derived even $2n$ and odd $2n+1$ numbers are also Collatz compliant.

Such a property involving both even, and odd natural numbers, might be considered sufficient for a simple initial empirical proof, showing all natural numbers are Collatz compliant.

However, one can obtain better, refined, and general heuristic proofs of the Collatz conjecture, as described below in the following paragraphs.

3.4. Collatz compliance of a sum of a Collatz compliant natural number set

The previous results about sums of two natural numbers, three in the case of the equation (3.5), and their Collatz compliance can be easily generalized.

For this purpose, we can now suppose known a set of different natural numbers:

$$\mathbb{A} = \{a_I \,|\, I = 1, N\} \subset \mathbb{N},$$

such that their elements are Collatz compliant, that is[2]:

$$\forall I = 1, N : C[a_I] = 1 \Rightarrow$$
$$C[\langle A|] = \langle \mathbf{1}_N| = (1,1,1,...,1) \Leftarrow \langle A| = (a_1, a_2, a_3, ..., a_N).$$

The setup shown above can be used as a first stage to prove that the sum of the elements of a Collatz compliant set $\mathbb{A}$, is Collatz compliant[3]:

$$\begin{aligned} \langle\langle \mathbb{A}|\rangle = \sum_{I=1}^{N} a_I \rightarrow C[\langle\langle \mathbb{A}|\rangle] = \sum_{I=1}^{N} C[a_I] = \sum_{I=1}^{N} 1 = N \\ \rightarrow C^{[2]}[\langle\langle \mathbb{A}|\rangle] = C[C[\langle\langle \mathbb{A}|\rangle]] = C[N] = 1. \end{aligned} \tag{3.6}$$

This result implies that a sum of Collatz compliant numbers is Collatz compliant whenever the total number of elements of the sum is Collatz compliant. That is, if the equality: $C[N] = 1$, also holds.

Considering that the sum of N different natural numbers greater than 1 is always higher than the number of elements of the sum itself, or: $\langle\langle \mathbb{A}|\rangle > N$.

Thus, one can suppose that to be Collatz compliant, a given natural number must rely on that all the lesser natural numbers have been previously found Collatz compliant.

The important thing to underline here is that a sum of N Collatz compliant natural numbers can be Collatz compliant whenever the *number of N terms of the sum* is Collatz compliant. In other words: if the cardinality of a natural number set is Collatz compliant, the whole elements' sum of the set is Collatz compliant.

One can be aware that we reach the *minimum* value of the sum of N ordered different natural numbers when all the sum terms are equal to the set $\mathbb{T}_N = \{0, 1, 2, \ldots, N-1\}$.

However, as the number of elements of $\mathbb{T}_N$ is N, if all of them are Collatz compliant, then N is Collatz compliant. That is so because if: $C[N-1] = 1$ as $N = (N-1) + 1 \rightarrow C[N] = 1$ using equations (3.4) and (3.5).

Therefore, when summing up the elements of a Collatz compliant natural number set having a cardinality N, it is only necessary to know the Collatz compliance of the number N of terms to be summed up to deduce the Collatz compliance of the resultant sum.

4. Natural and Collatz Vector Spaces

We can also define an N-dimensional natural (row) vector (*semi*)space[4] $\mathbb{V}_N(\mathbb{N})$ as the Cartesian power $\mathbb{N}^N$ of the row orderings of N natural numbers, that is:

$$\forall \langle \mathbf{a}| \in \mathbb{V}_N(\mathbb{N}) \Rightarrow \langle \mathbf{a}| = (a_1, a_2, a_3, \ldots, a_N) \wedge \{a_I | I = 1, N\} \subset \mathbb{N}.$$

One might call a natural vector space a Collatz vector space when the dimension of the natural vector space is Collatz compliant; that is when: $C[N] = 1$ holds.

In a Collatz space, a vector $\langle \mathbf{a}|$ will be called Collatz compliant when the whole set of its elements $\{a_I | I = 1, N\}$ is Collatz compliant. That is, one can write:

$$\forall I = 1, N : C[a_I] = 1 \Rightarrow$$
$$C[\langle \mathbf{a}|] = (C[a_1], C[a_2], C[a_3], \ldots, C[a_N],) = (1,1,1,...,1) = \langle \mathbf{1}_N|$$

for all Collatz compliant vectors.

In this case, if the Collatz conjecture holds, one can write a Collatz conjecture for natural spaces. We can write it as:

$$C[\mathbb{N}] = \langle \mathbf{1}| \Rightarrow \forall \langle \mathbf{a}| \in V_N(N) : C[\langle \mathbf{a}|] = \langle \mathbf{1}_N| \wedge C[N] = 1.$$

and that corresponds to a general conjecture related to ordered sets of natural numbers, including matrices and hypermatrices or tensors. It is well-known that one can reorder them as row vectors of the adequate dimension.

Moreover, for more information, any natural vector space (see references [27]–[29]) might be considered a Banach space, where one can define some vector norms. Among them, the simplest is the Minkowski norm, defined as:

$$\forall \langle \mathbf{a}| \in \mathbb{V}_N(\mathbb{N}) : M[\langle \mathbf{a}|] = \langle\langle \mathbf{a}|\rangle = \sum_{I=1}^{N} a_I \rightarrow M[\langle \mathbf{a}|] \in \mathbb{N},$$

[2] An ordered set of natural numbers can be also represented for the purposes of the present work as a row vector belonging to a row vector space, defined over the natural numbers, and using a Dirac bra notation to describe it: $A = \{a_I | I = 1, N\} \subset \mathbb{N} \Leftrightarrow \langle A| = (a_1, a_2, a_3, ..., a_N) \in V_N(\mathbb{N})$.

[3] The bracket symbol $\langle \quad \rangle$ is used as a symbolic algorithm to compute the complete sum over the subindices of the elements of a vector $\langle \mathbf{a}| = (a_1, a_2, ..., a_N)$: $\langle\langle \mathbf{a}|\rangle = \sum_{I=1}^{N} a_I$.

[4] The name (*semi*)space is used to stress the fact that no other addition operation is allowed than these associated to an addition semigroup. See references [28]–[30] for more details. The particle (*semi*) will be omitted from now on. Such spaces can be also called *orthants*. In this precise context are also related to lattices.

defined in the natural number context as the sum of the vector elements, which is of use in this paper. We can admit this, because the Minkowski norm of the unity vector yields the dimension of the natural space, or:

$$M\left[\langle\mathbf{1}_N|\right]=N.$$

Therefore, in Collatz vector spaces, one can write:

$$C\left[M\left\langle\langle\mathbf{1}_N|\right\rangle\right]=C\left[N\right]=1.$$

Now one must stress that this result, applied to Collatz natural vectors, looks similar to the descriptions and properties of the previous paragraphs. Similarly, as in the equations (3.2) and (3.6), a Collatz compliant vector defined in a Collatz vector space can be associated with the sum of the elements of the vector.

That is, in a Collatz space involving a vector, constructed with Collatz compliant natural numbers, one can write:

$$C\left[\mathbb{N}\right]=\langle\mathbf{1}|\Rightarrow\forall\langle\mathbf{a}|\in\mathbb{V}_N\left(\mathbb{N}\right):C\left[\langle\mathbf{a}|\right]=\langle\mathbf{1}_N|\wedge C\left[\langle\langle\mathbf{a}|\rangle\right]=1$$

which one can write compactly, using the previous paragraphs notation:

$$\forall\langle\mathbf{a}|\in\mathbb{V}_N\left(\mathbb{N}\right):C^{[2]}\left[\langle\mathbf{a}|\right]=1,$$

which one can interpret as:

$$C^{[2]}\left[\langle\mathbf{a}|\right]=C\left[C\left[\langle\langle\mathbf{a}|\rangle\right]\right]=C\left[\langle C\left[\langle\mathbf{a}|\right]\rangle\right]=C\left[N\right]=1.$$

Now we can propose a Collatz extended conjecture from what one has commented on before and compactly write it as:

$$C^{[2]}\left[\mathbb{V}_N\left(\mathbb{N}\right)\right]=\langle\mathbf{1}|.$$

5. N-dimensional Boolean Hypercubes and Binary Expression of any Natural Number

One can construct any N-dimensional Boolean hypercube $\mathbf{H}_N$, see references [27]–[30] for more information and applications, as a set of 2^N vertices. We can consider every vertex formed as a string of N bits. That is, with elements made of the two binary digits: $\mathbb{B}=\{0,1\}$.

One can name the vertices of such a construct as the set:

$$\mathbf{H}_N=\left\{\langle\mathbf{h}_0|;\langle\mathbf{h}_1|;\langle\mathbf{h}_2|;\ldots\left\langle\mathbf{h}_{\mu(N)}\right|\right\},$$

where the last subindex $\mu_2\left(N\right)=2^N-1$ corresponds to the already encountered Mersenne number, associated in turn with the unity (or Mersenne) vertex in *any* Boolean Hypercube dimension:

$$\forall N\in\mathbb{N}:\left\langle\mathbf{h}_{\mu(N)}\right|=\langle\mathbf{1}_N|=\left(1,1,1,\ldots,1\right).$$

Another characteristic vertex, which is well-structured in any dimension Boolean Hypercube, agrees with the zero vertex:

$$\forall N\in\mathbb{N}:\langle\mathbf{h}_0|=\langle\mathbf{0}_N|=\left(0,0,0,\ldots,0\right).$$

The remaining vertices of $\mathbf{H}_N$ are the remnant combinations of the binary set $\mathbb{B}$ taken by N by N.

However, one can interpret these vertices in various manners. The following section will deal with this.

5.1. Interpretations of the Boolean hypercube vertices

One alternative is considering the two bits of $\mathbb{B}$ as natural numbers. Then the Boolean hypercube transforms into a *natural* hypercube of the same dimension. One can also consider the natural hypercube vertices made by strings of the most straightforward natural set: $\mathbb{S}_2=\{0,1\}\subset\mathbb{N}$, constituting the decimal translation of the vertices of the monodimensional Boolean hypercube $\mathbf{H}_1$.

Another possibility is to consider them as a set of logical Kronecker deltas, see references [31]–[33] for more information and applications, which, taking L as any logical expression, can be defined as:

$$\delta\left(L=.False.\right)=0\wedge\delta\left(L=.True.\right)=1.$$

For example:

$$\left(1,0,0,1\right)\Rightarrow\left(\delta\left(L_3\right);\delta\left(L_2\right);\delta\left(L_1\right);\delta\left(L_0\right)\right),$$

where we also define a logical vector with the following values:

$$\langle\mathbf{L}|=\left(L_3;L_2;L_1;L_0\right)\equiv\left(.True.;.False.;.False.;.True.\right).$$

5.2. Binary expression of any natural number

Now, any natural number can be expressed as the complete sum of an inward (or Hadamard, or diagonal, ...) product of two vectors [28],[29],[34],[35], using as coordinates of one vector a vertex of an appropriate N-dimensional Boolean hypercube, and the other vector constructed by the powers of 2 ordered in the same way.

That is, we can construct the reference binary basis as a vector made of the convenient powers of 2:

$$\left\langle \mathbf{2}^N \right| = \left(2^{N-1};2^{N-2};...;2^2;2^1;2^0\right)$$

Then, constructing the elements of an appropriate Boolean hypercube vertex according to the rightmost bit being the less significative:

$$\langle \mathbf{h}_n| = \left(h_{(N-1)n},h_{(N-2)n},h_{(N-3)n},...,h_{1n},h_{0n}\right),$$

the 2^N numbers in the interval:

$$[0,\mu(N)] \to \mathbb{S}_N = \{0,1,2,\ldots,n,\ldots,\mu(N)\} \tag{5.1}$$

can be generated with the following algorithm[5]:

$$\forall n \in \mathbb{S}_N : n = \left\langle \langle \mathbf{h}_n| * \left\langle 2^N \right| \right\rangle = \sum_{I=0}^{N-1} h_{In} 2^I, \tag{5.2}$$

considering the bits of the vertex $\langle \mathbf{h}_n|$ equivalent to some elements of the natural set $\mathbb{S}_2$.

Alternatively, one can use a logical Kronecker's delta expression:

$$\forall n \in \mathbb{S}_N : n = \left\langle \langle \mathbf{h}_n| * \left\langle \mathbf{2}^N \right| \right\rangle = \sum_{I=0}^{N-1} \delta\left(h_{In} = 1\right) 2^I,$$

which is valid for both Boolean and natural options to construct the hypercube vertices.

5.3. Collatz operator acting on the recursive generation of natural numbers associated with a Boolean hypercube

The equation (5.1) has been used in reference [1] to design a manner to construct the natural number set recursively. That has been so because when describing the set defined in the equation (5.1), the attached Boolean hypercube dimension augments in one unit. One can write the resultant natural number set:

$$[0,\mu(N+1)] \to \mathbb{S}_{N+1} = \{0,1,2,\ldots,n,\ldots,\mu(N+1)\},$$

as the union of the initial set $\mathbb{S}_N$ with a new set, $\mathbb{A}_N$ say, which one can write in terms of $\mathbb{S}_N$, using the algorithm:

$$\begin{aligned}
\mathbb{A}_N &= 2^N \oplus \mathbb{S}_N \\
&= \left\{2^N;\left(2^N+1\right);\left(2^N+2\right);\ldots;\left(2^N+\mu(N)\right) = \mu(N+1)\right\} \\
&\Rightarrow \mathbb{S}_{N+1} = \mathbb{S}_N \cup \mathbb{A}_N;
\end{aligned}$$

where the symbol $2^N\oplus$ means that the power 2^N is summed to every element of the set $\mathbb{S}_N$.

Then, the application of the Collatz operator over the set $\mathbb{S}_N$, if previously found Collatz compliant:

$$C[\mathbb{S}_N] = \langle \mathbf{1}_{2^N}|,$$

as well as the already discussed property of powers of 2:

$$\forall N \in \mathbb{N} : C_N\left[2^N\right] = 1,$$

implies that, when used over the new natural set $\mathbb{A}_N$, one can write:

$$C[\mathbb{A}_N] = C\left[2^N \oplus \mathbb{S}_N\right] = C\left[2^N\right] \oplus C[\mathbb{S}_N] = 2\langle \mathbf{1}_{2^N}|,$$

implying that the new set acts over the Collatz operator as:

$$C[\mathbb{S}_{N+1}] = \langle \mathbf{1}_{2^{N+1}}|,$$

and therefore, $\mathbb{S}_{N+1}$ might be considered Collatz compliant.

We can also see such reasoning as an inductive way to prove the Collatz compliance of the natural number set heuristically.

[5] The scalar product of two vectors can be expressed as the complete sum of the inward product of two vectors:

$$\langle \mathbf{p}| = \langle \mathbf{a}| * \langle \mathbf{b}| = (a_1b_1,a_2b_2,...,a_Nb_N) \to \langle \langle \mathbf{a}| * \langle \mathbf{b}| \rangle = \langle \mathbf{a} \mid \mathbf{b} \rangle = \sum_{I=1}^{N} a_I b_I.$$

6. Application of the Collatz Algorithm or Operator to any Natural Number

Besides the results of the previous section, here is the possibility to obtain alternative heuristical proof that any natural number is Collatz compliant. Considering the Collatz operator applied up to completion over a natural number yielding the unit, one can apply it to the equation (5.2), for instance:

$$C[n] = \left\langle \langle \mathbf{h}_n| * C\left[\left\langle \mathbf{2}^N\right|\right]\right\rangle = \langle \langle \mathbf{h}_n| * \langle \mathbf{1}_{N+1}|\rangle = \langle \langle \mathbf{h}_n|\rangle, \tag{6.1}$$

and one might see the hypercube vertices as zero or unit weights or coordinates of the powers of 2 sum. As a definition of the operator action in similar cases, in the development of equations (5.2) and (6.1), one must consider that, it has been used both the pseudolinearity of the Collatz operator and the application of such an operator over the natural vector: $\left\langle \mathbf{2}^N\right|$ only, leaving the coefficients of the Boolean Hypercube vertex vector $\langle \mathbf{h}_n|$ intact.

In the case of the equation (6.1), the operator does not even need to be considered linear. We must accept that when applying the Collatz operator to any vector made by natural numbers, the result is another vector with the Collatz algorithm results of each natural number element of the vector, as discussed in paragraph **4**.

In this case, the result is the unity vector $\langle \mathbf{1}|$ of the appropriate dimension because every initial element is a power of 2.

The result of the sum (6.1), whenever $\forall n > 0$, might be considered from two points of view. Considering the vertex $\langle \mathbf{h}_n|$ as:

A. Binary, then: $\langle\langle \mathbf{h}_n|\rangle = 1$,
B. Natural, then: $\langle\langle \mathbf{h}_n|\rangle = \sigma_1\left(\langle \mathbf{h}_n|\right)$,

where $\sigma_1\left(\langle \mathbf{h}_n|\right)$ is the number of ones contained in the hypercube vertex: $\langle \mathbf{h}_n|$.

6.1. The definition of natural number (one)classes and Collatz compliance

One might consider the function $\sigma_1\left(\langle \mathbf{h}|\right)$ a simple tool to classify the vertices of the N-dimensional Boolean hypercube in $N+1$ (one)classes, as the vertices might possess zero, one, two, ... up to N unit numbers, 1, which one can find within their elements.

Consequently, one can also classify the natural numbers in this way, and accordingly, in any natural subset $\mathbb{S}_N$ of cardinality 2^N, there are present $N+1$ (one)classes.

For example, Mersenne numbers $\mu(N)$ are associated with the unit vector $\langle \mathbf{1}_N|$, attached to N ones. Thus, such numbers belong to the $N+1-th$ (one)class holding N ones, the unique occurrence of one vertex in this kind of $N-$ dimensional hypercubes.

One can construct the hypercube vertices associated with the powers of 2, which with the algorithm:

$$\begin{aligned} \forall P = 0, N-1 : \langle \mathbf{h}_{2^P}| = \left\{ h_{I;2^P} = \delta(I=P) \,|\, I = 0, N-1 \right\} \\ \rightarrow \sigma_1\left(\langle \mathbf{h}_{2^P}|\right) = \langle\langle \mathbf{h}_{2^P}|\rangle = \kappa_{2^P} = 1, \end{aligned}$$

are elements of the (one)class holding just one 1.

While the complementary vertices to the collection $\{\langle \mathbf{h}_{2^P}|\}$ represent the numbers:

$$\forall P = 0, N-1 : \chi(P) = \mu_2(N) - 2^P = 2^P\left(2^{N-P}-1\right) - 1 = 2^P \mu_2(N-P) - 1,$$

which we can write as:

$$\begin{aligned} \forall P = 0, N-1 : \left\langle \mathbf{h}_{\chi(P)}\right| = \left\{ h_{I;\chi(P)} = \delta(I \neq P) \,|\, I = 0, N-1 \right\} \\ \rightarrow \sigma_1\left(\left\langle \mathbf{h}_{\chi(P)}\right|\right) = \left\langle\left\langle \mathbf{h}_{\chi(P)}\right|\right\rangle = \kappa_{\chi(P)} = N-1 \end{aligned}$$

that is, the vector set $\left\{\left\langle \mathbf{h}_{\chi(P)}\right|\right\}$ belongs to the $N-th$ (one)class holding $N-1$ ones.

One must realize that the set cardinality duplicates from the set $\mathbb{S}_N$ to the set $\mathbb{S}_{N+1}$. Similarly, the number of vertices duplicates from the N-dimensional Boolean hypercube $\mathbf{H}_N$ to $\mathbf{H}_{N+1}$; the number of associated (one)classes augments in one unit.

That is: defining the cardinality of (one)classes in a natural subset $\mathbb{S}_N$ as $K(\mathbb{S}_N) = N+1$, then it can be written: $K(\mathbb{S}_{N+1}) = N+2$. However, if we write the cardinality of both sets as $L(\mathbb{S}_N) = 2^N$, then $L(\mathbb{S}_{N+1}) = 2^{N+1}$.

6.2. Collatz compliance in natural number and natural number classes

As a consequence of the above-obtained properties, to heuristically prove that a natural number is Collatz compliant, one has just to apply the Collatz algorithm to the natural number classes.

To apply the Collatz operator to the resultant (one)class κ_n of a natural number $n \in \mathbb{N}$, first, just consider that in any case:

$$C[n] = \langle\langle \mathbf{h}_n|\rangle = \sigma_1(\langle \mathbf{h}_n|) = \kappa_n \to 0 \leq \kappa_n \leq N.$$

Now, suppose that all the $N+1$ class numbers κ_n of the subset S_N are Collatz compliant, or what is the same[6]:

$$\forall I = 0, N : C[I] = 1.$$

Implying an induction reasoning might heuristically prove that (one)class numbers associated with the set $\mathbb{S}_N$ are Collatz compliant. When used in the set $\mathbb{S}_{N+1}$, one can consider that the following (one)class number $N+1$ is also Collatz compliant. Because using similar reasoning as in the equations (3.4) and (3.5), and the pseudolinearity of the Collatz operator, one can write:

$$C[N+1] = C[N] + 1 = 2 \wedge C[2] = 1 \to C^{[2]}[N+1] = 1.$$

That is, in general, for any natural number n, the following sequence holds:

$$\begin{aligned} \forall n \in N : C[n] = \langle\langle \mathbf{h}_n|\rangle = \sigma_1(\langle \mathbf{h}_n|) = \kappa_n \wedge C[\kappa_n] = 1 \\ \to C^{[2]}[n] = C[\langle\langle \mathbf{h}_n|\rangle] = C[\kappa_n] = 1, \end{aligned}$$

whenever the implied (one)class number κ_n is Collatz compliant.

We have to consider here the squared Collatz operator, as it has been pointed out reiteratively before, as the subsequent application of the Collatz operator over the result of some previous application of the Collatz algorithm n-path complete steps.

Note also that the number of ones in the Boolean hypercube vertex vector representing the number n, in any case, fulfills the relation: $\kappa_n < n$, and as n grows larger: $\kappa_n \ll n$.

7. Conclusion

The results found all along this paper lead to the empirical proof, such that one can write:

$$C^{[2]}[\mathbb{N}] = \langle \mathbf{1}| . \tag{7.1}$$

Then Collatz conjecture appears to be heuristically true: any natural number is *Collatz compliant*. But also considering this statement can be extended to N-tuple orderings of natural numbers in the way:

$$\forall N \in \mathbb{N} \wedge C[N] = 1 : C^{[2]}\left[\mathbb{N}^N\right] = \langle \mathbf{1}| . \tag{7.2}$$

The reported discussion and results are of empirical and heuristic nature.

Perhaps there are no other means to prove the Collatz conjecture. Suppose this statement is true, then equations (7.1) and (7.2) constitute an important landmark in studying the Collatz conjecture structure.
On the contrary, whenever a complete description of a mathematical proof might appear in the future, this paper's results will still constitute a reliable, first-step heuristic source of the natural number set Collatz conjecture compliance.

8. Appendix: Collatz Algorithm

Pseudocode depicting the original Collatz algorithm.

Algorithm: Collatz or $(3x+1)$ **procedure**

$$\begin{aligned} &Input : n \in \mathbb{N}; \\ &I = 0; \\ &Define\, C_I[n]; \\ &\textbf{while}\; n > 1; \\ &\quad I = I+1; c \leftarrow n/2; \\ &\quad \textbf{if}\; 2*c \neq n : n \leftarrow 3*n+1;\; \textbf{else}: n \leftarrow c; \end{aligned}$$

Acknowledgements

The authors would like to express their sincere thanks to the editor and the anonymous reviewers for their helpful comments and suggestions.

Funding

There is no funding for this work.

[6] As it was already defined in reference [1], the result: $C[0] = 1$ is also adopted here.

Availability of data and materials

Not applicable.

Competing interests

The authors declare that they have no competing interests.

Author's contributions

All authors contributed equally to the writing of this paper. All authors read and approved the final manuscript.

References

[1] R. Carbó-Dorca, *Boolean Hypercubes, Mersenne numbers and the Collatz conjecture*, J. Math. Sci. Mod., **3** (2020), 120-129.
[2] The Collatz conjecture. Wikipedia, https://en.wikipedia.org/wiki/Collatz_conjecture "What is the Importance of the Collatz Conjecture?" https://math.stackexchange.com/questions/2694/what-is-the-importanceof-the-collatz-conjecture.
[3] H. Nowak, *Collatz conjecture and emergent properties*, https://www.youtube.com/watch?v=QrzcHhBQ2b0.
[4] J. C. Lagarias, *The $3x+1$ problem and its generalizations*, Amer. Math. Monthly, **92**(1) (1985), 323.
[5] J. C. Lagarias, A. Weiss, *The $3x+1$ problem: two stochastic models*, Ann. Applied Prob. **2** (1992), 329-361.
[6] I. Korec, *A density estimate for the $3x+1$ problem*, Math. Slovaca, **44** (1994), 85-89.
[7] G. J. Wirsching, *The Dynamical System Generated by the $3n+1$ Function*, Lecture Notes in Math. 1681, Springer-Verlag, New York, 1998.
[8] J. C. Lagarias, K. Soundararajan, *Benford's law for the $3x+1$ function*, J. London Math. Soc., **74** (2006), 289-303.
[9] J. C. Lagarias, ed.; *The ultimate challenge: the $3x+1$ problem*. Providence, R. I.: Amer. Math. Soc., (2010).
[10] F. Oan, J. P. Draayer, *A polynomial approach to the Collatz conjecture*, arXiv.org: 1905.08462 [math. NT] (2019).
[11] F. Izadi, *A new approach on proving Collatz conjecture*, Journal of Mathematics, Hindawi, **2019** (2019), Article ID: 6129836, 12 pages.
[12] D. Barina, *Convergence verification of the Collatz problem*, The Journal of Supercomputing, **77**(3) (2021), 2681-2688.
[13] T. Tao, *Almost all orbits of the Collatz map attain almost bounded values*, In Forum of Mathematics, Pi (Vol. 10). Cambridge University Press, 2022.
[14] J. A. T. Machado, A. Galhano, D. Cao Labora, *A clustering perspective of the Collatz conjecture*, Mathematics, **9** (2021), 314-328.
[15] F. Izadi, *Complete proof of Collatz's conjectures*, arXiv:2101.06107v4 [math. GM], (2021).
[16] B. M. Gurbaxani, *An engineering and statistical look at the Collatz $(3n+1)$ conjecture* ResearchGate Preprint, 14 March (2021).
[17] B. B. Stefanov, *Two-parameter generalization of the Collatz function characterization of terminal cycles and empirical results*, Online Mathematics OMJ, **03**(01) (2021), 19-25.
[18] L.-O. Pochon, A. Favre, *La suite de Syracuse, un monde de conjectures*, (2021) ffhal01593181v3f.
[19] C. Castro Perelman, R. Carbó-Dorca, *The Collatz conjecture and the quantum mechanical harmonic oscillator*, J. Math. Chem. **60** (2022), 145-160.
[20] N. Fabiano, N. Mirkov, S. Radenovic, *Collatz hypothesis and Planck's black body radiation*, J. Siberian Fed. Univ. Mathematics & Physics, **2** (2021), 1-5.
[21] A. Rahn, E. Sultanov, M. Henkel, S. Ghosh, I. J. Aberkane, *An algorithm for linearizing the Collatz convergence*, Mathematics, **9** (2021), 1898-1930.
[22] J. Kleinnijenhuis, A. M. Kleinnijenhuis, *Pruning the binary tree, proving the Collatz conjecture*, ResearchGate Preprint (no file attached), August (2020).
[23] M. R. Schwob, P. Shiue, R. Venkat, *Novel theorems and algorithms relating to the Collatz conjecture*, Int. J. Math. Math. Sci., **2021** (2021), Article ID: 5754439, 10 pages, (2021).
[24] https://www.mersenne.org/primes/
[25] R. Carbó-Dorca, *Cantor-like infinity sequences and Gödel-like incompleteness revealed by means of Mersenne infinite dimensional Boolean Hypercube concatenation*, J. Math. Chem., **58** (2020), 1-5.
[26] R. Carbó-Dorca, *About Erdös discrepancy conjecture*, J. Math. Chem., **54** (2016), 657-660.
[27] R. Carbó-Dorca, *N-dimensional Boolean Hypercubes and the Goldbach conjecture*, J. Math. Chem., **54** (2016), 1213-1220.
[28] R. Carbó-Dorca, *Natural vector spaces, (Inward power and Minkowski norm of a natural vector, natural Boolean Hypercubes) and Fermat's last theorem*, J. Math. Chem., **55** (2017), 914-940.
[29] R. Carbó-Dorca, *Boolean Hypercubes and the structure of vector Spaces*, J. Math. Sci. Mod., **1** (2018), 1-14.
[30] R. Carbó-Dorca, *Role of the structure of Boolean Hypercubes when used as vectors in natural (Boolean) vector semispaces*, J. Math. Chem., **57** (2019), 697-700.
[31] R. Carbó, E. Besalú, *Definition, mathematical examples and quantum chemical applications of nested summation symbols and logical Kronecker deltas*, Computers & Chemistry **18** (1994), 117-126.
[32] E. Besalú, R. Carbó, *Definition and quantum chemical applications of nested summation symbols and logical Kronecker deltas: Pedagogical Artificial intelligence devices for formulae writing, sequential programming and automatic parallel implementation*, J. Math. Chem., **18** (1995), 37-72.
[33] R. Carbó-Dorca, *Logical Kronecker delta deconstruction of the absolute value function and the treatment of absolute deviations*, J. Math. Chem., **49** (2011), 619-624.
[34] R. Carbó-Dorca, *Inward matrix products: Extensions and applications to quantum mechanical foundations of QSAR*, J. Mol. Struct. Teochem, **537** (2001), 41-54.
[35] R. Carbó-Dorca, *Inward Matrix product algebra and calculus as tools to construct space-time frames of arbitrary dimensions*, J. Math. Chem., **30** (2001), 227-245.

Journal of Mathematical Sciences and Modelling, 5 (3) (2022) 92-98
Research Article

Journal of Mathematical Sciences and Modelling

Journal Homepage: www.dergipark.gov.tr/jmsm
ISSN 2636-8692
DOI: http://dx.doi.org/10.33187/jmsm.1132139

Stability of Finite Difference Schemes to Pseudo-Hyperbolic Telegraph Equation

Mahmut Modanlı[1] and Fatih Özbağ[1*]

[1]*Department of Mathematics, Faculty of Science and Arts, Harran University, Şanlıurfa, Turkey*
[*]*Corresponding author*

Article Info

Keywords: *Finite difference scheme, Pseudo-hyperbolic equation, Stability, Telegraph equation.*
2010 AMS: *35L82, 65M06*
Received: *17 June 2022*
Accepted: *2 September 2022*
Available online: *18 November 2022*

Abstract

Hyperbolic partial differential equations are frequently referenced in modeling real-world problems in mathematics and engineering. Therefore, in this study an initial-boundary value issue is proposed for the pseudo-hyperbolic telegraph equation. By operator method, converting the PDE to an ODE provides an exact answer to this problem. After that, finite difference method is applied to construct first order finite difference schemes to calculate approximate numerical solutions. The stability estimations of finite difference schemes are shown, as well as some numerical tests to check the correctness in comparison to the precise solution. The numerical solution is subjected to error analysis. As a result of the error analysis, the maximum norm errors tend to decrease as we increase the grid points. It can be drawn that the established scheme is accurate and effective.

1. Introduction

Mathematical models in physics, chemistry, engineering, biology and economics are often expressed using partial and ordinary differential equations [1]–[4]. Analytical and numerical solutions of partial differential equations play a significant role in understanding the underlying phenomena [5, 6]. Partial differential equations are classified into three types and in this study, hyperbolic type partial differential equations are considered.

Pseudo-hyperbolic equations are hyperbolic partial differential equations which contain mixed time and space partial derivatives. For these types of equations, there are several technics to calculate exact and approximate numerical solutions. In [7], the conformable double Laplace transform decomposition approach was used to solve linear and nonlinear singular pseudo-hyperbolic equations. In [8], by the regularization method and the method of continuation parameter the regular solvability of the boundary value problem for pseudo-hyperbolic equations with variable time direction were proved. In [9, 10], numerical schemes based on H^1-Galerkin mixed finite element method were constructed for pseudo-hyperbolic equations. Some other works on pseudo-hyperbolic equations are [11]–[15].

There has been a wide range of research on finite difference schemes for approximate solutions to telegraph equations and there are considerable approximation for stability of these difference schemes. The stability estimates of these difference schemes are constructed applying the operator splitting approach and some energy inequalities using certain assumptions on the grid step sizes τ and h [16].

In the present work we consider pseudo-hyperbolic telegraph equation. Telegraph equation is mostly used for modeling of wave propagation of electric signals in a cable transmission line. To get accurate and approximate numerical solutions of hyperbolic telegraph equations, a variety of numerical and analytical approaches are applied. In [17], exact solution of the telegraph equation was solved by (G'/G)-expansion method. In [18], a numerical technique was developed for the one-dimensional telegraph equation with purely integral conditions. Daftardar-Gejji-Jafaris (DGJ) method was used to obtain approximate solution of the hyperbolic telegraph equation [19]. In [20], Differential Transformation Method (DTM) has been utilized to obtain the exact solutions of the one-space-dimensional hyperbolic telegraph equation. In [21], a new numerical scheme was constructed to solve the second-order hyperbolic telegraph equation using the collocation method. Laplace transform homotopy perturbation method was used in [22] to solve the telegraph equation with the initial and boundary conditions. An operator method was studied in [23] for the difference equations and partial differential telegraph equation. In [24], a numerical method for the first and second-order of accuracy for telegraph equations was discussed and the stability of difference schemes were obtained. Numerical solutions were computed for the telegraph equations arising in transmission lines [25].

***Email addresses and ORCID numbers*: mmodanli@harran.edu.tr, 0000-0002-7743-3512 (M. Modanlı), fozbag@harran.edu.tr, 0000-0002-5456-4261 (F. Özbağ)**

In this work, numerical solution of the third-order pseudo-hyperbolic telegraph equation is investigated using the first-order finite difference technique. The numerical solution is subjected to an error analysis. The stability inequalities of finite difference schemes are presented, as well as some numerical experiments to verify the correctness in terms of precise solution.

2. Introducing Problem

We define the pseudo-hyperbolic telegraph equation below

$$\begin{cases} v_{\eta\eta}(\eta,\theta)+\lambda v_{\eta}(\eta,\theta)+\mu v(\eta,\theta)=v_{\eta\theta\theta}(\eta,\theta)+v_{\theta\theta}(\eta,\theta)+g(\eta,\theta), \\ v(0,\theta)=\varphi_1(\theta), \quad v_{\eta}(0,\theta)=\varphi_2(\theta), \quad 0<\theta<L, \\ v(\eta,0)=v(\eta,L)=0, \quad 0<\eta<T, \\ 0<\lambda, \quad 0<\mu. \end{cases} \tag{2.1}$$

We can rewrite equation (2.1) as

$$\begin{cases} v_{\eta\eta}(\eta)+\lambda v_{\eta}(\eta)+Av_{\eta}(\eta)+Av(\eta)+\mu v(\eta)=g(\eta) \quad 0\le\eta\le T, \\ v(0)=\varphi_1, \quad v'(0)=\varphi_2, \end{cases} \tag{2.2}$$

where $A\ge\delta I$ and A is positive definite self-adjoint operator. For positive δ and λ, the following restriction is requried

$$\delta+\mu\ge\frac{(\lambda+\delta)^2}{4}.$$

One can obtain equation (2.2) from (2.1) under the following conditions. In a Hilbert space $\mathscr{L}_2[0,L]$ define

$$Av(\theta)=-v_{\theta\theta}+\delta v(\theta), \tag{2.3}$$

then

$$(Av)_{\eta}=-v_{\theta\theta\eta}=-v_{\eta\theta\theta}$$

with the domain

$$D(A)=\{v(\theta):v,v_{\theta},v_{\theta\theta}\in\mathscr{L}_2, v(0)=v(L), v'(0)=v'(L)\}.$$

Here we set $g(\eta)=g(\eta,\theta)$ and $v(\eta)=v(\eta,\theta)$ which are given and will be determined abstract functions in $\mathscr{L}_2[0,L]$. $v(\eta)$ is a solution of (2.2) if it is three times continuously differentiable on $[0,T]$, $v(\eta)\in D(A)$ and $Av(\eta)$ is continuous on $[0,T]$. Also $v(\eta)$ must satisfy equation (2.2) and the initial conditions. If the operator A satisfies the properties given above, then the partial differential equation (2.1) turns into the ordinary differential equation (2.2). Thus the method used is know as the operator method [23]–[26].
Next we introduce the Hilbert space $\mathscr{L}_2(\overline{\Omega})$, where $\overline{\Omega}=\Omega\cup S$ and $\Omega\subset R^n$ is a bounded open domain with smooth boundary S, with the norm

$$\|g\|_{\mathscr{L}_2(\overline{\Omega})}=\left\{\int\cdots\int_{\theta\in\overline{\Omega}}|g(\theta)|^2dx_1...dx_n\right\}^{\frac{1}{2}}.$$

The problem (2.2) can easily be converted to a system of first order differential equation with initial conditions. Therefore we obtain

$$\begin{cases} v'(\eta)+\dfrac{\lambda+A}{2}v(\eta)+iK^{\frac{1}{2}}v(\eta)=z(\eta), \quad 0\le\eta\le T, \\ v(0)=\varphi_1, \quad v'(0)=\varphi_2, \\ \\ z'(\eta)+\frac{\lambda+A}{2}z(\eta)-iK^{\frac{1}{2}}z(\eta)=g(\eta), \\ z(0)=v'(0)+\left(\frac{\lambda+A}{2}+iK^{\frac{1}{2}}\right)v(0). \end{cases} \tag{2.4}$$

where $K=A+\mu-\frac{(\lambda+A)^2}{4}$. If we integrate (2.4), we obtain

$$v(\eta)=e^{-\left(\frac{\lambda+A}{2}+iK^{\frac{1}{2}}\right)\eta}v(0)+\int_0^{\eta}e^{-\left(\frac{\lambda+A}{2}+iK^{\frac{1}{2}}\right)(\eta-z)}z(s)ds, \tag{2.5}$$

$$z(\eta)=e^{-\left(\frac{\lambda+A}{2}-iK^{\frac{1}{2}}\right)\eta}z(0)+\int_0^{\eta}e^{-\left(\frac{\lambda+A}{2}-iK^{\frac{1}{2}}\right)\eta}g(s)ds. \tag{2.6}$$

Applying the method in [24] with the equations (2.5) and (2.6), we have the solution of the problem (2.2)

$$v(\eta)=e^{-\left(\frac{\lambda+A}{2}\right)\eta}c(\eta)\varphi_1+\frac{\lambda+A}{2}e^{-\left(\frac{\lambda+A}{2}\right)\eta}s(\eta)\varphi_1+e^{-\left(\frac{\lambda+A}{2}\right)\eta}s(\eta)\varphi_2+\int_0^{t}e^{-\left(\frac{\lambda+A}{2}+iK^{\frac{1}{2}}\right)(\eta-z)}\delta(\eta-z)g(z)dz, \tag{2.7}$$

where $c(\eta)=\frac{e^{i\eta K^{1/2}}+e^{-i\eta K^{1/2}}}{2}$ and $s(\eta)=K^{-1/2}\frac{e^{i\eta K^{1/2}}-e^{-i\eta K^{1/2}}}{2i}$.

Lemma 2.1. *Following estimates hold*

- $\|e^{-\left(\frac{\lambda+A}{2}\right)\eta}\|_{\mathscr{L}_2}\le 1$.
- $\|c(\eta)\|_{\mathscr{L}_2\to\mathscr{L}_2}\le 1$.
- $\|K^{1/2}s(\eta)\|_{\mathscr{L}_2\to\mathscr{L}_2}\le 1$.

- $\|A^{1/2}K^{-1/2}\|_{\mathscr{L}_2\to\mathscr{L}_2} \le M(\delta)$.
- $\|K^{-1/2}\varphi_1\|_{\mathscr{L}_2} \le \frac{1}{\sqrt{\delta}}\|\varphi_1\|_{\mathscr{L}_2}$.

For easy proof, see [27, 28]. Now we give the main theorem and prove it.

Theorem 2.2. *Let $\varphi_1 \in D(A)$, $\varphi_2 \in D(A^{1/2})$, $g(\eta)$ be a continuous differentiable function on [0,T] and $\delta+\mu \ge \frac{(\lambda+\delta)^2}{4}$. Then there exist a unique solution of (2.2) and its stability estimate is*

$$\max_{0\le\eta\le T}\|v(\eta)\|_{\mathscr{L}_2} \le M\left[\|\varphi_1\|_{\mathscr{L}_2} + \|A^{-1/2}\varphi_2\|_{\mathscr{L}_2} + \max_{0\le\eta\le T}\|A^{-1/2}g(\eta)\|_{\mathscr{L}_2}\right]$$

where M is independent from φ_1, φ_2 and $g(\eta)$.

Proof. By Lemma 2.1 with $A \ge \delta I$ and using the formula (2.7), we have the following inequalities

$$\begin{aligned}
\|v(\eta)\|_{\mathscr{L}_2} &\le \|c(\eta)\|_{\mathscr{L}_2\to\mathscr{L}_2}\|e^{-(\frac{\lambda+A}{2})\eta}\|_{\mathscr{L}_2}\|\varphi_1\|_{\mathscr{L}_2} + \|K^{1/2}s(\eta)\|_{\mathscr{L}_2\to\mathscr{L}_2}\|A^{1/2}K^{-1/2}\|_{\mathscr{L}_2\to\mathscr{L}_2}|\frac{\lambda+A}{2}e^{-(\frac{\lambda+A}{2})\eta}| \\
&\quad \|A^{-1/2}\varphi_1\|_{\mathscr{L}_2} + \|K^{1/2}s(\eta)\|_{\mathscr{L}_2\to\mathscr{L}_2}\|A^{1/2}K^{-1/2}\|_{\mathscr{L}_2\to\mathscr{L}_2}|e^{-(\frac{\lambda+A}{2})\eta}|\|A^{-1/2}\varphi_2\|_{\mathscr{L}_2} \\
&\quad + \int_0^\eta \|K^{1/2}s(\eta-z)\|_{\mathscr{L}_2\to\mathscr{L}_2}\|A^{1/2}K^{-1/2}\|_{\mathscr{L}_2\to\mathscr{L}_2}\|A^{-1/2}g(s)\|_{\mathscr{L}_2}ds \\
&\le M(\delta,\lambda)\left[\|\varphi_1\|\|_{\mathscr{L}_2} + \|A^{-1/2}\varphi_2\|_{\mathscr{L}_2} + \max_{0\le\eta\le T}\|A^{-1/2}g(\eta)\|_{\mathscr{L}_2}\right].
\end{aligned}$$

□

3. Stability for First Order Difference Scheme

We investigate the approximation in η of first order difference scheme

$$\begin{cases}
\frac{v_{k+1}-2v_k+v_{k-1}}{\tau^2} + \lambda\frac{v_k-v_{k-1}}{\tau} + A\frac{v_k-v_{k-1}}{\tau} + \mu v_k + Av_k = g_k, \\
g_k = g(\eta_k), \quad 1\le k\le N-1, \quad N\tau = T, \\
v_0 = \varphi_1, \quad \frac{v_1-v_0}{\tau} + (\mu+A)\tau v_0 = (1-(\lambda+A)\tau)\varphi_2
\end{cases} \tag{3.1}$$

for the numerical solution of the initial value problem (2.1). We can write (3.1) into the following difference problem

$$\begin{cases}
(1-(\lambda+A)\tau)v_{k-1} - (2-(\lambda+A)\tau-(\mu+A)\tau^2)v_k + v_{k+1} = \tau^2 g_k, \\
1\le k\le N-1, \\
v_0 = \varphi_1, \quad v_1 = (1-(\mu+A)\tau^2)v_0 + (1-(\lambda+A)\tau)\tau\varphi_2.
\end{cases} \tag{3.2}$$

The formula (3.2) can be simplified as

$$av_{k-1} - cv_k + bv_{k+1} = \varphi_k,$$

where $a = 1-(\lambda+A)\tau$, $\quad c = 2-((\lambda+A)\tau+(\mu+A)\tau^2)$, $\quad b = 1$ and $\varphi_k = \tau^2 g_k$.

Theorem 3.1. *Let $\varphi_1 \in D(A)$, $\varphi_2 \in D(A^{1/2})$ and $\delta+\mu \ge \frac{(\lambda+\delta)^2}{4}$. The following stability inequality for (3.1)*

$$\max_{0\le k\le 1}\|v_k\|_{\mathscr{L}_2} \le M(\lambda,\mu,\delta)\left[\|\varphi_1\|_{\mathscr{L}_2} + \|A^{-1/2}\varphi_2\|_{\mathscr{L}_2} + \max_{1\le k\le N-1}\|A^{-1/2}g_k\|_{\mathscr{L}_2}\right] \tag{3.3}$$

holds where $M(\lambda,\mu,\delta)$ is independent from $\tau, \varphi_1, \varphi_2$ and g_k, $1\le s\le N-1$.

The proof of Theorem 3.1 follows from [26] by using the formula for the solution of the difference scheme (3.2).
Now, we consider applications of Theorem 3.1. We begin by discretizing the problem (2.1). First we define the grid space

$$[0,L]_h = \{\theta = \theta_n : \theta_n = nh, 0\le n\le M, Mh = L\}.$$

$\mathscr{L}_{2h}$ with the grid space $[0,L]_h$ is defined as $\mathscr{L}_2([0,L]_h)$. The following $\mathscr{L}_{2h}$ norm

$$\|\varphi^h\|_{\mathscr{L}_{2h}} = \left(\sum_{\theta\in[0,L]_h}|\varphi(\theta)|^2 h\right)^{1/2}$$

is used for the grid functions $\varphi^h(\theta) = \{\varphi_n\}_0^M$. Then we define the difference operator A_h for the differential operator A in equation (2.3)

$$A_h\varphi^h(\theta) = \{-(\varphi_{\theta\theta})_n + \delta\varphi_n\}_1^{M-1}.$$

A_h is a positive definite and self-adjoint operator in $\mathscr{L}_{2h}$ and satifies the conditions $\varphi_0 = \varphi_M$ and $\varphi_1 - \varphi_0 = \varphi_M - \varphi_{M-1}$. Now we can write

$$\begin{cases} v^h_{\eta\eta}(\eta,\theta)+\lambda v^h_\eta(\eta,\theta)+A^h v^h_\eta(\eta,\theta)+A^h v^h(\eta,\theta)+\mu v(\eta,\theta)=g^h(\eta,\theta), \\ v^h(0,\theta)=\varphi^h_1(\theta), \quad v^h_\eta(0,\theta)=\varphi^h_2(\theta), \quad 0<\eta<T, \theta\in[0,L]_h. \end{cases} \tag{3.4}$$

After replacing (3.4) with the difference scheme (3.1), we obtain

$$\begin{cases} \frac{v^h_{k+1}(\theta)-2v^h_k(\theta)+v^h_{k-1}(\theta)}{\tau^2}+\lambda\frac{v^h_k(\theta)-v^h_{k-1}(\theta)}{\tau}+A^h\frac{v^h_k(\theta)-v^h_{k-1}(\theta)}{\tau} \\ +\mu v^h_k(\theta)+A^h v^h_k(\theta)=g^h_k(\theta), \\ g^h_k(\theta)=g^h(\eta_k,\theta), \quad 1\le k\le N-1, \theta\in[0,L]_h, \eta_k=k\tau, N\tau=T, \\ v^h_0(\theta)=\varphi^h_1(\theta), \quad \frac{v^h_1(\theta)-v^h_0(\theta)}{\tau}+(\mu I_h+A^h)\tau v^h_0(\theta)=(I_h-(\lambda I_h+A^h)\tau)\varphi^h_2(\theta). \end{cases} \tag{3.5}$$

Theorem 3.2. *The stability estimate of the solution $\{v^h_k(\theta)\}_0^N$ of the discretized problem (3.5)*

$$\max_{1\le k\le N}\|v^h_k\|_{\mathscr{L}_{2h}}\le M\left[\|\varphi^h_1\|_{\mathscr{L}_{2h}}+\|\varphi^h_2\|_{\mathscr{L}_{2h}}+\max_{1\le k\le N-1}\|g^h_k\|_{\mathscr{L}_{2h}}\right]$$

holds where M is independent from $\varphi^h_1(\theta), \varphi^h_2(\theta)$ and $g^h_k(\theta)$, $1\le k\le N-1$.

Proof of Theorem 3.2 follows from stability estimate (3.3).

4. Simulations

In this chapter, a numerical example is provided to support the theoretical statements. Some numerical results are given as an application of the Theorem 3.1. Consider the following problem

$$\begin{cases} v_{\eta\eta}(\eta,\theta)+v_\eta(\eta,\theta)+v(\eta,\theta)=v_{\eta\theta\theta}(\eta,\theta)+v_{\theta\theta}(\eta,\theta)+g(\eta,\theta), \\ g(\eta,\theta)=e^{-\eta}(\theta-\theta^2), 0<\theta<1, 0<\eta<1, \\ v(0,\theta)=\theta-\theta^2, \quad v_\eta(0,\theta)=-(\theta-\theta^2), \quad 0\le\theta\le1, \\ v(\eta,0)=v(\eta,1)=0, \quad 0\le\eta\le1. \end{cases} \tag{4.1}$$

By using Modified Double Laplace Decomposition method the exact solution of the problem (4.1) is $v(\eta,\theta)=e^{-\eta}(\theta-\theta^2)$. See [29, 30, 31] for similar examples.
The first order difference scheme of the problem (4.1) is as follows

$$\begin{cases} \frac{v^{k+1}_n-2v^k_n+v^{k-1}_n}{\tau^2}+\frac{v^k_n-v^{k-1}_n}{\tau}+v^k_n=\frac{1}{\tau}\left(\frac{v^k_{n-1}-2v^{k+1}_n+v^k_{n+1}}{h^2}-\frac{v^{k-1}_{n-1}-2v^k_n+v^{k-1}_{n+1}}{h^2}\right)+\frac{v^k_{n+1}-2v^k_n+v^k_{n-1}}{h^2}+g^k_n, \\ \theta_n=nh, \quad \eta_k=k\tau, 1\le k\le N-1, \quad 1\le n\le M-1, \\ v^0_n=\theta-\theta^2, \quad \frac{v^1_n-v^0_n}{\tau}=-(\theta-\theta^2), \quad 0\le n\le M, \\ v^k_0=v^k_M=0, \quad 0\le k\le N. \end{cases} \tag{4.2}$$

Next, we consider the following matrix equation

$$\mathscr{A}v_{n+1}+\mathscr{B}v_n+\mathscr{C}v_{n-1}=I\varphi_n$$

where $v_n=[v^1_n,v^2_n,...,v^{N-1}_n]$, $\varphi_n=[\varphi^1_n,\varphi^2_n,...,\varphi^{N-1}_n]^T$. We have $(N+1)\times(N+1)$ system of equation with the coefficient matrices $\mathscr{A}$, $\mathscr{B}$ and $\mathscr{C}$. Following the same approach as in [23], we compute the maximum difference between the approximate and exact solution by

$$\varepsilon=\max_{\substack{1\le k\le N-1\\1\le n\le M-1}}|v(\eta,\theta)-v(\eta_k,\theta_n)|.$$

Calculated results are presented in Table 1 for (4.2).

$\tau=\frac{1}{N}, h=\frac{1}{M}$	ε
$N=25, M=5$	0.1600
$N=100, M=10$	0.0900
$N=225, M=15$	0.0622
$N=400, M=20$	0.0475
$N=625, M=25$	0.0384
$N=900, M=30$	0.0322
$N=1600, M=40$	0.0244
$N=2500, M=50$	0.0196

Table 1: Error Analysis

From Table 1, one can observe that maximum norm errors tend to decrease as we increase the grid points. This shows the established scheme's precision. Moreover numerical results in Table 1 are calculated by taking $\tau=h^2$. To show the precision of the numerical results, we calculate the error of the difference scheme (4.2) by taking $\tau = h$. For example, for $N = M = 20$ maximum norm error is 0.0811 which is greater than for $N = 400$, $M = 20$. Also this maximum norm error is increasing as N and M are increasing.

Figures 4.1 and 4.2 show how the solutions to the example (4.1) look very similar. In addition, in Figure 4.3, 2d-line plot is given to see how the solutions fit together.

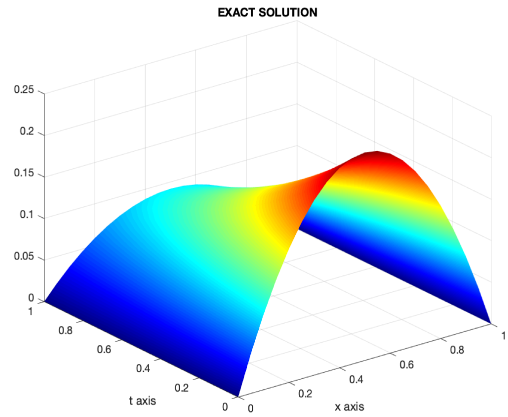

Figure 4.1: For $N = 400$ and $M = 20$, graph of the exact solution of the problem (4.1).

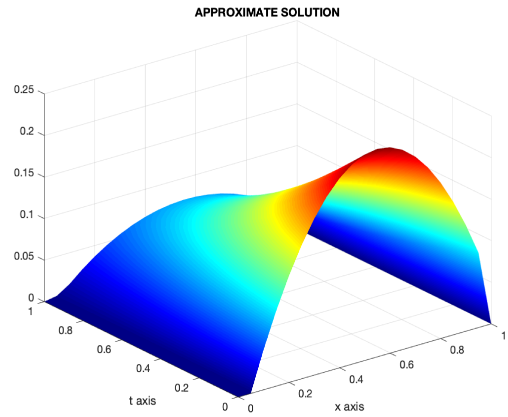

Figure 4.2: For $N = 400$ and $M = 20$, the graph with maximum error 0.0475.

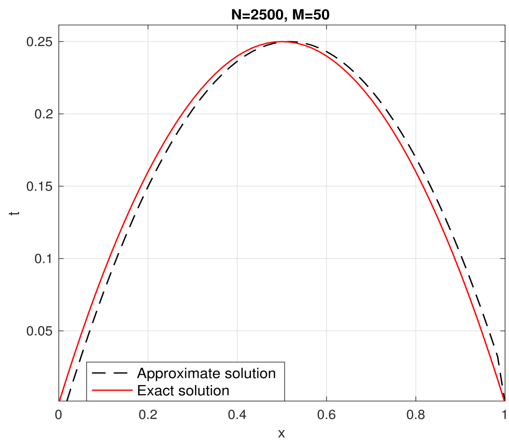

Figure 4.3: For $N = 2500$ and $M = 50$, comparison of the approximate and exact solutions.

5. Conclusion

In this paper, the pseudo-hyperbolic telegraph equation was addressed and its stability estimates were calculated. In the literature, finite difference technic has not been applied for the numerical solution of this equation. Although the Modified Double Laplace Decomposition method gave the exact solution of this problem, we also constructed the first order finite difference scheme. Besides, stability estimates of the scheme were obtained. Then, we performed the difference scheme technique on the considered numerical example to confirm the correctness. Error calculations showed that the established scheme has good results and is effective for this equation. Also, some simulations were plotted to see it clearly and assist with the results. MATLAB programming was used to calculate the numerical solutions for the test example.

Acknowledgements

The authors would like to express their sincere thanks to the editor and the anonymous reviewers for their helpful comments and suggestions.

Funding

There is no funding for this work.

Availability of data and materials

Not applicable.

Competing interests

The authors declare that they have no competing interests.

Author's contributions

All authors contributed equally to the writing of this paper. All authors read and approved the final manuscript.

References

[1] A. Din, Y. Li, F. M. Khan, Z. U. Khan, P. Liu, *On analysis of fractional order mathematical model of Hepatitis B using Atangana-Baleanu Caputo (ABC) derivative*, Fractals, **30**(01) (2022), 2240017.
[2] A. Din, Y. Li, T. Khan, G. Zaman, *Mathematical analysis of spread and control of the novel corona virus (COVID-19) in China*, Chaos Solitons Fractals, **141** (2020), 110286.
[3] P. Veeresha, M. Yavuz, C. Baishya, *A computational approach for shallow water forced Korteweg-De Vries equation on critical flow over a hole with three fractional operators*, Int. J. Optim. Control: Theor. Appl. , **11**(3) (2021), 52-67.
[4] F. Özbağ, *Numerical simulations of traveling waves in a counterflow filtration combustion model*, Turk. J. Math., **46**(4) (2022), 1424-1435.
[5] L. Zada, R. Nawaz, K. S. Nisar, M. Tahir, M. Yavuz, *New approximate-analytical solutions to partial differential equations via auxiliary function method*, Partial Differ. Eq. Appl. Math., **4** (2021), 100045.
[6] Z. Hammouch, M. Yavuz, N. Özdemir, *Numerical solutions and synchronization of a variable-order fractional chaotic system*, Math. Model. Numer. Simul. App., **1**(1) (2021), 11-23.
[7] H. Eltayeb, S. Mesloub, Y. T. Abdalla, A. Kilicman, *A note on double conformable Laplace transform method and singular one dimensional conformable pseudo-hyperbolic equations*, Mathematics, **7**(10) (2019), 949.
[8] S. V. Potapova, *Boundary value problems for pseudo-hyperbolic equations with a variable time direction*, J. Pure Appl. Math., **3**(1) (2012), 75-91.
[9] Y. Zhang, Y. Niu, D. Shi, *Nonconforming H^1 -Galerkin mixed finite element method for pseudo-hyperbolic equations*, American J. Comp. Math., **2** (2012), 269-273.
[10] Y. Liu, J. Wang, H. Li, W. Gao, S. He, *A new splitting H^1-Galerkin mixed method for pseudo-hyperbolic equations*, Int. J. Math. Comp. Sci., **5**(3) (2011), 1444-1449.
[11] I. Fedotov, M.Y. Shatalov, J. Marais, *Hyperbolic and pseudo-hyperbolic equations in the theory of vibration*, Acta Mech., **227**(11) (2016), 3315-3324.
[12] G. Chen, Z. Yang, *Initial value problem for a class of nonlinear pseudo-hyperbolic equations*, Acta Math. App. Sinica, **9**(2) (1993), 166-173.
[13] P. A. Krutitskii, *An initial-boundary value problem for the pseudo-hyperbolic equation of gravity-gyroscopic waves*, J. Math. Kyoto Univ., **37**(2) (1997), 343-365.
[14] Z. Zhao, H. Li, *A continuous Galerkin method for pseudo-hyperbolic equations with variable coefficients*, J. Math. Anal. App., **473**(2) (2019), 1053-1072.
[15] M. Modanli, F. Özbağ, A. Akgülma, *Finite difference method for the fractional order pseudo telegraph integro-differential equation*, J. Appl. Math. Comput. Mech., **21**(1) (2022), 41-54.
[16] H. W. Liu, L. B. Liu, *An unconditionally stable spline difference scheme of $O(k^2+h^4)$ for solving the second-order 1D linear hyperbolic equation*, Math. Comp. Model., **49** (2009), 1985-1993.
[17] M. M. Islam, M. S. Hasan, *A study on exact solution of the telegraph equation by (G'/G)-expansion method*, African J. Math. Comp. Sci. Res., **11**(7) (2018), 103-108.
[18] A. Merad, A. Bouziani, *Solvability the telegraph equation with purely integral conditions*, J. App. Eng. Math., **3**(2) (2013), 245-253.
[19] M. Sarı, A. Günay, G. Gürarslan, *A solution to the telegraph equation by using DGJ method*, Int. J. Nonlinear Sci., **17**(1) (2014), 57-66.
[20] B. Soltanalizadeh, *Differential transformation method for solving one-space-dimensional telegraph equation*, Comput. Appl. Math., **30**(3) (2016), 639-653.
[21] M. Dehghan, A. Shokri, *A numerical method for solving the hyperbolic telegraph equation*, Numer. Methods for Partial Differ. Eq., **24**(4) (2008), 1080-1093.
[22] M. Javidi, N. Nyamoradi, *Numerical solution of telegraph equation by using LT inversion technique*, Int. J. Adv. Math. Sci., **1**(2) (2013), 64-77.
[23] A. Ashyralyev, M. Modanli, *An operator method for telegraph partial differential and difference equations*, Boundary V. Prob., **1**(41) (2015).
[24] A. Ashyralyev, M. Modanli, *Nonlocal boundary value problem for telegraph equations*, AIP Conf. Proc., **1676** (2015).
[25] M. E. Köksal, *An operator-difference method for telegraph equations arising in transmission lines*, Discrete Dyn. Nature Soc., **2011**(6) (2011), 17.
[26] A. Ashyralyev, P.E. Sobolevskii, *New difference schemes for partial differential equations*, Operator Theory: Advances and Applications, **148**, (2004).
[27] V. Pogorelenko, P. E. Sobolevskii, *The "counter-example" to W. Littman counter-example of Lp-energetical inequality for wave equation*, Funct. Differ. Equ., **4**(1-2) (1997), 165-172.
[28] V. A Kostin, *Analytic semigroups and cosine functions*, Dokl. Akad. Nauk SSSR, **307**(4) (1989), 796-799.
[29] M. Modanli, B. Bajjah, *Double Laplace decomposition method and finite difference method of time-fractional Schrödinger pseudoparabolic partial differential equation with Caputo derivative*, J. Math., **2021** (2021), 10.

[30] M. Modanlı, F. Şimşek, *Pseudo-hiperbolik telegraf kısmi diferansiyel denklemin modifiye çift Laplace metodu ile Çözümü*, Karadeniz Fen Bilimleri Dergisi, **12**(1) (2022), 43-50.
[31] M. Modanli, B. Bajjah, S. Kuşulay, *Two numerical methods for solving the Schrödinger parabolic and pseudoparabolic partial differential equations*, Adv. Math. Phys., **2022** (2022), 10.

Journal of Mathematical Sciences and Modelling, 5 (3) (2022) 99-104
Research Article

Journal of Mathematical Sciences and Modelling

Journal Homepage: www.dergipark.gov.tr/jmsm
ISSN 2636-8692
DOI: http://dx.doi.org/10.33187/jmsm.1123178

Novel Solutions of Perturbed Boussinesq Equation

Şeyma Tülüce Demiray[1] **and Uğur Bayrakcı**[1*]

[1]*Department of Mathematics, Faculty of Science and Arts, Osmaniye Korkut Ata University, Osmaniye, Turkey*
[*]*Corresponding author*

Article Info

Keywords: *Generalized Kudryashov method, Perturbed Boussinesq equation, Sine-Gordon expansion method, Soliton solutions*
2010 AMS: *35A20, 35A25, 35C07*
Received: *30 May 2022*
Accepted: *28 September 2022*
Available online: *18 November 2022*

Abstract

In this article, we have worked on the perturbed Boussinesq equation. We have applied the generalized Kudryashov method (GKM) and sine-Gordon expansion method (SGEM) to the perturbed Boussinesq equation. So, we have obtained some new soliton solutions of the perturbed Boussinesq equation. Furthermore, we have drawn some 2D and 3D graphics of these results by using Wolfram Mathematica 12.

1. Introduction

Perturbed Boussinesq equation (BE) is a category of nonlinear evolution equations (NLEEs). NLEEs have very important applications in areas such as plasma physics, mathematical physics, optical fibers, mathematical chemistry, hydrodynamics, fluid dynamics, geochemistry, control theory, meteorology, optics, mechanics, chemical kinematics, biophysics, biogenetics, and so on. NLEE's important work is carried out by scientists in many disciplines, especially mathematics and physics [1]-[12].
Perturbed BE is given as:

$$u_{tt}-k^2u_{xx}+p(u^{2n})_{xx}+ru_{xxxx}=\beta u_{xx}+\rho u_{xxxx}, \tag{1.1}$$

where ρ is the higher-order stabilization term and β shows the coefficient of dissipation [13, 14]. The perturbed BE is defined for areas such as plasma waves, quantum mechanics, acoustic waves, nonlinear optics, the elasticity of longitudinal waves in bars. Recently perturbed BE has been studied by some researchers.
Ebadi et al. have worked exponential function method and G'/G method [13]. Akbar et al. have applied the modified auxiliary equation technique for the perturbed BE [14]. Daripa and Dash have used the Pseudospectral method [15]. Dash and Daripa have established weakly nonlocal solitary wave solutions of the regularized sixth-order BE [16]. Jiao have used approximate symmetry method for (2+1)-dimensional perturbed BE [17].
Our aim in this study is to detect soliton solutions of perturbed BE through GKM [18]-[21] and SGEM [22]-[25]. In part 2, GKM and SGEM's structures are given. In part 3, some soliton solutions of perturbed BE is obtained by applying GKM and SGEM.

2. Methods

2.1. Structure of GKM

We take notice of a general nonlinear partial differential equation (NLPDE) in the following form:

$$P(u,u_t,u_x,u_{xx},u_{xt},...)=0. \tag{2.1}$$

Email addresses and ORCID numbers: **seymatuluce@gmail.com, 0000-0002-8027-7290 (Ş. Tülüce Demiray), ubayrakci42@gmail.com, 0000-0002-1765-2318 (U. Bayrakcı)**

Step 1. Firstly, we regard the travelling wave transform like as in the below form;

$$u(x,t) = u(\xi), \xi = x - vt, \tag{2.2}$$

by inserting Eq. (2.2) into Eq. (2.1). We reduce the Eq. (2.1) to the ordinary differential equation form:

$$R(u, u^{'}, u^{''}, u^{'''}, \cdots) = 0. \tag{2.3}$$

Step 2. Solutions of the obtained ordinary differential equation are taken as follows;

$$u(\xi) = \frac{\sum_{i=0}^{T} p_i Z^i(\xi)}{\sum_{j=0}^{K} r_j Z^j(\xi)} = \frac{A[Z(\xi)]}{B[Z(\xi)]}, \tag{2.4}$$

where Z is $\frac{1}{1 \pm e^{\xi}}$. Z is a solution to the $Z_\xi = Z^2 - Z$ equation,
Step 3. We use the homogeneous balance principle to find the values of K and T in Eq. (2.4). For this purpose, we balance between the highest order derivative and highest order nonlinear term in Eq. (2.3).
Step 4. We put Eq. (2.4) into Eq. (2.3). So we get a polynomial $R(Z)$ of Z. By equating all coefficients of $R(Z)$ to zero, we get a system of algebraic equations. By solving obtained system, we find c and the variable coefficients of $p_0, p_1, p_2, \ldots, p_T, r_0, r_1, r_2, \ldots, r_K$. Finally we can get the solutions of Eq. (2.1).

2.2. Structure of SGEM

We will give the general basic of SGEM. For this, we first handle the sine-Gordon equation

$$u_{xx} - u_{tt} = m^2 \sin(u), \tag{2.5}$$

where m is a real constant and $u = u(x,t)$ is a function.
Performing wave transformation $u(x,t) = u(\xi), \xi = \mu(x - kt)$ to Eq. (2.5),

$$u'' = \frac{m^2}{\mu^2 \left(1 - k^2\right)} \sin(u) \tag{2.6}$$

is obtained. Integrating Eq. (2.6) and setting the integration constant to zero, we have,

$$\left[\left(\frac{u}{2}\right)'\right]^2 = \frac{m^2}{\mu^2 \left(1 - k^2\right)} \sin^2\left(\frac{u}{2}\right). \tag{2.7}$$

Subsituting $w(\xi) = \frac{u}{2}$ and $b^2 = \frac{m^2}{\mu^2(1-k^2)}$ in Eq. (2.7), we get,

$$w' = b \sin(w). \tag{2.8}$$

If we receive $b = 1$ in Eq. (2.8), we have,

$$w' = \sin(w). \tag{2.9}$$

From the Eq. (2.9), we get,

$$\sin(w) = \sin(w(\xi)) = \left.\frac{2de^{\xi}}{d^2 e^{2\xi} + 1}\right|_{d=1} = \operatorname{sech}(\xi), \tag{2.10}$$

$$\cos(w) = \cos(w(\xi)) = \left.\frac{d^2 e^{2\xi} - 1}{d^2 e^{2\xi} + 1}\right|_{d=1} = \tanh(\xi), \tag{2.11}$$

To find the solution of the following nonlinear partial differential equation;

$$F(u, u_x, u_t, u_{xx}, u_{tt}, u_{xt}, \ldots) = 0, \tag{2.12}$$

we handle the equation given below,

$$u(\xi) = \sum_{i=1}^{n} \tanh^{i-1}(\xi) \left[B_i \operatorname{sech}(\xi) + A_i \tanh(\xi)\right] + A_0. \tag{2.13}$$

Considering the Eqs. (2.10) and (2.11), we can write the Eq. (2.13) as follows:

$$u(w) = \sum_{i=1}^{n} \cos^{i-1}(w) \left[B_i \sin(w) + A_i \cos(w)\right] + A_0. \tag{2.14}$$

Here we specify the value of n in Eq. (2.14) by means of balance principle, replace Eq. (2.14) into Eq. (2.12), and comparison the terms, we get a system of equations. By solving obtained system of equations, we acquire travelling wave solutions of the Eq. (2.12).

3. Application of Methods

3.1. GKM

To get the exact solutions of Eq. (1.1) we take account of the following transformation:

$$u(x,t)=u(\xi),\xi=x-vt. \tag{3.1}$$

Replacing Eq. (3.1) into Eq. (1.1) and integrating by taking the integration constant as zero, we get the following equation,

$$(v^2-k^2-\beta)u+p(u^{2n})+(r-\rho)u^{''}=0. \tag{3.2}$$

In Eq. (3.2), $u=q^{\frac{2}{2n-1}}$ transformation is applied. Thus, Eq. (3.2) is converted into the following form.

$$(v^2-k^2-\beta)q^2+pq^4+(r-\rho)\frac{2(3-2n)}{(2n-1)^2}\left(q^{'}\right)^2+(r-\rho)\frac{2}{(2n-1)}qq^{''}=0. \tag{3.3}$$

By using balance principle in Eq. (3.3), we get $T=K+1$. Takes the value $T=2$ for $K=1$, so we get

$$u(\xi)=\frac{a_0+a_1Z+a_2Z^2}{b_0+b_1Z}, \tag{3.4}$$

$$u^{'}(\xi)=\left(Z^2-Z\right)\left[\frac{(a_1+2a_2Z)(b_0+b_1Z)-b_1\left(a_0+a_1Z+a_2Z^2\right)}{(b_0+b_1Z)^2}\right], \tag{3.5}$$

$$\begin{aligned} u^{''}(\xi) &= \frac{(Z^2-Z)(2Z-1)}{(b_0+b_1Z)}\left[(a_1+2a_2Z)(b_0+b_1Z)-b_1\left(a_0+a_1Z+a_2Z^2\right)\right] \\ &+\frac{(Z^2-Z)^2}{(b_0+b_1Z)^3}\left[2a_2(b_0+b_1Z)^2-2b_1(a_1+2a_2Z)(b_0+b_1Z)+2b_1^2\left(a_0+a_1Z+a_2Z^2\right)\right]. \end{aligned} \tag{3.6}$$

We find the solution cases as follows;
Case 1:

$$\begin{aligned} &a_0=0, \quad a_2=-a_1, \quad b_0=\frac{i(-1+2n)\sqrt{p}a_1}{2\sqrt{2}\sqrt{(1+2n)(r-\rho)}}, \quad b_1=-\frac{i(-1+2n)\sqrt{p}a_1}{\sqrt{2r+4nr-2\rho-4n\rho}}, \\ &v=-\frac{\sqrt{k^2(1-2n)^2-4r+\beta+4(-1+n)n\beta+4\rho}}{(1-2n)}. \end{aligned} \tag{3.7}$$

Soliton solutions of Eq. (1.1) are found by writing values in (3.7) into Eq. (3.4).

$$u_1(x,t)=\left(\frac{\sqrt{2}\sqrt{(1+2n)(r-\rho)}csc[ivt-ix]}{(1-2n)\sqrt{p}}\right)^{\frac{2}{2n-1}}. \tag{3.8}$$

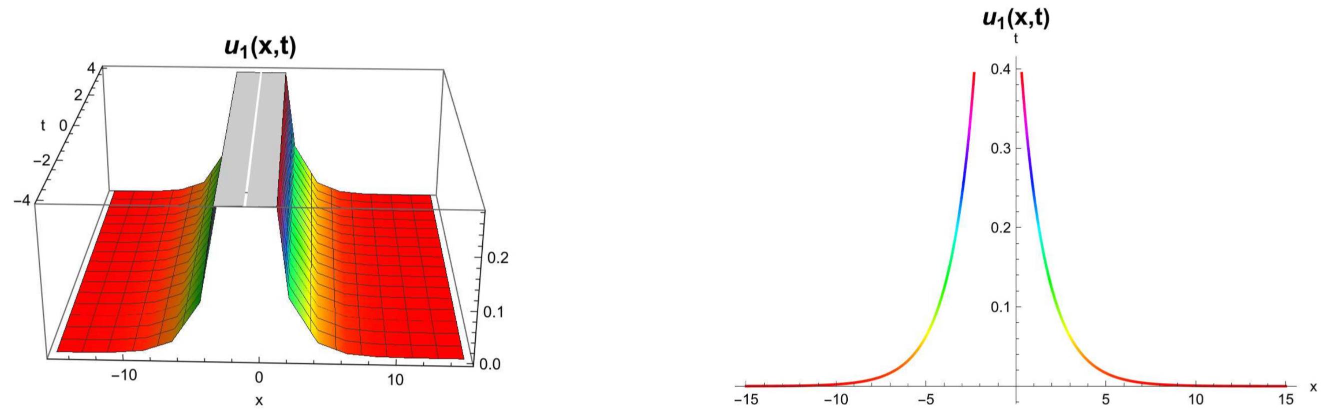

Figure 3.1: The 3D graph of the solution (3.8) for $n=2,\ r=2,\ \rho=1.5,\ v=-1,\ p=3,-15\leq x\leq 15,\ -4\leq t\leq 4$ and 2D graph for this values and $t=1$.

Case 2:

$$a_0 = 0, \quad a_1 = -a_2, \quad b_0 = -\frac{b_1}{2}, \quad \beta = \frac{-k^2(1-2n)^2 + 4r + (1-2n)^2 v^2 - 4\rho}{(1-2n)^2}, \quad p = \frac{2(1+2n)(-r+\rho)b_1^2}{(1-2n)^2 a_2^2}. \tag{3.9}$$

Soliton solutions of Eq. (1.1) are found by writing values in (3.9) into Eq. (3.4).

$$u_2(x,t) = \left(\frac{csch[x-vt]a_2}{b_1}\right)^{\frac{2}{2n-1}}. \tag{3.10}$$

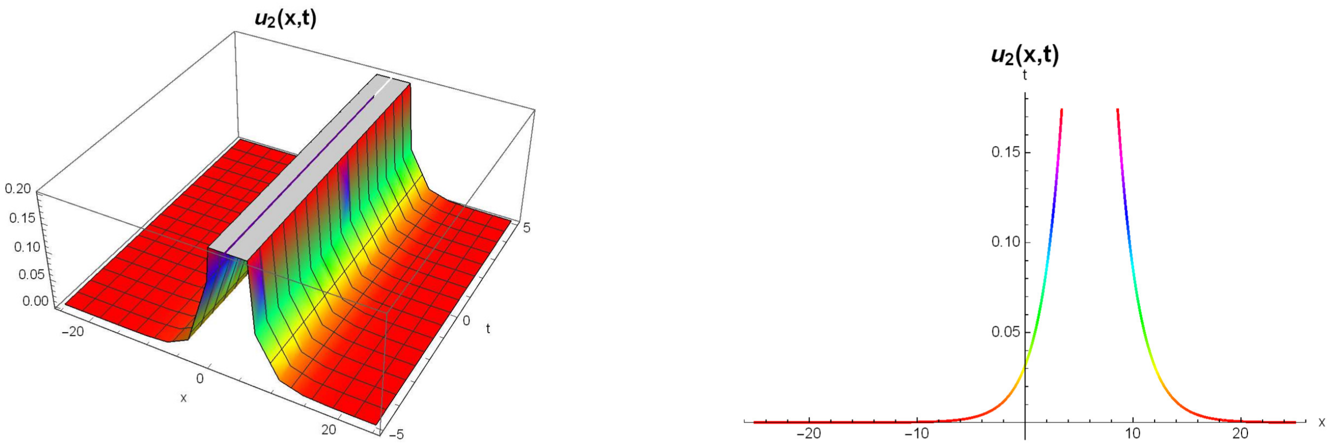

Figure 3.2: The 3D graph of the solution (3.10) for $n = 2.5,\ v = 1, a_2 = 1,\ b_1 = 5,\ -25 \le x \le 25,\ -5 \le t \le 5$ and 2D graph for this values and $t = 3$.

3.2. SGEM

By using balance principle in Eq. (3.3), we find $N = 1$. Using the value of $N = 1$ in Eq. (2.14), we get:

$$u(w) = B_1 \sin(w) + A_1 \cos(w) + A_0, \tag{3.11}$$

$$u'(w) = B_1 \cos(w)\sin(w) - A_1 \sin^2(w), \tag{3.12}$$

$$u''(w) = B_1 \cos^2(w)\sin(w) - B_1 \sin^3(w) - 2A_1 \sin^2(w)\cos(w). \tag{3.13}$$

Placing Eq. (3.11), (3.12) and (3.13) into Eq. (3.3), we are generating trigonometric equations. We obtain an equation system by performing some mathematical operations in these trigonometric equations. Solving the obtained system of equations, we can result:

$$A_0 = 0, \quad A_1 = 0, \quad B_1 = -\frac{\sqrt{2(1+2n)(r-\rho)}}{\sqrt{(1-2n)^2 p}}, \quad k = -\frac{\sqrt{4r + (1-2n)^2(v^2-\beta) - 4\rho}}{\sqrt{(1-2n)^2}}. \tag{3.14}$$

For values (3.14) we get the following result:

$$u_3(x,t) = \left(-\frac{\sqrt{2(1+2n)(r-\rho)}\,\mathrm{sech}[x-vt]}{\sqrt{(1-2n)^2 p}}\right)^{\frac{2}{2n-1}}. \tag{3.15}$$

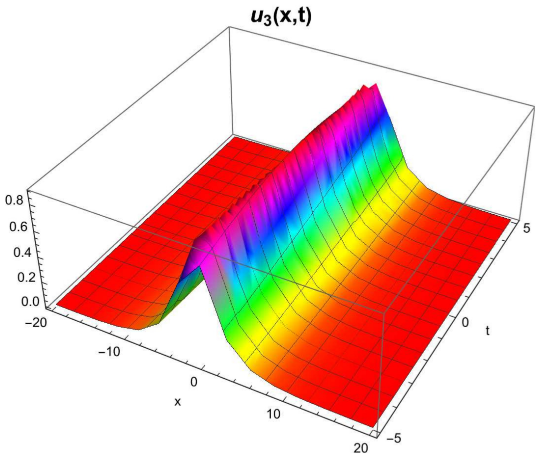

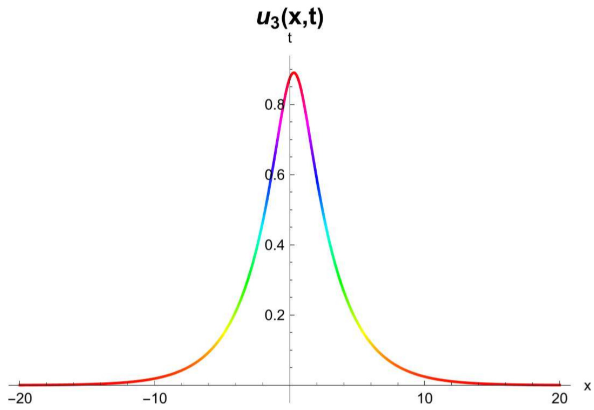

Figure 3.3: The 3D graph of the solution (3.15) for $n=3, r=2, \rho=3, v=0.2, p=-1, -20\leq x\leq 20, -5\leq t\leq 5$ and 2D graph for this values and $t=1.5$.

4. Results and Discussion

In this study, the perturbed BE is discussed. GKM and SGEM have been applied to this equation and thus the solutions of the equation have been sought. As a result, bright soliton solutions of the equation have been acquired. As far as we researched, these obtained bright soliton solutions are new and have not been demonstrated before compared to previous studies. Both 2D and 3D graphical representations have been made for the physical representation of these obtained solutions.

5. Conclusion

In this study, the perturbed BE was studied. First, it is reduced to an ordinary differential equation by applying the traveling wave transform to the equation. Afterward, some n-dimensional soliton solutions of the equation were found by applying GKM and SGEM to this ordinary differential equation. 2D and 3D graphics were drawn thanks to Wolfram Mathematica 12 by giving certain values to the acquired solutions. According to our study, GKM and SGEM appear to be effective and reliable methods for finding NLEEs solutions. Thus, it is seen that GKM and SGEM are methods that facilitate the solution of NLEEs emerging in mathematical physics, applied mathematics and engineering.

Acknowledgements

The authors would like to express their sincere thanks to the editor and the anonymous reviewers for their helpful comments and suggestions.

Funding

There is no funding for this work.

Availability of data and materials

Not applicable.

Competing interests

The authors declare that they have no competing interests.

Author’s contributions

All authors contributed equally to the writing of this paper. All authors read and approved the final manuscript.

References

[1] A. R. Seadawy, N. Cheemaa, *Applications of extended modified auxiliary equation mapping method for high-order dispersive extended nonlinear Schrödinger equation in nonlinear optics*, Mod. Phys. Lett. B, **33**(18) (2019), 1-11.
[2] F. Düşünceli, E. Çelik, M. Aşkın, H. Bulut, *New exact solutions for the doubly dispersive equation using the improved Bernoulli sub-equation function method*, Indian J. Phys., **95**(2) (2021), 309-314.
[3] S. Chettouh, H. Triki, A. El-Akrmi, Q. Zhou, S. P. Moshokoa, M. Z. Ullah, A. Biswas, M. Belic, *Dipole solitons in an extended nonlinear Schrödinger’s equation with higher-order even and odd terms*, Optik, **145** (2017), 644-649.
[4] M. A. Akbar, N. H. M. Ali, *The improved F-expansion method with Riccati equation and its applications in mathematical physics*, Cogent Math., **4**(1) (2017), 1-19.
[5] S. T. R. Rizvi, K. Ali, M. Ahmad, *Optical solitons for Biswas-Milovic equation by new extended auxiliary equation method*, Optik, **204** (2020), 164181.
[6] M. Tahir, A. U. Awan, *Optical singular and dark solitons with Biswas-Arshed model by modified simple equation method*, Optik, **202** (2020), 163523.
[7] Y. Gürefe, E. Mısırlı, Y. Pandır, A. Sönmezoğlu, M. Ekici, *New exact solutions of the Davey-Stewartson equation with power-law nonlinearity*, Bull. Malays. Math. Sci. Soc., **4** (2015), 1223-1234.

[8] A. Akbulut, M. Kaplan, F. Taşcan, *The investigation of exact solutions of nonlinear partial diferential equations by using* $\exp(-\phi(\xi))$ *method*, Optik, **132** (2017), 382-387.

[9] O. Taşbozan, Y. Çenesiz, A. Kurt, *New solutions for conformable fractional Boussinesq and combined KdV-mKdV equations using Jacobi elliptic function expansion method*, Eur. Phys. J. Plus., **131**(244) (2016), 1-14.

[10] S. Tülüce Demiray, H. Bulut, *New exact solutions for generalized Gardner equation*, Kuwait J. Sci., **44**(1) (2017), 1-8.

[11] S. Tülüce Demiray, H. Bulut, G. Onargan, *An application of generalized* tanh *function method for the sixth-order Boussinesq (sB) equation and (1+1) dimensional dispersive long wave equation*, Appl. Math. Sci., **9**(16) (2015), 773-790.

[12] O. A. İlhan, H. Bulut, T. A. Sulaiman, H. M. Başkonuş, *On the new wave behavior of the Magneto-Electro-Elastic(MEE) circular rod longitudinal wave equation*, Optik, **10**(1) (2020), 1-8.

[13] G. Ebadi, S. Johnson, E. Zerrad, A. Biswas, *Solitons and other nonlinear waves for the perturbed Boussinesq equation with power law nonlinearity*, J. King Saud Univ. Sci., **24**(3) (2012), 237-241.

[14] M. A. Akbar, N. H. M. Ali, T. Tanjim, *Adequate soliton solutions to the perturbed Boussinesq equation and the KdV-Caudrey-Dodd-Gibbon equation*, J. King Saud Univ. Sci., **342**(6) (2020), 2777-2785.

[15] P. Daripa, R. K. Dash, *Weakly non-local solitary wave solutions of a singularly perturbed Boussinesq equation*, Math. Comput. Simul., **55**(4-6) (2002), 393-405.

[16] R. K. Dash, P. Daripa, *Analytical and numerical studies of a singularly perturbed Boussinesq equation*, Appl. Math. Comput., **126**(1) (2002), 1-30.

[17] X. Y. Jiao, *Truncated series solutions to the (2+1)-dimensional perturbed Boussinesq equation by using the approximate symmetry method*, Chin. Phys. B, **27**(10) (2018), 1-7.

[18] S. Tülüce Demiray, U. Bayrakçı, *Soliton Solutions of Generalized Third-Order Nonlinear Schrödinger Equation by Using GKM*, Journal of the Institute of Science and Technology, **11**(2) (2021), 1481-1488.

[19] S. Tülüce Demiray, H. Bulut, *Soliton solutions of some non-linear evolution problems by GKM*, Neural. Comput. Appl., **31** (2019), 287-294.

[20] Y. Pandır, S. Eren, *Exact solutions of the two dimensional KdV-Burger equation by generalized Kudryashov method*, Journal of the Institute of Science and Technology, **11**(1) (2021), 617-624.

[21] S. Tülüce Demiray, H. Bulut, *Generalized Kudryashov method for nonlinear fractional double sinh-poisson equation*, Journal of Nonlinear Science and Applications, **9** (2016), 1349-1355.

[22] S. Tülüce Demiray, U. Bayrakçı, *Construction of soliton solutions for Chaffee-Infante equation*, Afyon Kocatepe University Journal of Science and Engineering, **21**(5) (2021), 1046-1051.

[23] O. Taşbozan, A. Kurt, *The new travelling wave solutions of time fractional Fitzhugh-Nagumo equation with Sine-Gordon expansion method*, ADYU J. Sci., **10**(1) (2020), 256-263.

[24] G. Yel, H. Bulut, E. İlhan, *A new analytical method to the conformable chiral nonlinear Schrödinger equation in the quantum Hall effect*, Pramana, **96** (2022), 54.

[25] K. K. Ali, A. R. Seadawy, A. Yokuş, R. Yılmazer, H. Bulut, *Propagation of dispersive wave solutions for* $(3+1)$*-dimensional nonlinear modified Zakharov-Kuznetsov equation in plasma physics*, Int. J. Mod. Phys. B, **35**(25) (2020), 2050227.

Journal of Mathematical Sciences and Modelling, 5 (3) (2022) 105-112
Research Article

Journal of Mathematical Sciences and Modelling

Journal Homepage: www.dergipark.gov.tr/jmsm
ISSN 2636-8692
DOI: http://dx.doi.org/10.33187/jmsm.1059716

Existence Results for Fractional Integral Equations in Fréchet Spaces

Said Baghdad

Computer Science and Mathematics Laboratory, Ibn khaldoun University of Tiaret, Algeria

Article Info

Keywords: *Fixed-point theorems, Fréchet spaces, Hadamard-Volterra-Stieltjes integral equations, Measure of noncompactness.*
2010 AMS: *26A33, 45G05, 47H08, 47H10*
Received: *18 January 2022*
Accepted: *5 September 2022*
Available online: *1 December 2022*

Abstract

The objective of this paper is to present results on the existence of solutions for a class of fractional integral equations in Fréchet spaces of Banach space-valued functions on the unbounded interval. Our main tool is the technique of measures of noncompactness and fixed points theorems.

1. Introduction

One of the most widely used techniques of proving that certain operator equation has a solution is to reformulate the problem as a fixed point problem and see if the latter can be solved via a fixed point argument. Measures of noncompactness play an important role in fixed point theory and have many applications in various branches of nonlinear analysis, including differential equations, integral and integro-differential equations, optimization, etc. Roughly speaking, a measure of noncompactness is a function defined on the family of all nonempty and bounded subsets of a certain metric space such that it is equal to zero on the whole family of relatively compact sets. This significant concept in mathematical science was defined by many authors in different manners [1,2]. In the last years there appeared many papers devoted to the applications of the measure noncompactness for establish some existence and stability results for various types of nonlinear integral equations [3,4]. In some recent works on this subject, authors utilize a new method of a family of measures of noncompactness and fixed point theorems for condensing operators in Fréchet spaces see [5,6]. The additional advantage of this works is the possibility of extension of the study for several problems to an unbounded domains.

Let us mention that Fréchet spaces have played an important role in functional analysis from its very beginning: Many vector spaces of holomorphic, differentiable or continuous functions which arise in connection with various problems in analysis and its applications are defined by (at most) countably many conditions, whence they carry a natural Fréchet topology (if they are, in addition, complete) [7,8].

This paper is devoted to the study of the following integral equation

$$u(x) = \varphi(x) + \frac{1}{\Gamma(r)} \int_1^x \left(\ln\frac{x}{t}\right)^{r-1} \frac{f(t,u(t))}{t} dg(t);\; x \in J, \tag{1.1}$$

where $J = [1, +\infty)$, $r > 0$, $\varphi : J \to E$ is continuous function, $f : J \times E \to E$, $g : J \to \mathbb{R}$ are given functions, $(E, \|\cdot\|)$ is a Banach space and $\Gamma(\cdot)$ is the Euler gamma function. We investigate the existence of solutions of Eq. (1.1) with an application of the fixed point theorems and the technique of measure of noncompactness under some sufficient conditions.

As we know, fractional calculus have been the focus of many researchers in recent years due to their wide application in various fields of engineering, modeling of natural phenomena, optimal control, and biological mathematics [9–12]. Given the wide application of this branch of mathematics in human life, it makes sense for researchers to spend more time identifying equations that can interpret many physical phenomena and come up with newer and more powerful solutions to them. For this reason, in the last decade, many articles have been

Email address and ORCID number: **said_bg@ymail.com, 0000-0001-7165-670X**

published in the field of ordinary and partial differential equations (see, for example, [13–15]). Let us mention that integral equations of fractional order create an interesting and important branch of the theory of integral equations. The theory of such integral equations is developed intensively in recent years together with the theory of differential equations of fractional order. On the other hand, during the last decades there has been developed the theory of functional integral equations of Stieltjes type. Nevertheless, it turns out that a lot of interesting and important problems which can be formulated inside the theory of Volterra–Stieltjes integral equations are not satisfactory solved by the results obtained up to now [16]. In the theory in question, several types of integral operators, both of linear and nonlinear types are investigated in numerous papers and monographs, we refer [17–19].

2. Preliminaries

This section is devoted to collect some definitions and auxiliary results which will be needed in further considerations.

Definition 2.1 ([20]). *A function $f : J = [a,b] \to \mathbb{R}$ is called of bounded variation if $\bigvee_J f < \infty$, where $\bigvee_J f = \sup \sum_{i=0}^{k} |f(t_{i+1}) - f(t_i)|$, and the supremum is taken over all finite subdivision of J of the forme $a = t_0 < t_1 < t_2 \cdots < t_k = b$.*

Proposition 2.2 ([20]).
- *A function f is of bounded variation on J if and only if f is the difference between two monotone increasing real-valued functions on J.*
- *If f is of bounded variation on J, then f has countable discontinuities in J.*

The Stieltjes integral exists under several conditions, One of the most frequently used requires that f is continuous and g is of bounded variation on J, and the following inequality holds

$$\left| \int_J f(t)dg(t) \right| \leq \int_J |f(t)| \bigvee_J g.$$

Theorem 2.3 ([20]). *Suppose that g is a monotonically increasing function such that g' is Riemann integrable on J and f is continuous on J. Then*

$$\int_a^b f(t)dg(t) = \int_a^b f(t)g'(t)dt.$$

In what follows, we consider the Hadamard-Stieltjes integral of order $q > 0$ for a function u of the form

$$\left({}^{HS}I_1^q u \right)(x) = \frac{1}{\Gamma(q)} \int_1^x \left(\ln \frac{x}{t} \right)^{q-1} \frac{u(t)}{t} dg(t).$$

Lemma 2.4 ([21]). *Assume that the functions $\Phi, \phi_1, \phi_2 : \mathbb{R}_+ \to \mathbb{R}_+$ are continuous functions such that Φ satisfies the following inequality:*

$$\Phi(t) \leq \phi_1(t) + \int_0^t \phi_2(\tau)\Phi(\tau)d\tau;\ t \geq 0,$$

then

$$\Phi(t) \leq \phi_1(t) + \int_0^t \phi_1(\tau)\phi_2(\tau) \exp\left(\int_\tau^t \phi_2(s)ds \right) d\tau;\ t \geq 0.$$

We present now some basic facts concerning measures of noncompactness. If A is a subset of a Fréchet space X then the symbols $\overline{A}$, Conv$A$ stand for the closure and convex hull of A, respectively. Moreover, for any fixed function $h : \mathbb{R}_+ \to (0,\infty)$ let us denote

$$\mathtt{M}_X = \{x \in X;\ \|x(t)\|_E \leq h(t),\ t \in J\},$$

the family of all nonempty and bounded subsets of X and by $\mathtt{N}_X$ its subfamily consisting of all relatively compact sets.
For the Fréchet space we accept the following definition of the family of measures of noncompactness.

Definition 2.5 ([6]). *A family of mappings $\mu_n : M_X \to \mathbb{R}_+$ is said to be a family of measures of noncompactness in the Fréchet space X if it satisfies the following conditions*

1. *The family $ker\{\mu_n\} = \{A \in M_X;\ \mu_n(A) = 0 \text{ for } n \in \mathbb{N}\}$ is nonempty and $ker\{\mu_n\} \subset N_X$.*
2. *$\mu_n(A) \leq \mu_n(B)$ for $A \subset B$, $n \in \mathbb{N}$.*
3. *$\mu_n(ConvA) = \mu_n(A)$ for $n \in \mathbb{N}$.*
4. *If (A_i) is a sequence of closed sets from $\mathtt{M}_X$ such that $A_{i+1} \subset A_i$ $(i = 1,2,\cdots)$ and if $\lim_{i\to\infty} \mu_n(A_i = 0$ for each $n \in \mathbb{N}$, then the intersection set $A_\infty = \bigcap_{i=1}^\infty A_i$ is nonempty.*
5. *$\mu_n(\lambda A) = |\lambda|\mu_n(A)$ for $\lambda \in \mathbb{R}$, $n = 1,2,\cdots$*
6. *$\mu_n(A+B) \leq \mu_n(A) + \mu_n(B)$ for $n = 1,2,\cdots$*
7. *$\mu_n(A \cup B) = \max\{\mu_n(A), \mu_n(B)\}$ for $n = 1,2,\cdots$*

We call the family $\{\mu_n\}_{n\in\mathbb{N}}$ to be *homogeneous*, *subadditive*, *sublinear*, has the *maximum property* if 5., 6., (5.6.), 7. hold respectively.

Definition 2.6. *The family of measures of noncompactness $\{\mu_n\}_{n\in\mathbb{N}}$ is said to be regular if it is full ($ker\{\mu_n\} = N_F$), sublinear and has maximum property.*

Remark 2.7. *In Fréchet space X we can also consider families of measures $\{\mu_T\}_{T\geq 0}$ indexed by nonnegative numbers instead of families $\{\mu_n\}_{n\in\mathbb{N}}$ indexed by natural numbers.*

Theorem 2.8 ([6,22]). *Let Ω be a nonempty, bounded, closed and convex subset of a Fréchet space X and let $L:\Omega\to\Omega$ be a continuous mapping. If L is a contraction with respect to a family of measures of noncompactness $\{\mu_n\}_{n\in\mathbb{N}}$ i.e for each $n\in\mathbb{N}$ and a nonempty $A\subset\Omega$ there exist a constants $k_n\in[0,1)$ such that*

$$\mu_n(L(A))\leq k_n\mu_n(A),$$

then L has at least one fixed point in the set Ω.

The above Theorem is a generalization of the classical Darbo fixed point Theorem for the Fréchet space.

Theorem 2.9 ([23]). *Let Ω be a nonempty, bounded, closed and convex subset of a Hausdorff locally convex space X such that $0\in\Omega$, and let L be a continuous mapping of Ω into itself. If the implication*

$$(V=\text{ conv }L(V)\text{ or }V=L(V)\cup\{0\})\Rightarrow V\text{ is relatively compact},$$

holds for every subset V of Ω, then L has a fixed point.

In the sequel we will work in the space

$$C(J,E)=\{u:J\to E;\ u\text{ is continuous}\},$$

equipped with the family of seminorms

$$\|u\|_n=\sup\{\|u(t)\|;\ t\in[1,n]\},\ n=1,2,\cdots$$

$C(J,E)$ became a Fréchet space.

Proposition 2.10 ([24]).
1. *A nonempty subset $Q\subset C(J,E)$ is said to be bounded if $\sup\{\|x\|_n;\ x\in Q\}<\infty$, $n=1,2,\cdots$*
2. *A sequence (u_n) is convergent to u in $C(J,E)$ if and only if (u_n) is uniformly convergent to u on compact subsets of J.*
3. *A family $Q\subset C(J,E)$ is relatively compact if and only if for each $T>1$, the restriction to $[1,T]$ of all functions from Q form an equicontinuous set and $Q(t)$ is relatively compact in E for each $t\in J$.*

In order to define a measure of noncompactness in the space $C(J,E)$, let us fix a nonempty bounded subset Q of the space $C(J,E)$. For $u\in Q$, $\varepsilon>0$, $t,s\in[1,n]$ such that $|t-s|\leq\varepsilon$, we denote by $\omega_0^n(u,\varepsilon)$ the modulus of continuity of the function u on the interval $[1,n]$ i.e

$$\omega_0^n(u,\varepsilon)=\sup\{\|u(t)-u(s)\|;\ t,s\in[1,n],\ |t-s|\leq\varepsilon\},$$

so

$$\begin{aligned}\omega_0^n(Q,\varepsilon)&=\sup\{\omega_0^n(u,\varepsilon);\ u\in Q\}\\ \omega_0^n(Q)&=\lim_{\varepsilon\to0}\omega_0^n(Q,\varepsilon)\end{aligned}$$

Finally, consider the family $\{\mu_n\}_{n\geq1}$ in $C(J,E)$ defined by the formula

$$\mu_n(Q)=\omega_0^n(Q)+\psi_n(Q);\ Q\in\mathtt{M}_{C(J,E)},\ n=1,2,\cdots,\tag{2.1}$$

where $\psi_n(Q)=\sup\limits_{t\in[1,n]}\psi(Q(t))$ and ψ is a regular measure of noncompactness in the Banach space E.

It can be shown that the family of maps $\{\mu_n\}_{n\geq1}$ is a family of measures of noncompactness in the space $C(J,E)$. The kernel (ker μ_n) consists of nonempty and bounded sets Q such that functions from Q are equicontinuous on compact subsets of J and $Q(t)$ is relatively compact in E for each $t\in J$.

Lemma 2.11 ([24]). *Assume $Q\subset C(J,E)$ is equicontinuous on compact intervals of J and $Q(t)$ is bounded for all $t\in J$. Then*

- *The function $t\mapsto\psi(Q(t))$ is continuous on J.*
- *For each $t\in J$*

$$\psi\left(\int_1^t Q(\tau)d\tau\right)\leq\int_1^t\psi(Q(\tau))d\tau.$$

3. Main results

The equation (1.1) will be considered under the following assumptions :

(H_1) The function f is continuous and there exist two continuous functions $p,q:J\longrightarrow\mathbb{R}_+$ such that

$$\|f(x,u)\|\leq p(x)\|u\|+q(x);\ x\in J;\ u\in E.$$

(H_2) The function g is continuous and of bounded variation on J.

(H_3) For each $A\in\mathtt{M}_E$ and for each $x\in J$, we have

$$\psi(f(x,A))\leq p(x)\psi(A).$$

(H_4) For each $T>1$, there exists a constant $\theta_T>0$ such that

$$\left|\int_1^T\left(\ln\frac{T}{t}\right)^{r-1}dg(t)\right|\leq\theta_T.$$

With

$$k_T=\frac{\theta_T p^*}{\Gamma(r)}<1,$$

where $p^*=\sup\{p(x);\ x\in[1,T]\}$.

Theorem 3.1. *Under the assumptions $(H_1)-(H_4)$ the integral equation (1.1) has at least one solution $u=u(x)$ in the space $C(J,E)$.*

Proof. Consider the operator L on the space $C(J,E)$ defined by

$$(Lu)(x)=\varphi(x)+\frac{1}{\Gamma(r)}\int_1^x\left(\ln\frac{x}{t}\right)^{r-1}\frac{f(t,u(t))}{t}dg(t);\, x\in J,$$

observe that in view of our assumptions, for any function $u\in C(J,E)$ the function Lu is continuous on J. For an arbitrary function $u\in C(J,E)$ and a fixed $x\in J$ we have

$$\begin{aligned}\|Lu(x)\| &= \left\|\varphi(x)+\frac{1}{\Gamma(r)}\int_1^x\left(\ln\frac{x}{t}\right)^{r-1}\frac{f(t,u(t))}{t}dg(t)\right\|\\ &\leq \|\varphi(x)\|+\frac{1}{\Gamma(r)}\int_1^x\left(\ln\frac{x}{t}\right)^{r-1}\|f(t,u(t))\|dg(t)\\ &\leq \|\varphi(x)\|+\frac{1}{\Gamma(r)}\int_1^x\left(\ln\frac{x}{t}\right)^{r-1}[p(t)\|u(t)\|+q(t)]\,dg(t)\\ &\leq m(x)+\frac{1}{\Gamma(r)}\int_1^x\left(\ln\frac{x}{t}\right)^{r-1}p(t)\|u(t)\|dg(t),\end{aligned}$$

where

$$m(x)=\|\varphi(x)\|+\frac{1}{\Gamma(r)}\int_1^x\left(\ln\frac{x}{t}\right)^{r-1}q(t)dg(t).$$

Next, consider the following integral inequality

$$\omega(x)\leq m(x)+\frac{1}{\Gamma(r)}\int_1^x\left(\ln\frac{x}{t}\right)^{r-1}p(t)\omega(x)dg(t).$$

In view of Lemma 2.4, we get

$$\omega(x)\leq m(x)+\frac{1}{\Gamma(r)}\int_1^x\left(\ln\frac{x}{t}\right)^{r-1}p(t)m(t)\exp\left(\int_t^x\left(\ln\frac{x}{s}\right)^{r-1}p(s)ds\right)dg(t).$$

The function

$$\Phi(x)=m(x)+\frac{1}{\Gamma(r)}\int_1^x\left(\ln\frac{x}{t}\right)^{r-1}p(t)m(t)\exp\left(\int_t^x\left(\ln\frac{x}{s}\right)^{r-1}p(s)ds\right)dg(t),$$

is continuous and nonnegative. Observe that the following implication is true :

$$\|u(x)\|\leq\Phi(x)\Rightarrow\|Lu(x)\|\leq\Phi(x);\ \text{for } x\in J.$$

We take the set

$$Q=\Big\{u\in C(J,E);\ \|u(x)\|\leq\Phi(x);\ x\in J\Big\}.$$

We see that Q is nonempty, bounded, closed and convex subset of $C(J,E)$. Moreover, the operator L transforms the set Q into itself. Further, let $T>1$, $x_1,x_2\in[1,T]$ with $x_1<x_2$ and $x_2-x_1<\varepsilon$. For a given $u\in Q$, we have

$$\begin{aligned}\|Lu(x_2)-Lu(x_1)\| &= \left\|\varphi(x_2)+\frac{1}{\Gamma(r)}\int_1^{x_2}\left(\ln\frac{x_2}{t}\right)^{r-1}\frac{f(t,u(t))}{t}dg(t)-\varphi(x_1)-\frac{1}{\Gamma(r)}\int_1^{x_1}\left(\ln\frac{x_1}{t}\right)^{r-1}\frac{f(t,u(t))}{t}dg(t)\right\|\\ &\leq \|\varphi(x_2)-\varphi(x_1)\|+\frac{1}{\Gamma(r)}\left\|\int_1^{x_2}\left(\ln\frac{x_2}{t}\right)^{r-1}f(t,u(t))dg(t)-\int_1^{x_2}\left(\ln\frac{x_1}{t}\right)^{r-1}f(t,u(t))d_tg(x_2,t)\right.\\ &\quad\left.+\int_1^{x_2}\left(\ln\frac{x_1}{t}\right)^{r-1}f(t,u(t))dg(t)-\int_1^{x_1}\left(\ln\frac{x_1}{t}\right)^{r-1}f(t,u(t))dg(t)\right\|\\ &\leq \|\varphi(x_2)-\varphi(x_1)\|+\frac{1}{\Gamma(r)}\int_1^{x_1}[(\ln x_2)^r-(\ln x_1)^r]\,\|f(t,u(t))\|dg(t)+\int_{x_1}^{x_2}\left(\ln\frac{x_1}{t}\right)^{r-1}\|f(t,u(t))\|dg(t)\\ &\leq \|\varphi(x_2)-\varphi(x_1)\|+\frac{p^*\Phi^*+q^*}{\Gamma(r)}\left[\int_1^{x_1}[(\ln x_2)^r-(\ln x_1)^r]\,dg(t)+\int_{x_1}^{x_2}\left(\ln\frac{x_1}{t}\right)^{r-1}dg(t)\right]\\ &= W(T,\varepsilon),\end{aligned}$$

since φ and the logarithm function are locally uniformly continuous, so, $W(T,\varepsilon)\to 0$ when $\varepsilon\to 0$.

Remark 3.2. *In this case, the set Q is the family consisting of functions equicontinuous on compact intervals of J.*

Next, we will show that $L:Q\to Q$ is continuous. Let us fix $T>1$, $\delta>0$ and take $u_0\in Q$. Then, for $x\in[1,T]$ and any function $u\in Q$ such that $\|u(x)-u_0(x)\|<\delta$, we get

$$\begin{aligned}\|Lu(x)-Lu_0(x)\| &= \left\|\frac{1}{\Gamma(r)}\int_1^x\left(\ln\frac{x}{t}\right)^{r-1}\frac{f(t,u(t))}{t}dg(t)-\frac{1}{\Gamma(r)}\int_1^x\left(\ln\frac{x}{t}\right)^{r-1}\frac{f(t,u_0(t))}{t}dg(t)\right\|\\ &\leq \frac{1}{\Gamma(r)}\int_1^x\left(\ln\frac{x}{t}\right)^{r-1}\|f(t,u(t))-f(t,u_0(t))\|dg(t).\end{aligned}$$

Since f is continuous on $[1,T]\times E$, we have $\sup_{x\in[1,T]}\|f(x,u(x))-f(x,u_0(x))\|<\varepsilon(\delta)$ with $\varepsilon(\delta)\to 0$ as $\delta\to 0$. This implies

$$\sup_{x\in[1,T]}\|Lu(x)-Lu_0(x)\|\leq\frac{\theta_T}{\Gamma(r)}\varepsilon(\delta),$$

hence, the operator L is continuous on the set Q.
Further, fix arbitrarily $T>1$ and take a nonempty $\Omega\subset Q$. In view of the assumption (H_3), Remark 3.2 and by Lemma 2.11, we obtain

$$\psi(L\Omega(x)) \quad =\psi\left(\varphi(x)+\frac{1}{\Gamma(r)}\int_1^x\left(\ln\frac{x}{t}\right)^{r-1}\frac{f(t,\Omega(t))}{t}dg(t)\right)\leq\frac{1}{\Gamma(r)}\int_1^x\left(\ln\frac{x}{t}\right)^{r-1}p(t)\psi(\Omega(t))dg(t)\leq\frac{p^*\theta_T}{\Gamma(r)}\psi(\Omega(t)).$$

Thus

$$\psi_n(L\Omega)\leq k_T\psi_n(\Omega). \tag{3.1}$$

Observe, that linking (3.1) and the definition of the family of measure of noncompactness μ_n given by the formula (2.1), we obtain

$$\mu_n(L\Omega)\leq k_T\mu_n(\Omega). \tag{3.2}$$

Finally, in view of the Theorem 2.8 we deduce that L has at least one fixed point in Q which is a solution of Eq. (1.1).

□

In this section, we will give an other result using Mönch's fixed point Theorem.

The Eq. (1.1) will be considered under the following assumptions :

(C_1) The function f is continuous and there exists a continuous function $p:J\longrightarrow\mathbb{R}_+$ such that

$$\|f(x,u)\|\leq p(x);\ x\in J;\ u\in E.$$

(C_2) The function g is continuous and of bounded variation on J.
(C_3) There exists a continuous function $b:J\longrightarrow\mathbb{R}_+$ such that for each $A\in \mathtt{M}_E$ and for each $x\in J$, we have

$$\psi(f(x,A))\leq b(x)\psi(A). \tag{3.3}$$

(C_4) For each $T>1$, there exists a constant $\theta_T>0$ such that

$$\left|\int_1^T\left(\ln\frac{T}{t}\right)^{r-1}dg(t)\right|\leq\theta_T.$$

With

$$k_T=\frac{\theta_T b^*}{\Gamma(r)}<1,$$

where $b^*=\sup\{b(x);\ x\in[1,T]\}$.

Theorem 3.3. *Suppose the hypotheses $(C_1)-(C_4)$ are satisfied. Then Eq. (1.1) has at least one solution $u=u(x)$ in the space $C(J,E)$.*

Proof. Consider the operator L on the space $C(J,E)$ defined by

$$(Lu)(x)=\varphi(x)+\frac{1}{\Gamma(r)}\int_1^x\left(\ln\frac{x}{t}\right)^{r-1}\frac{f(t,u(t))}{t}dg(t);\ x\in J,$$

observe that in view of our assumptions, for any function $u\in C(J,E)$ the function Lu is continuous on J. For an arbitrary function $u\in C(J,E)$ and a fixed $x\in J$ we have

$$\begin{aligned}\|Lu(x)\| &= \left\|\varphi(x)+\frac{1}{\Gamma(r)}\int_1^x\left(\ln\frac{x}{t}\right)^{r-1}\frac{f(t,u(t))}{t}dg(t)\right\|\\ &\leq \|\varphi(x)\|+\frac{1}{\Gamma(r)}\int_1^x\left(\ln\frac{x}{t}\right)^{r-1}\|f(t,u(t))\|dg(t)\\ &\leq \|\varphi(x)\|+\frac{1}{\Gamma(r)}\int_1^x\left(\ln\frac{x}{t}\right)^{r-1}p(x)dg(t),\end{aligned}$$

hence, for $x\in[1,n]$ we infer that

$$\|Lu\|_n=\|\varphi\|_n+\frac{\theta_n p^*}{\Gamma(r)}.$$

Further, let $T>1$, $x_1,x_2\in[1,T]$ with $x_1<x_2$ and $x_2-x_1<\varepsilon$. For a given $u\in C(J,E)$, we have

$$\begin{aligned}
\|Lu(x_2)-Lu(x_1)\| &= \left\|\varphi(x_2)+\frac{1}{\Gamma(r)}\int_1^{x_2}\left(\ln\frac{x_2}{t}\right)^{r-1}\frac{f(t,u(t))}{t}dg(t)-\varphi(x_1)-\frac{1}{\Gamma(r)}\int_1^{x_1}\left(\ln\frac{x_1}{t}\right)^{r-1}\frac{f(t,u(t))}{t}dg(t)\right\| \\
&\leq \|\varphi(x_2)-\varphi(x_1)\|+\frac{1}{\Gamma(r)}\left\|\int_1^{x_2}\left(\ln\frac{x_2}{t}\right)^{r-1}f(t,u(t))dg(t)-\int_1^{x_2}\left(\ln\frac{x_1}{t}\right)^{r-1}f(t,u(t))dg(t)\right. \\
&\quad \left.+\int_1^{x_2}\left(\ln\frac{x_1}{t}\right)^{r-1}f(t,u(t))dg(t)-\int_1^{x_1}\left(\ln\frac{x_1}{t}\right)^{r-1}f(t,u(t))dg(t)\right\| \\
&\leq \|\varphi(x_2)-\varphi(x_1)\|+\frac{1}{\Gamma(r)}\int_1^{x_1}[(\ln x_2)^r-(\ln x_1)^r]\,p(t)dg(t)+\int_{x_1}^{x_2}\left(\ln\frac{x_1}{t}\right)^{r-1}p(t)dg(t) \\
&\leq \|\varphi(x_2)-\varphi(x_1)\|+\frac{p^*}{\Gamma(r)}\left[\int_1^{x_1}[(\ln x_2)^r-(\ln x_1)^r]\,dg(t)+\int_{x_1}^{x_2}\left(\ln\frac{x_1}{t}\right)^{r-1}dg(t)\right] \\
&\leq W(T,\varepsilon),
\end{aligned}$$

We take the set

$$D=\left\{u\in C(J,E);\ \|u\|_n\leq l_n=\|\varphi\|_n+\frac{\theta_n p^*}{\Gamma(r)};\ \text{and}\ \omega_0^n(u,\varepsilon)\leq W(T,\varepsilon);\ n\leq T\right\}.$$

Obviously D is nonempty, bounded, closed and convex subset of $C(J,E)$ and the operator L transforms the set D into itself. Moreover, the set D is the family consisting of functions equicontinuous on compact intervals of J.
Now, we show that L is continuous on the set D. Let $(u_n)_n\subset D$ be a sequence converging to u in D i.e

$$\lim_{n\to\infty}\sup_{1\leq t\leq T}\|u_n(t)-u(t)\|=0;\ T>1.$$

Then we get

$$\begin{aligned}
\sup_{1\leq t\leq T}\|(Lu_n)(x)-(Lu)(x)\| &\leq \frac{1}{\Gamma(r)}\sup_{1\leq x\leq T}\int_1^x\left(\ln\frac{x}{t}\right)^{r-1}\|f(t,u_n(t))-f(t,u(t))\|\times dg(t) \\
&\leq \frac{\theta_T}{\Gamma(r)}\sup_{1\leq t\leq T}\|f(t,u_n(t))-f(t,u(t))\|,
\end{aligned}$$

so

$$\lim_{n\to\infty}\sup_{1\leq t\leq T}\|(Lu_n)(x)-(Lu)(x)\|\leq\frac{\theta_T}{\Gamma(r)}\lim_{n\to\infty}\sup_{1\leq t\leq T}\|f(t,u_n(t))-f(t,u(t))\|.$$

Since f is continuous on $[1,T]\times E$, we obtain

$$\lim_{n\to\infty}\sup_{1\leq t\leq T}\|(Lu_n)(x)-(Lu)(x)\|=0,$$

hence the operator L is continuous on the set D.

Further, let $V\subset D$ such that $V=L(V)\cup\{0\}$, fix $x\in[1,T]$ and using our assumptions we arrive at the following estimates

$$\begin{aligned}
\psi(LV(x)) &= \psi\left(\varphi(x)+\frac{1}{\Gamma(r)}\int_1^x\left(\ln\frac{x}{t}\right)^{r-1}\frac{f(t,V(t))}{t}dg(t)\right) \\
&\leq \frac{1}{\Gamma(r)}\int_1^x\left(\ln\frac{x}{t}\right)^{r-1}\psi(f(t,V(t)))dg(t) \\
&\leq \frac{1}{\Gamma(r)}\int_1^x\left(\ln\frac{x}{t}\right)^{r-1}b(t)\psi(V(t))dg(t) \\
&\leq \frac{b^*\theta_T}{\Gamma(r)}\sup_{x\in[1,T]}\psi(V(x)),
\end{aligned}$$

thus

$$\sup_{x\in[1,T]}\psi(V(x))\leq k_T\sup_{x\in[1,T]}\psi(V(x)).$$

Since for each $T>1$ we have $k_T<1$, we deduce that

$$\sup_{x\in[1,T]}\psi(V(x))=0.$$

Hence, $V(x)$ is relatively compact in E for each $x\in[1,T]$, and from the choice of the set D, we conclude that V is relatively compact in $C(J,E)$ (in view of proposition 2.10). Combining with Theorem 2.9 we complete the proof.

□

4. Example

Let $E = l^{\infty}$ be the space of all bounded sequences $(w_p)_{p\in\mathbb{N}}$ of real numbers endowed with the norm

$$\|w\|_{\infty} = \max_{p\in\mathbb{N}} |w_p|;\ w \in E.$$

We consider an infinite system of fractional integral equations

$$u_p(z) = \frac{z+p}{z^2+2p} + \frac{1}{\Gamma(r)} \int_1^z \left(\ln\frac{z}{t}\right)^{r-1} \frac{\sqrt{e^{-2t}u_p^2(t) + \frac{1}{pt}}}{t}\, d\left(\frac{1}{t} - \frac{1}{t^2}\right);\ p \in \mathbb{N};\ r > 1. \tag{4.1}$$

It is clear that equation (4.1) can be written as equation (1.1), where

$$\begin{array}{rcl} u : J = [1,\infty) & \to & l^{\infty} \\ z & \mapsto & (u_p(z))_{p\in\mathbb{N}}, \end{array}$$

Set

$$\varphi(z) = (\varphi_p(z))_{p\in\mathbb{N}} = \frac{z+p}{z^2+2p}; \quad g(t) = \frac{1}{t} - \frac{1}{t^2},$$

$$f(z,u(z)) = (f_p(z,u_p(z)))_{p\in\mathbb{N}} = \sqrt{e^{-2z}u_p^2(z) + \frac{1}{pz}}.$$

Remark 4.1. *We can see that for each $u(z) \in l^{\infty}$ and $z \in J$ we have $(f_p(z,u_p(z)))_{p\in\mathbb{N}} \in l^{\infty}$, so, the function $f : J \times l^{\infty} \to l^{\infty}$ is well defined.*

Let us show that conditions $(H_1)-(H_4)$ hold. The function $t \mapsto \dfrac{1}{t} - \dfrac{1}{t^2}$ is continuous on J, increasing on $[1,2]$ and decreasing on $[2,\infty)$. Moreover, we have

$$\lim_{t\to+\infty}\left(\frac{1}{t} - \frac{1}{t^2}\right) = 0.$$

So it is of bounded variation on J. It follows that

$$\begin{aligned} \left|f_p(z,u_p(z))\right| &= \sqrt{e^{-2z}u_p^2(z) + pz} \\ &\leq \sqrt{e^{-2z}u_p^2(z)} + \sqrt{\frac{1}{pz}} \\ &\leq e^{-z}|v_p(z)| + \sqrt{\frac{1}{pz}}, \end{aligned}$$

thus

$$\sup_{p\in\mathbb{N}} \left|f_p(z,u_p(z))\right| \leq e^{-z} \sup_{p\in\mathbb{N}} |v_p(z)| + \sqrt{\frac{1}{pz}}.$$

Then

$$\|f(z,u(z))\|_{\infty} \leq e^{-z}\|u(z)\|_{\infty} + \sqrt{\frac{1}{pz}}. \tag{4.2}$$

So $p(z) = e^{-z}$; $\quad p^* = \frac{1}{e}$; $\quad q(z) = \sqrt{\frac{1}{pz}}$ and for a fixed $T > 1$ we have

$$\begin{aligned} \left|\int_1^T \left(\ln\frac{T}{t}\right)^{r-1} d\left(\frac{1}{t} - \frac{1}{t^2}\right)\right| &\leq (\ln T)^r \left|\int_1^T d\left(\frac{1}{t} - \frac{1}{t^2}\right)\right| \\ &\leq (\ln T)^r \left(\frac{1}{T} - \frac{1}{T^2}\right) \\ &= \theta_T. \end{aligned}$$

Observe that

$$k = \frac{\theta_T p^*}{\Gamma(r)} = \frac{(\ln T)^r (T-1)}{eT^2\Gamma(r)} < 1;\ \text{for each } T > 1.$$

In view of (4.2), we deduce that

$$\psi(f(t,A)) \leq e^{-t}\psi(A);\ \text{for each } A \in \mathtt{M}_E.$$

Consequently from Theorem 3.1 the Eq. (4.1) has at least solution in $C(J,E)$.

5. Conclusion

In this work, we have presented an existence result for a type of integral equation by application of MNCs and the fixed point theorems. The interest of this work is the possibility of dealing with several nonlinear problems on unbounded domains, on the other hand, we have given an illustrative example which indicates the applicability of this study to deal with an infinite system of integral equations. Some of the results in this direction are our future plan especially the choice of MNCs which allows us to characterize the qualitative aspect of the solutions.

Acknowledgements

The authors would like to express their sincere thanks to the editor and the anonymous reviewers for their helpful comments and suggestions.

Funding

There is no funding for this work.

Availability of data and materials

Not applicable.

Competing interests

The authors declare that they have no competing interests.

Author's contributions

All authors contributed equally to the writing of this paper. All authors read and approved the final manuscript.

References

[1] J. Banaś, K. Geobel, *Measures of Noncompactness in Banach Spaces*, Lecture Notes in Pure and Appl. Math., 60, Marcel Dekker, New York and Basel, 1980.
[2] M. Mursaleen, Syed M. H. Rizvi, B. Samet, *Measures of Noncompactness and their Applications*, *Advances in Nonlinear Analysis via the Concept of Measure of Noncompactness,* 59-125, Springer, Singapore, 2017.
[3] S. Baghdad, *Existence and stability of solutions for a system of quadratic integral equations in Banach algebras*, Ann. Univ. Paedagog. Crac. Stud. Math., **19** (2020), 203-218.
[4] S. Baghdad, M. Benchohra, *Global existence and stability results for Hadamard-Volterra-Stieltjes integral equation*, Commun. Fac. Sci. Univ. Ank. Ser. A1. Math. Stat., **68**(2) (2019), 1387-1400.
[5] M. Benchohra, M. A. Darwish, *On quadratic integral equations of Urysohn type in Fréchet spaces*, Acta Math. Univ. Comenian. (N.S.), **79**(1) (2010), 105-110.
[6] L. Olszowy, *Fixed point theorems in the Fréchet space $C(\mathbb{R}_+)$ and functional integral equations on an unbounded interval*, Appl. Math. Comput. **218**(18) (2012), 9066-9074.
[7] K. D. Bierstedt, J. Bonet, *Some aspects of the modern theory of Fréchet spaces*, RACSAM. Rev. R. Acad. Cienc. Exactas Fís. Nat. Ser. A Mat., **97**(2) (2003), 159-188.
[8] V. Dietmar, *Lectures on Fréchet Spaces*, Bergische Universität Wuppertal Sommersemester, 2000.
[9] D. Baleanu, A. Jajarmi, H. Mohammadi, S. Rezapour, *A new study on the mathematical modelling of human liver with Caputo-Fabrizio fractional derivative*, Chaos Solitons Fractals, **134** (2020), 109705.
[10] A. A. Kilbas, H. M. Srivastava, J. J. Trujillo, *Theory and Applications of Fractional Differential Equations*, North-Holland Mathematics Studies, 204, Elsevier Science B.V., Amsterdam, 2006.
[11] H. Mohammadi, S. Kumar, S. Rezapour; S. Etemad, A theoretical study of the Caputo-Fabrizio fractional modeling for hearing loss due to Mumps virus with optimal control, Chaos Solitons Fractals, **144** (2021), 110668.
[12] Y.-M. Chu, S. Rashid, F. Jarad, M. A. Noor, H. Kalsoom, *More new results on integral inequalities for generalized $\mathscr{K}$-fractional conformable integral operators*, *Discrete Contin. Dyn. Syst. Ser. S* **14**(7) (2021), 2119-2135.
[13] S. Abbas, M. Benchohra, G. M. N'Guérékata *Advanced Fractional Differential and Integral Equations*, Nova Science Publishers, New York, 2015.
[14] D. Baleanu, S. Etemad, S. Rezapour, *A hybrid Caputo fractional modeling for thermostat with hybrid boundary value conditions*, Bound. Value Probl., **2020**(1) (2020), Article number: 64, 16 pages.
[15] P. O. Mohammed, T. Abdeljawad, F. Jarad, Y. M. Chu, *Existence and uniqueness of uncertain fractional backward difference equations of Riemann-Liouville type*, Math. Probl. Eng., 2020 (2020), Article ID: 6598682, 8 pages.
[16] J. Banaś; T. Zając, *A new approach to the theory of functional integral equations of fractional order*, J. Math. Anal. Appl., **375**(2) (2011), 375-387.
[17] S. Abbas, M. Benchohra, J. Henderson, *Asymptotic behavior of solutions of nonlinear fractional order Riemann-Liouville Volterra-Stieltjes quadratic integral equations*, Int. Elect. J. Pure Appl. Math., **4**(3) (2012), 195-209.
[18] S. Abbas, M. Benchohra, J. J. Nieto, *Global attractivity of solutions for nonlinear fractional order Riemann-Liouville Volterra-Stieltjes partial integral equations*, Electron. J. Qual. Theory Differ. Equ., **81** (2012), 1-15.
[19] S. Samko, A. Kilbas, O. I. Marichev, *Fractional Integrals and Derivatives (Theorie and Applications)*, Gordon and Breach Science Publishers, Yverdon, 1993.
[20] I. P. Natanson, *Theory of Functions of a Real Variable*, Ungar, New York, 1960.
[21] B. G. Pachpatte, *Inequalities for Differential and Integral Equations*, William F. Ames, Georgia Institute of Technology, 1998.
[22] L. Olszowy, S. Dudek, *On generalization of Darbo-Sadovskii type fixed point theorems for iterated mappings in Fréchet spaces*, J. Fixed Point Theory Appl., **20**(4) (2018), Article number: 146, 12 pages.
[23] J. Daneš, *Some fixed point theorems*, Comment. Math. Univ. Carolinae, **9** (1968), 223-235.
[24] F. Wang, H. Zhou, *Fixed point theorems in locally convex spaces and a nonlinear integral equation of mixed type*, Fixed Point Theory Appl., **2015**(1) (2015), Article number: 228228, 11 pages.

Journal of Mathematical Sciences and Modelling, 5 (3) (2022) 113-124
Research Article

Journal of Mathematical Sciences and Modelling

Journal Homepage: www.dergipark.gov.tr/jmsm
ISSN 2636-8692
DOI: http://dx.doi.org/10.33187/jmsm.1115792

Comparison of Recent Meta-Heuristic Optimization Algorithms Using Different Benchmark Functions

Mahmut Dirik

Sirnak University, Department of Computer Engineering, Turkey

Article Info

Keywords: *Benchmark test function, Bio-inspired, Global optimization, Meta-heuristics, Optimization*
2010 AMS: *65Yxx, 65D15*
Received: *12 May 2022*
Accepted: *20 October 2022*
Available online: *1 December 2022*

Abstract

Meta-heuristic optimization algorithms are used in many application areas to solve optimization problems. In recent years, meta-heuristic optimization algorithms have gained importance over deterministic search algorithms in solving optimization problems. However, none of the techniques are equally effective in solving all optimization problems. Therefore, researchers have focused on either improving current meta-heuristic optimization techniques or developing new ones. Many alternative meta-heuristic algorithms inspired by nature have been developed to solve complex optimization problems. It is important to compare the performances of the developed algorithms through statistical analysis and determine the better algorithm. This paper compares the performances of sixteen meta-heuristic optimization algorithms (AWDA, MAO, TSA, TSO, ESMA, DOA, LHHO, DSSA, LSMA, AOSMA, AGWOCS, CDDO, GEO, BES, LFD, HHO) presented in the literature between 2021 and 2022. In this context, various test functions, including single-mode, multi-mode, and fixed-size multi-mode benchmark functions, were used to evaluate the efficiency of the algorithms used.

1. Introduction

Optimization has received more attention in recent years, and various new optimization methods have been developed [1–15].These newly discovered techniques are applied to real-world challenges. An optimization problem is about finding the optimal answer from a collection of possible solutions. The main goal of optimization is to find selection variables that lead to the minimization or maximization of an objective function. These problems are classified as constrained or unconstrained, discrete or continuous, static or dynamic, and single-or multi-objective. Most real-world problems are nonlinear, incur significant computational costs, and have many complicated solution spaces. For this reason, several researchers have proposed optimization techniques to solve these problems, often referred to as mathematical programming approaches or meta-heuristic methods. Therefore, solving problems with a large number of variables and constraints is very challenging. Since most traditional optimization techniques are based on classical mathematical and probabilistic assumptions, they are not able to provide useful answers to the increasingly complicated optimization problems of recent years. Often, basic optimization problems can be effectively solved using traditional optimization approaches such as mathematical programming. However, solving real-world engineering optimization problems using classical optimization methods is very difficult. Therefore, several researchers [16–24] have proposed novel solution strategies, called meta-heuristic algorithms, to solve difficult optimization problems within reasonable time and cost. Most conventional optimization approaches are based on classical mathematics and probabilistic assumptions that cannot provide useful answers to emerging, complicated optimization problems. Meta-heuristics, which have gained popularity among researchers due to their numerous advantages over conventional optimization strategies, have a number of advantages over conventional optimization strategies, including their simplicity, non-differentiation, adaptability, and avoidance of local optima [25]. The main advantage of these techniques over conventional optimization methods is that they are able to solve optimization problems without requiring gradient information. Moreover, they can be adapted to a variety of working situations. The efficiency and effectiveness of meta-heuristic optimization algorithms in addressing known constrained mathematical and engineering design problems is one of their main advantages. Evolutionary algorithms, physics-based algorithms, swarm intelligence algorithms, and human-based algorithms are the four types of meta-heuristic algorithms [26,27]. Table 1.1 shows some of the optimization algorithms presented in the literature between 2021 and 2022 that were investigated in this study.

Email address and ORCID number: **mhmd.dirik@gmail.com, 0000-0003-1718-5075**

Algorithms	Year
Artificial Water Drop Algorithm (AWDA) [28]	2022
Mexican Axolotl Optimization (MAO) [3]	2022
Tunicate Swarm Algorithm (TSA) [2]	2022
Tuna Swarm Optimization (TSO) [1, 8]	2022
Equilibrium Slime Mould Algorithm (ESMA) [8, 26]	2021
Dingo Optimization Algorithm (DOA) [29]	2021
Leader Harris hawks optimization (LHHO) [5, 30]	2021
Differential Squirrel Search Algorithm (DSSA) [9, 10]	2021
Leader Slime Mould Algorithm (LSMA) [31]	2021
Adaptive Opposition Slime Mould Algorithm (AOSMA) [32]	2021
Hybrid Augmented Grey Wolf Optimizer & Cuckoo Search (AGWOCS) [33, 34]	2021
Child Drawing Development Optimization Algorithm (CDDO) [34]	2021
Golden Eagle Optimizer (GEO) [35]	2021
Bald eagle search Optimization algorithm (BES) [14]	2021
Lévy Flight Distribution (LFD) [6]	2021
Harris hawks optimization (HHO) [36]	2021

Table 1.1: Optimization algorithms

In this study, the performance of some meta-heuristic algorithms, listed in Table 1.1, was evaluated using a series of test functions. These are meta-heuristic algorithms inspired by the behavior of natural organisms. Meta-optimization is the process of optimizing the performance of an algorithm by changing its parameters. This strategy not only increases the efficiency of the algorithm, but also allows us to better understand how the algorithm responds to different types of challenges. These techniques fall into two broad categories: offline and online. Offline techniques specify the parameter settings of the algorithm before execution and work with a training set as an example. Offline approaches work well when the selected examples have the same structure as the other examples in the training set. However, these approaches may fail if the class of instances is heterogeneous. This is because finding the appropriate parameter settings for each class of instances takes a lot of time in this case. Online approaches, on the other hand, collect feedback and try to determine the optimal parameter values while the algorithm is solving a problem scenario. These approaches reduce computation time by trying to find the parameter settings while the algorithm is running. Although several optimization methods have been proposed in the literature, no algorithm is able to provide the optimal answer to all optimization questions [37]. As a result, the established optimization techniques and the field of new meta-heuristic optimization algorithms are constantly being improved through innovations and further developments. By evaluating the success of newly developed meta-heuristic optimization algorithms and comparing them with previously published algorithms, new studies on improving existing optimization algorithms or developing new optimization algorithms based on successful algorithms are added to the literature on a daily basis. In this context, Artificial Water Drop Algorithm [28], Mexican Axolotl Optimization: a novel bio-inspired heuristic [3], Tunicate Swarm Algorithm [2], Tuna Swarm Optimization [1, 8], Equilibrium Slime Mould Algorithm [8, 26], Dingo Optimization Algorithm [29], Leader Harris hawks optimization [5], Differential Squirrel Search Algorithm [9, 10], Leader Slime Mould Algorithm [31], Adaptive Opposition Slime Mould Algorithm [32], CLA- New Meta-Heuristic Algorithm [38], Hybrid Augmented Grey Wolf Optimizer and Cuckoo Search [33, 34], Child Drawing Development Optimization Algorithm [34], Golden Eagle Optimizer [35], Bald eagle search Optimization algorithm [14], Chimp Optimization Algorithm [39], Lévy Flight Distribution [6] and Harris hawks optimization [36] are some of them. This paper compares the performances of sixteen meta-heuristic optimization algorithms presented in the literature between 2021 and 2022. Various test functions, including single-modal, multi-modal and fixed-size multi-modal comparison functions, have been used to evaluate the effectiveness of the algorithms used in this context.
The rest of the article is structured as follows: Section 2 describes the methodology and mathematical framework of the benchmark functions; Section 3 presents the experimental results. Finally, section 4 presents the conclusion.

2. Methodology

An important aspect of testing and validating a new algorithm is comparing it to existing algorithms that use benchmark functions. This type of bench-marking is also crucial to better understand the advantages and weaknesses of the algorithm. Typically, the new technique is evaluated against a set of test functions that ideally have different properties such as mode shapes. However, these bench-marking methods suffer from a crucial weakness. Although it is a comparative function, it is rarely used in practice. There are several reasons for this. While real-world scenarios are much more complex and different than these test items, an explanation is usually well thought out and concise. Another problem is that these test functions often use unconstrained or regular fields, whereas in the real world, non-linear, complex constraints often apply, and the field may contain multiple isolated partitions or islands. The functions used to compare the performances of the algorithms discussed here are detailed below.

2.1. Mathematical framework of benchmark functions

The following functions are among the most used for evaluating optimization strategies. They are categorized based on their basic physical properties and shapes (see Table 1.1). Uni-modal, Multi-modal and Fixed-dimension multi-modal benchmark test functions were used in this study. In Table 2.1, D indicates the size of the function, Range is the variation range of the optimization variable, and F_{min} is the minimum. Twenty-three test functions were used to evaluate the performance of the sixteen algorithms considered in this study. Figure 2.1, Figure 2.2, and Figure 2.3 show two-dimensional (2D) views of the different functions.

	Function	D	Range	F_{min}
Uni-modal	$F_1(X)=\sum_{i=1}^{n} x_i^2$	30	[-100, 100]	0
	$F_2(X)=\sum_{i=1}^{n}\lvert X_i\rvert+\prod_{i=1}^{n}\lvert X_i\rvert$	30	[-10, 10]	0
	$F_3(X)=\sum_{i=1}^{n}\left(\sum_{j-1}^{1} x_i\right)^2$	30	[-100, 100]	0
	$F_4(X)=\max_i\left(\lvert x_i\rvert .1\leq i\leq n\,\right\rvert$	30	[-30, 30]	0
	$F_5(X)=\sum_{i=1}^{n-1}\left[100\left(x_{i+1}-x_i^2\right)^2+\left(x_i-1\right)^2\right]$	30	[-100, 100]	0
	$F_6(X)=\sum_{i=1}^{n}\left([x_i+0.5]\right)^2$	30	[-100, 100]	0
	$F_7(X)=\sum_{i=1}^{n} ix_i^4+\text{random}[0.1)$	30	[-1.28, 1.28]	0
Multi-modal	$\mathrm{F}_8(\mathrm{x})=\sum_{i=1}^{n}-\mathrm{x}_i\sin\left(\sqrt{\lvert\mathrm{x}_i\rvert}\right)-418.9829\times d$	30	[-500, 500]	-418.9829xd
	$F_9(x)=\sum_{i=1}^{n}\left[x_i^2-10\cos\left(2\pi x_i\right)+10\right]$	30	[-5.12, 5.12]	0
	$F_{10}(x)=-20\exp\left(-0.2\sqrt{\frac{1}{n}\sum_{i=1}^{n}x_i^2}\right)-\exp\left(\frac{1}{n}\sum_{i=1}^{n}\cos\left(2\pi x_i\right)\right)+20+e$	30	[-32, 32]	0
	$F_{11}(x)-\frac{1}{4000}\sum_{i=1}^{n}x_i^2-\prod_{i=1}^{n}\cos\left(\frac{x_i}{\sqrt{i}}\right)+1$	30	[-600, 600]	0
	$F_{12}(x)=\frac{\pi}{n}\left\{10\sin\left(\pi y_1\right)+\sum_{i=1}^{n-1}\left(y_i-1\right)^2\left[1+10\sin 2\left(\pi y_{i+1}\right)\right]+\left(y_n-1\right)^2\right\}$ $+\sum_{i=1}^{n}u\left(x_i,10,100,4\right)$	30	[-50, 50]	0
	$y_i=1+\frac{x_i+1}{4}\times u(x_i,a,k,m)=\begin{cases}k\left(x_i-a\right)^m x_i>a\\ 0-a<x_i<a\\ k(-x_i-a)^m x_i<-a\end{cases}$			
	$F_{13}(x)=0.1\mid\sin 2\left(3\pi x_1\right)+\sum_{i=1}^{n}\left(x_i-1\right)^2\left[1+\sin 2\left(3\pi x_i+1\right)\right]$ $+\left(x_n-1\right)^2\left[1+\sin 2\left(2\pi x_n\right)\mid l+\sum_{i=1}^{n}u\left(x_1,5,100,4\right)\right.$	30	[-50, 50]	0
Fixed-dimension multi-modal	$F_{14}(x)=\left(\frac{1}{500}+\sum_{j=1}^{25}\frac{1}{j+\sum\left(x_i-a_j\right)^6}\right)^{-1}$	2	[-65, 65]	0.998
	$F_{15}(x)=\sum_{i=1}^{11}\left[a_i-\frac{x_1\left(b_1^2+b_1x_2\right)}{b_i^2+b_1x_3+x_4}\right]^2$	4	[-5,5]	0.00030
	$F_{16}(x)=4x_1^2-2.1x_1^4+\frac{1}{3}x_1^6+x_1x_2-4x_2^2+4x_2^4$	2	[-5, 5]	-1.0316
	$F_{17}(x)=\left(x_2-\frac{5.1}{4\pi^2}x_1^3+\frac{5}{\pi}x_1-6\right)^3+10\left(1-\frac{1}{8\pi}\right)\cos x_1+10$	2	[-5,5]	0.398
	$F_{18}(x)=\left[1+\left(x_1+x_2+1\right)^2\left(19-14x_1+3x_1^2-14x_2+6x_1x_2+3x_2^2\right)\right]$ $\times\left[30+\left(2x_1-3x_2\right)^2\times\left(18-32x_1+12x_1^2+48x_2+36x_1x_2+27x_2^2\right)\right]$	2	[-2, 2]	3
	$\mathrm{F}_{19}(\mathrm{x})=-\sum_{i=1}^{4}\mathrm{c}_i\exp\left(-\sum_{i=1}^{3}\mathrm{a}_{ij}\left(\mathrm{x}_j-\mathrm{p}_{ij}\right)^2\right)$	3	[1,3]	-3.86
	$\mathrm{F}_{20}(\mathrm{x})=-\sum_{i=1}^{4}\mathrm{c}_i\exp\left(-\sum_{i=1}^{5}\mathrm{a}_{ij}\left(x_j-\mathrm{p}_{ij}\right)^2\right)$	6	[0,1]	-3.32
	$\mathrm{F}_{21}(\mathrm{x})=-\sum_{i=1}^{5}\left[\left(\mathrm{X}-\mathrm{a}_i\right)\left(\mathrm{X}-\mathrm{a}_i\right)^{\mathrm{T}}+\mathrm{c}_i\right]^{-1}$	4	[0,10]	-10.1532
	$\mathrm{F}_{22}(\mathrm{x})=-\sum_{i=1}^{7}\left[\left(\mathrm{X}-\mathrm{a}_i\right)\left(\mathrm{X}-\mathrm{a}_i\right)^{\mathrm{T}}+\mathrm{c}_i\right]^{-1}$	4	[0,10]	-10.4028
	$\mathrm{F}_{23}(\mathrm{x})=-\sum_{i=1}^{10}\left[\left(\mathrm{X}-\mathrm{a}_i\right)\left(\mathrm{X}-\mathrm{a}_i\right)^{\mathrm{T}}+\mathrm{c}_i\right]^{-1}$	4	[0,10]	-10.5363

Table 2.1: A mixture of uni-modal, multi-modal, and fixed-dimension multi-modal benchmark functions.

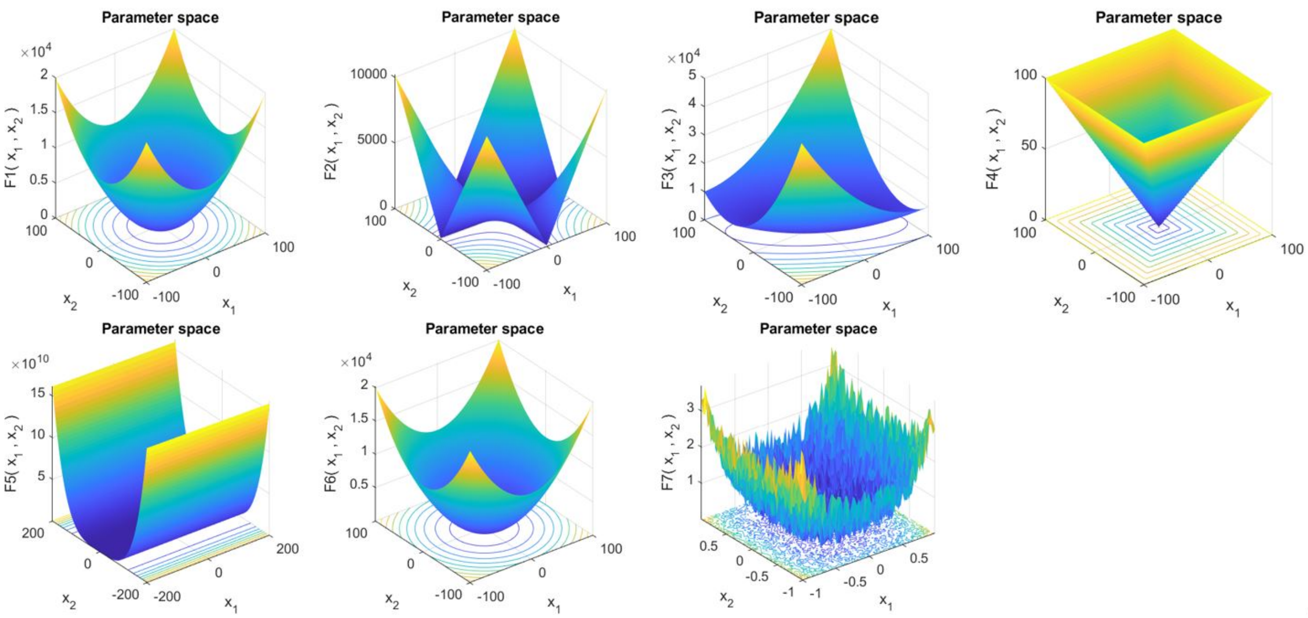

Figure 2.1: 2-D version of uni-modal benchmark function.

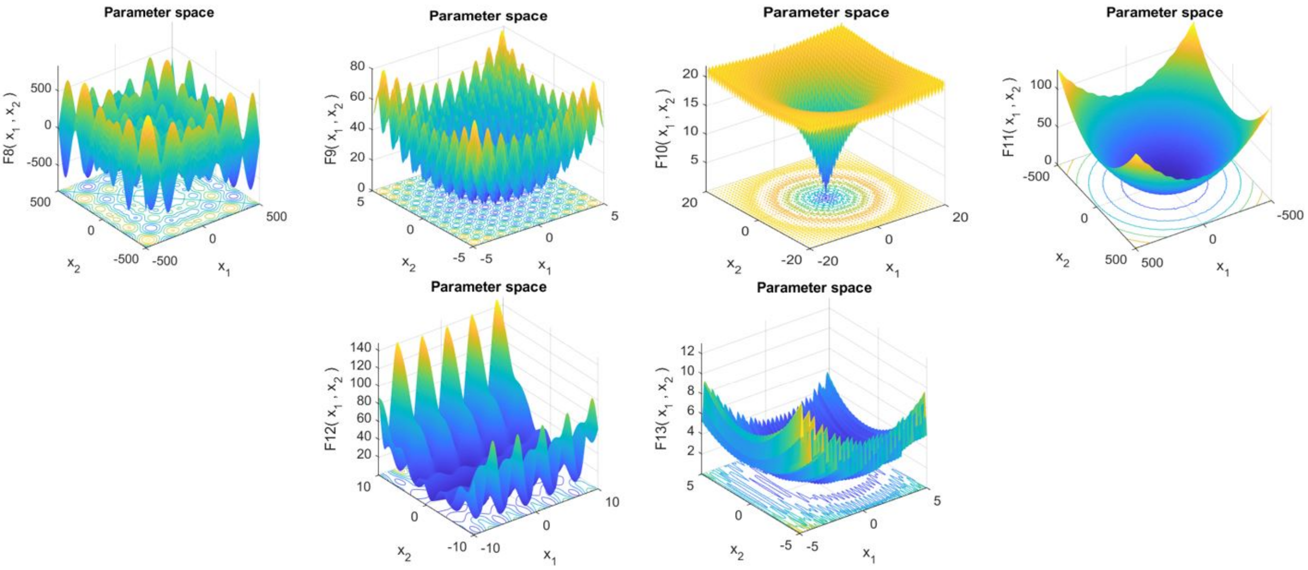

Figure 2.2: 2-D version of multi-modal benchmark function

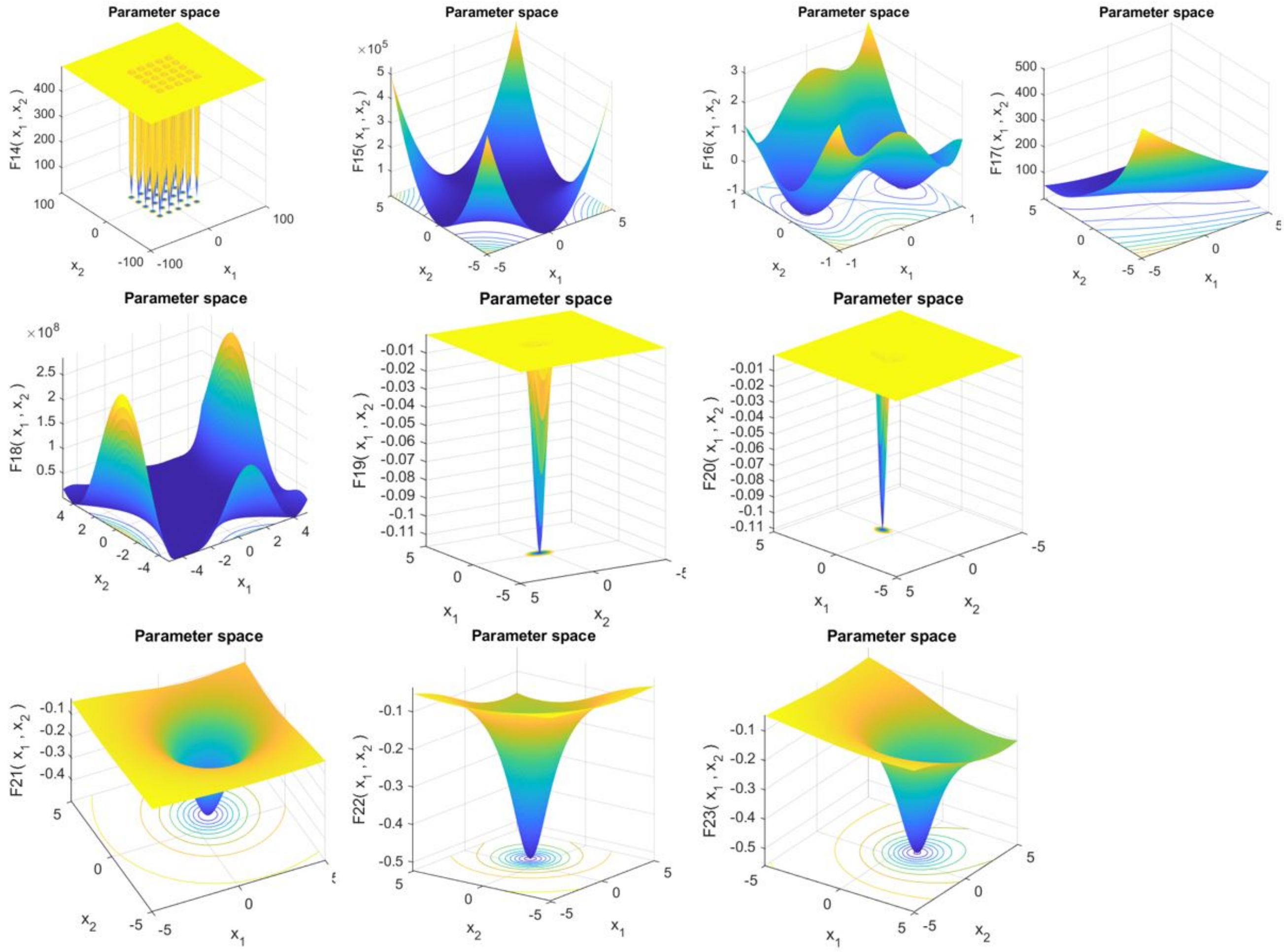

Figure 2.3: 2-D version of fixed-dimension multi-modal benchmark function

3. Experimental Results

In this section, we demonstrate the effectiveness of the algorithm used for 23 commonly used uni-modal, multi-modal and fixed-dimensional multi-modal bench-marking functions using qualitative metrics such as best, worst, mean, standard deviation and median scores. Table 2.1 illustrates these functions with category representations of three mathematical functions. Figure 2.1, Figure 2.2, and Figure 2.3 also represent two-dimensional shapes. The first group includes functions with a single solution path (F1-F7), which have a single ideal solution and are intentionally difficult to use. The second group includes functions (F8-F13) that have many optimal solutions. While the local optimal solutions are used in these functions to evaluate the algorithm's exploration performance, an algorithm must be able to search the space globally to find the global optimum and avoid being trapped in the local optimum. The third group contains multi-modal functions with fixed dimensions (F14-F23), which are similar to multi-modal functions but have fixed dimensions. The dimensions of these functions, as well as the constant coefficients used in this work, are accessible in [40, 41]. For each test category, 30 particles with 500 iterations were used. Each function was run 30 times and its average values were used for a fair evaluation. Table 3.1 shows how the parameters of each algorithm are configured.

Algorithms	Parameter	Value
For all algorithms	Population	30
	Maximum Iterations	500
AGWOCS	Control Parameter (a)	[2 1]
		[1 3]
AOSMA	Control Parameter (a, b)	
		[1 0]
	diffusion factor(pp)	0.1
AWDA	upper limit	5
	lower limit	2
BES	Control parameter (a)	[1.5 2]
	Control parameter (r)	[0 1]
	child level rate(LR)	0.01
CDDO	Child skill rate(SR)	0.9
	Creativity Rate (CR)	0.1
	alpha	0.85
CLA	zeta	0.6
	pConf	0.25
	mu	0.05
DOA	Hunting or Scavenger rate (p)	0.5
	Group attack or persecution (Q)	0.7
	Gliding constant (Gc)	1.9;
DSSA	Crossover rate (Cr)	Cr=0.5;
	Random gliding distance (dg)	dg=0.8;
	Predator presence probability(Pdp)	Pdp=0.1;
ESMA	adjustable param (q)	0.2
	vectors of random numbers in the range (r, λ)	[0 1]
GEO	Propensity to attack (pa)	[0.5 2]
	Propensity to cruise (pc)	[1 0.5]
	escaping energy (E0)	[-1 1]
	are random number (q)	[0.5 0.5]
HHO	Harris Hawks Number	30
	β	1.5
	E0 variable	ε [-1, 1]
	Search agents	30
	Threshold	2
	CSV	0.5
	β	1.5
LFD	$\alpha1$	10
	$\alpha2$	0.00005
	$\alpha3$	0.005
	$\partial1$	0.9
	$\partial2$	0.1
	Harris Hawks Number	30
LHHO	β	1.5
	E0 variable	ε [-1, 1]
	Entropic parameter (r)	0.5
LSMA	N	20
	z	0.03
	CrossOver Probability (cop)	0.5
	damage probability(dp)	0.5
MAO	regeneration probability (rp)	0.1
	tournament size (k)	3
	differentiation constant (λ)	0.5
	Search agents	30
TSA	Parameter P_{min}	1
	Parameter P_{max}	4
TSO	a	0.7
	z	0.05

Table 3.1: Algorithm parameter settings

The results of the performance comparison are shown in Table 3.2 for uni-modal, Table 3.3 for multi-modal and Table 3.4 for multi-modal fixed dimensions. Due to the stochastic nature of meta-heuristic algorithms, the results of two consecutive runs often do not match. Since we performed many independent experiments with each method, the average values of the results for each function are tabulated. The experiments were conducted in MATLAB 2021a on an Intel Core i7, with 16 GB RAM and in a Windows 10 environment. The algorithms of each benchmark function were run 30 times under the same conditions. The tables contain statistical data in the form of best value, worst value, median value, mean value and corresponding standard deviation.

Algorithms		F1	F2	F3	F4	F5	F6	F7
	Best	3.3506e-49	1.6539e-30	1.2297e-12	3.6704e-15	0.029243	0.0021407	1.7915e-06
AGWOCS	Mean	0.25209	0.0016347	2.0228	0.0031702	130.791	0.25954	7.0832e-05
	Std	1.14	0.0060045	5.5347	0.0081379	735.3995	1.1485	0.0002045
	Best	0	0	0	0	0.0051288	3.6623e-06	2.7551e-06
AOSMA	Mean	5.5695	52.0231	75.962	0.045495	17156.5852	4.7483	0.013632
	Std	92.779	45.0205	349.9254	0.21304	354706.9755	103.5421	0.24843
	Best	0.11767	0.00095195	1.0586	0.015044	6.0371	0.031703	7.2871e-05
AWDA	Mean	1.8643	0.016292	3.8985	0.028343	1045.6344	1.9835	0.0006933
	Std	2.8366	0.032433	2.1564	0.010301	2800.0147	2.8459	0.0014098
	Best	0	0	0	0	0.65699	3.9129e-21	2.3361e-06
BES	Mean	1.1926e-15	6.1888e-10	2.9025e-08	2.5315e-09	0.79875	0.0076214	8.3538e-06
	Std	2.6668e-14	1.3839e-08	6.4902e-07	5.6606e-08	0.087603	0.029749	2.9198e-05
	Best	2.1644e-60	1.4406e-171	0	1.7792e-173	0.9624	0.052593	2.653e-05
CDDO	Mean	1.2876	0.0033599	8.7454	0.0058665	2015.8209	1.406	0.00036195
	Std	9.7277	0.042286	143.1281	0.075178	44221.5524	26.4666	0.0038432
	Best	1.1469e-148	4.477e-124	8.6369e-219	4.6275e-164	0.96158	0.18751	3.7285e-05
DOA	Mean	7.157	16322776.9037	21.7977	0.013491	20147.9618	5.993	0.010845
	Std	114.5315	365353138.5064	347.2062	0.16287	448149.7826	96.0457	0.17488
	Best	0	2.5337e-184	2.4815e-233	1.2598e-173	0	0	3.8027e-05
DSSA	Mean	12.7504	4122824.3096	29.7994	0.025507	37561.7976	16.4352	0.020802
	Std	167.4216	65122224.9887	382.15	0.26481	483778.2616	180.258	0.25229
	Best	0	5.2536e-256	0	3.6113e-247	0.0081807	3.7081e-05	6.4925e-06
ESMA	Mean	13.8772	228481.2873	53.2054	0.0089188	15700.6462	5.6668	0.010327
	Std	176.0067	5108996.7524	486.9561	0.12994	350975.4737	102.2555	0.20037
	Best	5.6973e-27	4.9817e-32	2.5913e-24	2.115e-20	3.6978e-33	1.0374e-32	1.2008e-3
GEO	Mean	0.000979	0.0002412	4.9683e-05	0.00011026	0.00020344	0.00072641	0.00031885
	Std	0.0069597	0.00077319	0.00013601	0.00060643	0.0016597	0.0046885	0.0022391
	Best	3.2657e-114	1.3239e-56	9.4819e-94	2.6659e-52	0.00029177	2.1529e-05	1.4017e-05
HHO	Mean	7.1772	517294.4506	27.5972	0.015173	19452.9728	6.4293	0.01276
	Std	121.1378	11567055.3729	329.9414	0.1707	386839.017	116.7763	0.20452
	Best	1.0547e-08	0.00052114	2.5953e-07	2.2107e-05	1.6065	0.081866	0.00016718
LFD	Mean	25.1795	2.4779605994158	213.2922	0.041412	86637.4102	23.6023	0.071877
	Std	295.4489	5.5404824897375	1880.1345	0.31196	1142071.398	252.4117	0.73438
	Best	4.0603e-161	4.1437e-80	1.0195e-112	1.6601e-80	4.0084e-06	4.8004e-08	1.0863e-06
LHHO	Mean	2.4816	219.2769	5.6402	0.0065608	668.1418	0.86073	0.00065924
	Std	52.2959	4903.0323	73.9713	0.094363	14709.5343	16.1954	0.012678
	Best	0	0	0	6.0899e-320	0.0056562	5.9639e-05	1.9479e-06
LSMA	Mean	8.1105	74.5910	384.4104	0.018095	18847.2574	6.626	0.0067008
	Std	125.5814	16.6790	1203.5107	0.17735	358882.8341	112.3465	0.12339
	Best	13.7968	0.15669	31.1561	0.55386	96.4628	9.8023	0.0017507
MAO	Mean	87.4892	416.7457	154.6912	1.0213	119163.5785	72.2031	0.024319
	Std	162.0843	5648.4623	306.2596	0.64014	448476.2389	157.1719	0.09077
	Best	1.301e-202	1.8046e-103	1.5165e-185	1.8193e-92	0.955	0.20092	1.1951e-05
TSA	Mean	7.3101	88640985.7881	9.4265	0.018317	21884.5316	8.1195	0.013698
	Std	114.2715	1982072697.8507	163.5931	0.19395	418587.6844	117.503	0.25689
	Best	2.1705e-257	5.4605e-128	3.9708e-224	9.279e-118	0.03069	1.9959e-05	2.737e-05
TSO	Mean	19.8437	4187.2582	82.5075	0.018975	26214.3009	14.8457	0.014592
	Std	151.2259	93628.9913	490.0847	0.18541	489293.5139	145.0812	0.19667

Table 3.2: The results of benchmark functions with uni-modality, (D= 30, Max it=500)

Table 3.2 shows the convergence of the algorithms used. In this step, the performance of the algorithms was evaluated against the benchmark functions in which they were run. In this evaluation step, the initial population number was assumed to be 30 and the iteration number was assumed to be 500. Figure3.1 shows convergence plots of uni-modal benchmark functions. In the evaluation algorithm, the solutions tend to search extensively for promising regions of the search spaces and exploit the optimal point. In these uni-modal model functions, it is observed that there is an effective balance between exploration and exploitation so that the solutions move toward the optimal point. In the initial steps, a repetition of sudden changes can be observed, which gradually decreases as the iteration progresses. The convergence behavior of an algorithm at a point in the search space leads to solution fitness. The convergence diagram of solution fitness is shown in Figure 3.1. The graphs show decreasing behavior across all test functions. They show that the approximate optimum significantly improves the point at all iterations. Figure 3.1−Figure3.4 shows the convergence plot of 23 functions compared to different algorithms (16 algorithms). Those that can reach the point of global optimum (0) with high performance in functions F1-F7 of the algorithms.

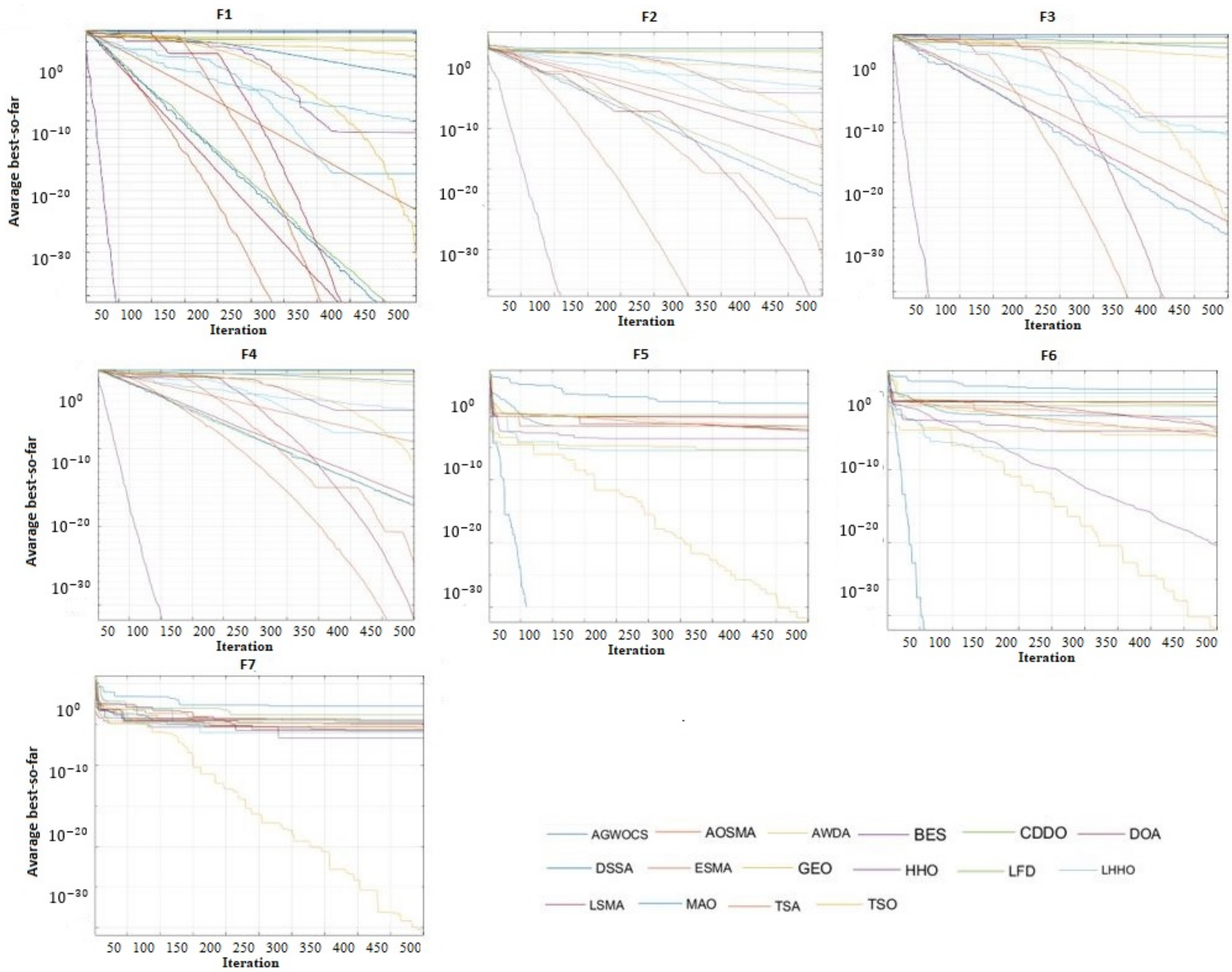

Figure 3.1: Convergence curves of the algorithms on F1–F7

Table 3.3 evaluates the convergence of the algorithms. The performance of the algorithms is tested at this stage using the multi-modal (F8-F13) benchmark functions. The initial population is 30 and the number of iterations in this evaluation stage is 500. The consistency diagrams for multi-modal benchmark functions are shown in Figure 3.2. It was found that there is an efficient balance between search and utilization for these multi-modal model functions, which ensures that the solutions approach the optimal point. The initial phases show a pattern of dramatic shifts that diminishes as the iteration progresses. At a certain point in the search space, the convergence behavior of an algorithm leads to solution fitness. For all test functions, the graphs show decreasing convergence.

Table 3.4 shows the convergence performance of the fixed-dimension multi-modal algorithms (F14-F23) in this phase. In this evaluation phase, the initial population is 30 and the number of iterations is 500. The consistency diagrams for fixed-dimension multi-modal benchmark functions are shown in Figure3.3. The early phases show a pattern of dramatic shifts that decrease as the iteration progresses. The diagrams show decreasing convergence for all test functions. The convergence plots for functions F14-F23 are shown in Figure 3.3.

		Multimodal benchmark functions					
Algorithms		F8	F9	F10	F11	F12	F13
	Best	-7.8365	0	8.8818e-18	0	0.00010519	0.00092445
AGWOCS	Mean	-7.3794	0.041007	0.00097152	0.0027997	1.3831	220.9848
	Std	0.24301	0.082966	0.0027633	0.012436	17.098	1239.4441
	Best	-418.9827	0	2.9606e-17	0	9.9386e-07	6.7812e-06
AOSMA	Mean	-415.9582	0.075541	0.0047513	0.044797	52393.0677	55823.3721
	Std	20.5681	0.95516	0.046634	0.99497	1171544.4371	1248248.3047
	Best	-2.5589	0.039849	0.0060703	0.0018924	0.0041695	0.0029728
AWDA	Mean	-2.0609	0.076849	0.012512	0.015766	3153.6857	10144.2236
	Std	0.39046	0.021872	0.0044522	0.015993	5547.4062	16607.6865
	Best	-192.849	0	2.9606e-17	0	3.9419e-25	0.098869
BES	Mean	-159.6664	3.0316e-17	1.6406e-12	1.1145e-16	0.00047515	0.098944
	Std	21.8772	6.779e-16	3.6684e-11	2.4921e-15	0.0033075	0.00019872
	Best	-414.9186	4.1436	1.4803e-16	0	1.9783e-06	0.010553
CDDO	Mean	-409.2277	4.1992	0.0029311	0.005143	143.3606	802.3993
	Std	30.587	0.43545	0.030446	0.1003	3205.583	17941.9473
	Best	-174.9058	0	2.9606e-17	0	0.024691	0.078147
DOA	Mean	-159.6674	0.67532	0.0060553	0.10222	35187.4366	96073.2885
	Std	18.7455	2.6085	0.052274	1.2424	785684.0574	2032984.8721
	Best	-2.718491268946872e+68	0	2.9606e-17	0	5.2351e-34	4.4993e-34
DSSA	Mean	-1.90597575847278e+66	0.12554	0.0058799	0.12345	72488.5008	202488.5563
	Std	1.717311818082357e+67	1.2337	0.060015	1.5571	1072057.3871	2600745.5342
	Best	-418.9721	0	2.9606e-17	0	2.4456e-05	1.7282e-06
ESMA	Mean	-410.9383	0.10006	0.0038052	0.058521	43636.2202	69284.3225
	Std	31.5805	0.99944	0.039319	0.83932	975735.3523	1549156.0305
	Best	5.3515e-32	4.1497e-32	4.1512e-16	5.7436e-21	2.0543e-33	1.1894e-28
GEO	Mean	0.00039421	0.00013089	0.00047771	0.00013806	0.00015149	0.0012698
	Std	0.004072	0.00049639	0.0047613	0.0023189	0.00084138	0.0046525
	Best	-418.9774	0	2.9606e-17	0	2.801e-06	7.0288e-07
HHO	Mean	-414.5949	0.11334	0.0051101	0.054826	41053.6651	113010.0108
	Std	29.3184	1.0612	0.048748	0.99619	902002.1664	2150141.3942
	Best	-937.7924	7.4903e-06	2.6392e-05	2.5532e-09	0.00049674	0.16477
LFD	Mean	-413.8811	3.3044	0.0091952	0.28953	300136.7078	233181.9774
	Std	235.8705	5.0429	0.065979	2.6183	3366941.541	3359582.3175
	Best	-418.9829	0	2.9606e-17	0	1.0112e-08	4.471e-07
LHHO	Mean	-416.4481	0.091388	0.0023909	0.017484	673.9148	9749.6928
	Std	21.7364	0.79404	0.027909	0.37956	15066.1738	216313.5404
	Best	-418.9775	0	2.9606e-17	0	6.7502e-06	9.812e-05
LSMA	Mean	-407.2941	0.084856	0.0047234	0.052499	49885.3932	99542.8596
	Std	36.8422	0.86632	0.048209	0.98755	1115471.0593	1892313.5595
	Best	-92.5983	0.9515	0.27227	0.22361	0.13535	12.4004
MAO	Mean	-68.2304	1.9137	0.37329	1.1615	459699.3387	792254.9447
	Std	17.0243	0.90728	0.10648	1.8415	1991167.4424	2327180.6163
	Best	-105.0841	0.06663	1.4803e-16	0	0.022997	0.075074
TSA	Mean	-98.7788	0.64792	0.0067426	0.06771	43727.5153	53020.4358
	Std	5.8538	2.1449	0.054204	0.99494	949251.061	1106040.1279
	Best	-418.9829	0	2.9606e-17	0	1.3514e-06	2.7818e-06
TSO	Mean	-412.5186	0.21564	0.01235	0.097162	41742.4897	98319.3265
	Std	30.9786	0.90544	0.05926	1.0356	933389.2961	1697227.7022

Table 3.3: The results of the benchmark functions with multi modality, with 30 dimensions

Although the comparison has a slower convergence rate at the beginning of the search for most functions, after a few iterations it shows good convergence performance and gives a better answer for most functions, especially for fixed multi-modal functions. The frequency diagram can be seen in Figure3.4. In this way, the performance of all algorithms in all functions is shown together. The frequency by best case indicates the number of algorithms that can reach the optimal point in the functions. According to this scheme, the algorithm GEO has the highest frequency, while the algorithms AWDA and LFD have the lowest frequency. To allow a fair comparison, the necessary conditions for the algorithms have remained the same. It is worth noting that due to the meta-heuristic nature of the algorithms, the comparisons made here are not constant and do not always give the same result.

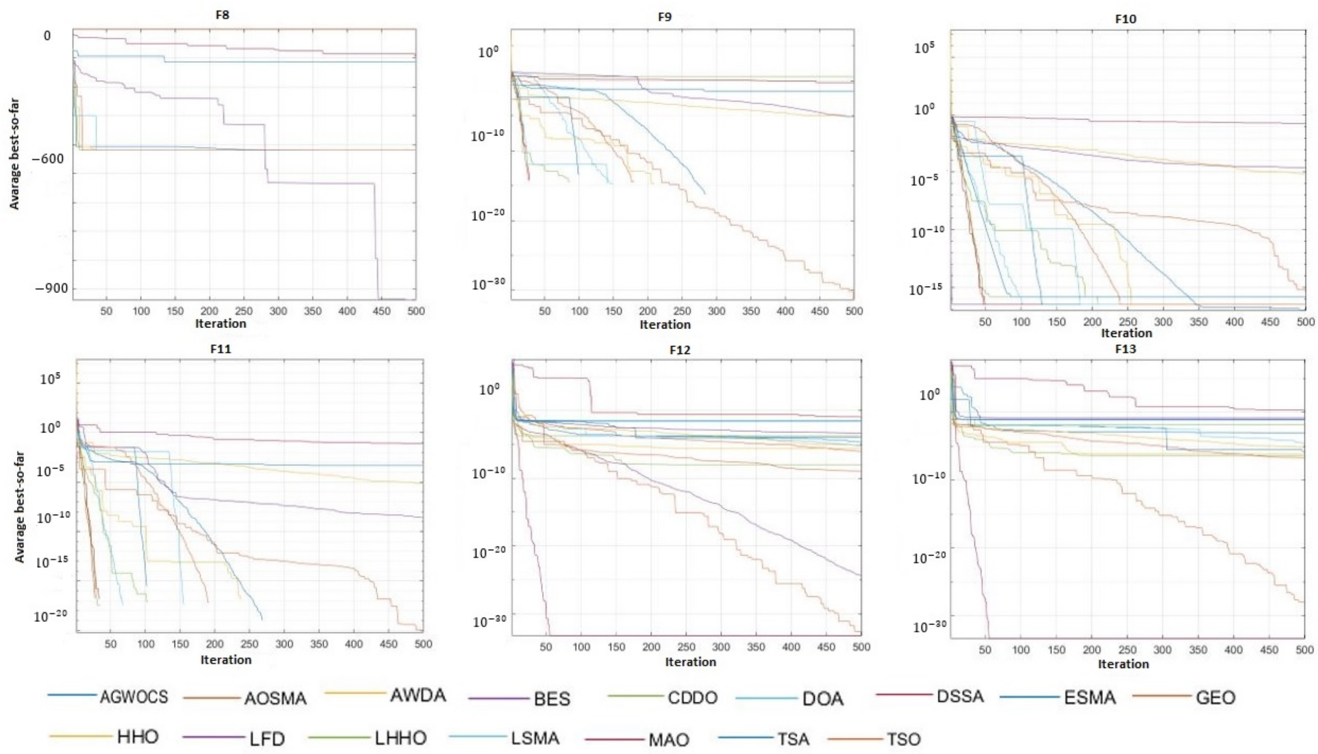

Figure 3.2: Convergence curves of the algorithms on F8–F13

		Fixed-dimension multi-modal benchmark functions									
Alg.		F14	F15	F16	F17	F18	F19	F20	F21	F22	F23
	Best	0.0033135	3.5141e-07	-0.0011462	0.00044281	0.0033333	-0.0042913	-0.0036521	-0.0074093	-0.0079195	-0.0038682
AGWOCS	Mean	0.0036284	1.0034e-06	-0.0011444	0.00046888	0.0035728	-0.0042828	-0.0036105	-0.0057	-0.005937	-0.0030972
	Std	0.0014804	5.3683e-06	3.0457e-05	0.00047603	0.0028832	7.3445e-05	0.00015844	0.0015926	0.0019506	0.00048692
	Best	0.033267	1.4088e-05	-0.034388	0.013263	0.1	-0.12876	-0.10658	-0.33844	-0.34676	-0.35121
AOSMA	Mean	0.05901	7.2452e-05	-0.034346	0.013281	0.13901	-0.12868	-0.10537	-0.32794	-0.33328	-0.34115
	Std	0.16589	0.00044571	0.00053593	0.00016387	0.47073	0.00030876	0.0068892	0.049831	0.047258	0.030526
	Best	0.0033135	1.0092e-06	-0.0011463	0.0033335	0.0033335	-0.004292	-0.0036895	-0.0029809	-0.011482	-0.0030016
AWDA	Mean	0.0034069	4.743e-05	-0.0011413	0.00617	0.0042119	-0.0041809	-0.0033073	-0.0025423	-0.0065387	-0.0026121
	Std	0.0003169	0.00015492	1.0756e-05	0.0035232	0.0025558	0.00021722	0.00048191	0.00075494	0.0038831	0.00032105
	Best	0.033267	1.025e-05	-0.034388	0.013263	0.1	-0.12876	-0.11073	-0.16851	-0.34676	-0.35121
BES	Mean	0.03489	1.6113e-05	-0.034383	0.013293	0.10002	-0.12868	-0.11038	-0.16805	-0.34264	-0.34873
	Std	0.010095	0.00010823	7.938e-05	0.00020801	0.00049561	0.0013077	0.0035659	0.0059867	0.026726	0.019388
	Best	0.033267	8.2041e-05	-0.034346	0.013268	0.10234	-0.12618	-0.094687	-0.3371	-0.33279	-0.34979
CDDO	Mean	0.035301	0.00013376	-0.034288	0.013495	0.34636	-0.12422	-0.094687	-0.32306	-0.28744	-0.34583
	Std	0.045474	9.0075e-05	0.00083044	0.0014674	0.40121	0.00189	2.9173e-16	0.041391	0.05882	0.013276
	Best	0.033267	0.00067878	-0.034388	0.013263	0.1	-0.12876	-0.11055	-0.33844	-0.34676	-0.35121
DOA	Mean	0.03453	0.00073193	-0.034305	0.013619	0.10346	-0.12807	-0.11018	-0.33236	-0.34238	-0.34561
	Std	0.0080879	0.00067655	0.0012122	0.0030308	0.046907	0.0026997	0.0027794	0.036855	0.031086	0.03435
	Best	0.033267	2.0486e-05	-0.034012	0.013335	0.38346	-0.12736	-0.095157	-0.17003	-0.34676	-0.35121
DSSA	Mean	0.12317	4.6844e-05	-0.033502	0.013935	0.45034	-0.12705	-0.089494	-0.16933	-0.3419	-0.3495
	Std	0.84121	0.00024589	0.0016329	0.0021464	0.46138	0.00024224	0.0057824	0.0096559	0.032963	0.021966
	Best	0.033267	1.0342e-05	-0.034388	0.013263	0.1	-0.12876	-0.10677	-0.33844	-0.34676	-0.35118
ESMA	Mean	0.047522	5.1199e-05	-0.034055	0.013476	0.22587	-0.12864	-0.10438	-0.33534	-0.32294	-0.34799
	Std	0.14829	0.00041763	0.003931	0.002481	0.95846	0.00059844	0.0049511	0.019334	0.060308	0.027668
	Best	1.5268e-30	1.915e-30	6.6766e-33	0	4.2114e-33	1.5216e-15	4.1227e-23	8.7103e-32	1.7117e-30	6.5173e-31
GEO	Mean	6.3114e-05	0.00040485	0.00068608	2.2865e-05	0.00043754	0.00011214	0.00016022	0.00067317	0.00064407	0.0001355
	Std	0.0004438	0.0027602	0.0031767	8.8517e-05	0.0035416	0.0010354	0.00066701	0.005151	0.0055138	0.0009007
	Best	0.033267	1.0422e-05	-0.034388	0.013263	0.1	-0.12856	-0.098654	-0.16851	-0.16946	-0.17081
HHO	Mean	0.072033	2.4821e-05	-0.034353	0.013447	0.25284	-0.12721	-0.090329	-0.16665	-0.16705	-0.16894
	Std	0.57258	0.00010526	0.00032258	0.0031932	1.0818	0.0012712	0.0044844	0.01272	0.013189	0.012809
	Best	0.033267	6.1611e-05	-0.034388	0.10129	0.10834	-0.12869	-0.10531	-0.33844	-0.12414	-0.17095
LFD	Mean	0.10675	0.00024484	-0.034195	0.10975	0.11857	-0.12842	-0.10396	-0.30615	-0.10692	-0.15115
	Std	0.16519	0.0015185	0.0011812	0.017921	0.032809	0.0019299	0.006337	0.083296	0.030128	0.039268
	Best	0.033267	1.0269e-05	-0.034388	0.013263	0.1	-0.12876	-0.10361	-0.33833	-0.16959	-0.3512
LHHO	Mean	0.036795	2.604e-05	-0.034358	0.013475	0.10315	-0.12868	-0.099576	-0.30315	-0.16949	-0.28795
	Std	0.028064	0.00017386	0.00041314	0.0027182	0.069287	0.00075748	0.0020618	0.070785	0.00068774	0.088846
	Best	0.033267	1.0297e-05	-0.034388	0.013263	0.1	-0.12876	-0.11073	-0.33843	-0.34676	-0.35121
LSMA	Mean	0.043432	3.426e-05	-0.034116	0.014432	0.48988	-0.12824	-0.10629	-0.32716	-0.32563	-0.30189
	Std	0.033784	9.4922e-05	0.00088212	0.005674	3.3495	0.002802	0.010143	0.029421	0.065147	0.081489
	Best	0.066401	0.00036673	-0.034387	0.78119	0.82362	-0.12841	-0.10869	-0.27841	-0.080423	-0.086101
MAO	Mean	1.3265	3.2519	0.13343	3.636	2.2516	-0.12241	-0.094856	-0.15349	-0.059535	-0.066526
	Std	4.0638	74.4946	3.3885	7.9148	8.2122	0.016864	0.024606	0.10096	0.021443	0.01934
	Best	0.45395	0.00028049	-0.034388	0.01334	0.1	-0.12843	-0.10819	-0.20731	-0.056239	-0.33368
TSA	Mean	0.47901	0.00086876	-0.032249	0.014729	0.49815	-0.12746	-0.10047	-0.17529	-0.050901	-0.23924
	Std	0.56031	0.0045565	0.0072198	0.0051053	1.0072	0.0047008	0.01357	0.043324	0.0075194	0.055414
	Best	0.033267	4.0772e-05	-0.034388	0.013263	0.1	-0.12876	-0.11073	-0.33844	-0.34676	-0.35121
TSO	Mean	0.038004	0.0001935	-0.034156	0.013405	0.11071	-0.12866	-0.10999	-0.3307	-0.34009	-0.33744
	Std	0.017447	0.0016314	0.0016097	0.0016331	0.1609	0.00091173	0.0059657	0.042262	0.034612	0.048519

Table 3.4: The results of the benchmark functions with fixed-dimension multi modality, with 30 dimensions

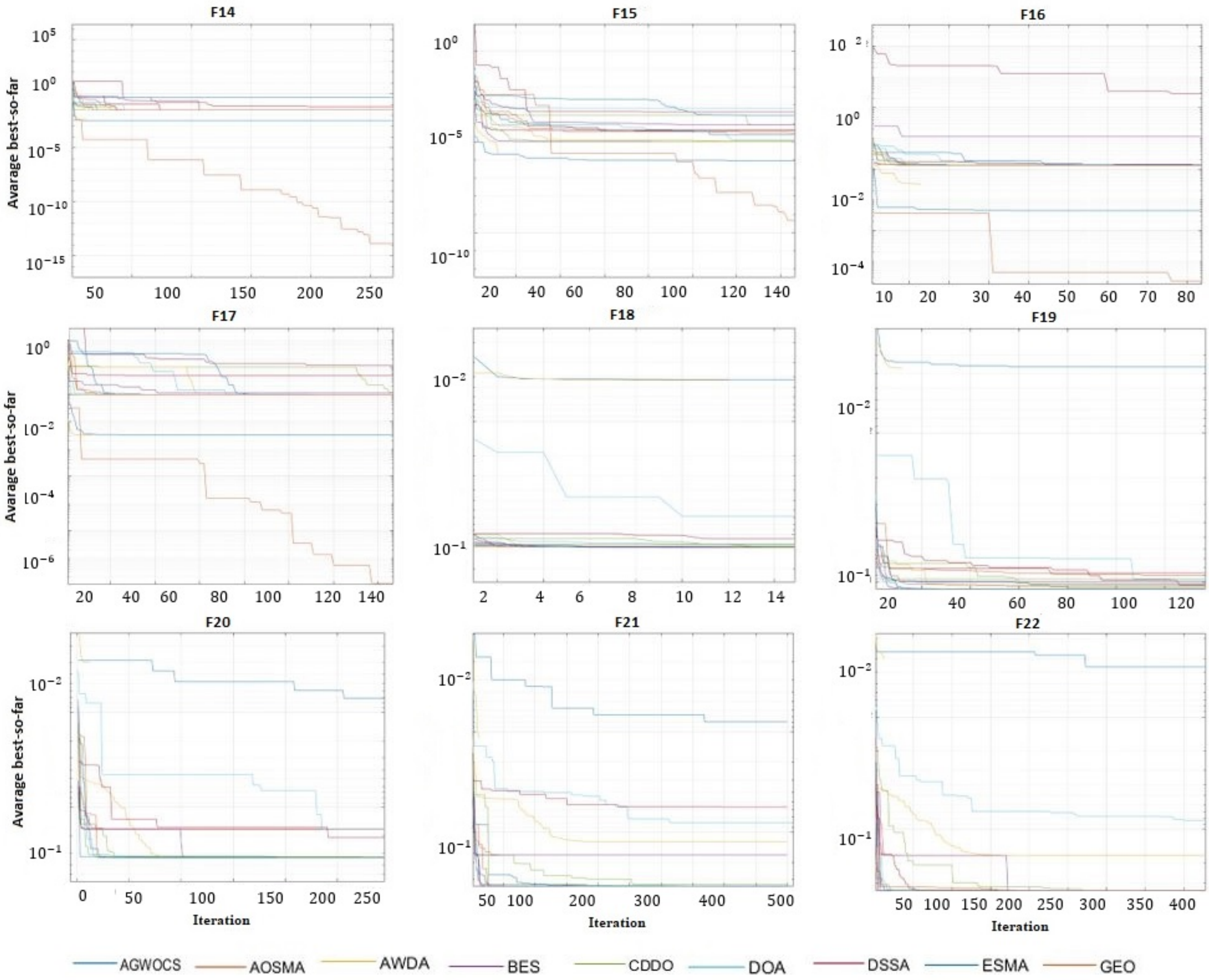

Figure 3.3: Convergence curves of the algorithms on F14–F23

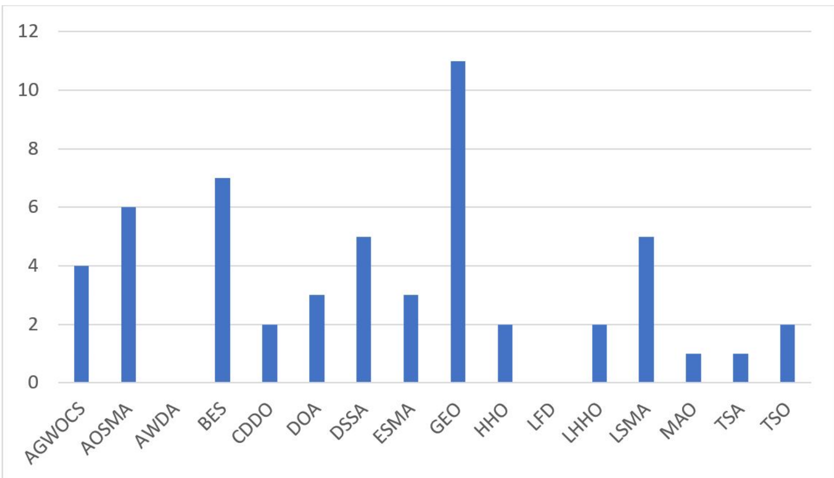

Figure 3.4: Performance histogram of the algorithms depending on the benchmark functions used

4. Conclusion

This paper compares the performance of sixteen meta-heuristic algorithms inspired by natural events. In this work, uni-modal, multi-modal, and fixed-dimension multi-modal benchmark functions were utilized to evaluate the efficiency of the optimization algorithms (AWDA, MAO, TSA, TSO, ESMA, DOA, LHHO, DSSA, LSMA, AOSMA, AGWOCS, CDDO, GEO, BES, LFD, HHO). The functions used contain sixteen test functions of three different types to test their performance in terms of usage, avoidance of local optimum, and convergence. The results are presented in the form of tables and diagrams. For future work, the use of different types of functions with a greater variety of curvatures, slopes and intercepts in the optimization of real problems is considered.

Acknowledgements

The author would like to express their sincere thanks to the editor and the anonymous reviewers for their helpful comments and suggestions.

Funding

There is no funding for this work.

Availability of data and materials

Not applicable.

Competing interests

The author declare that they have no competing interests.

References

[1] L. Xie, T. Han, H. Zhou, Z. R. Zhang, B. Han, A. Tang, *Tuna swarm optimization: a novel swarm-based metaheuristic algorithm for global optimization*, Computational intelligence and Neuroscience, **2021** Article ID 9210050 — https://doi.org/10.1155/2021/9210050,
[2] S. Kaura, L. K. Awasthia, G. Dhiman, *Tunicate Swarm Algorithm: A new bio-inspired based metaheuristic paradigm for global optimization*, Engineering Applications of Artificial Intelligence, **90** (2020),103-541.
[3] Y. V. Rey, J. L. Velázquez-Rodríguez, M. D. Alanis-Tamez, M. Moreno-Ibarra, C. Yáñez-Márquez, *Mexican axolotl optimization: a novel bioinspired heuristic*, Mathematics, **9(7)** (2021), https://doi.org/10.3390/math9070781.
[4] M. K. Naik, R. Panda, A. Abraham, *Normalized square difference based multilevel thresholding technique for multispectral images using leader slime mould algorithm*, Journal of King Saud University-Computer and Information Sciences, **2020**, https://doi.org/10.1016/j.jksuci.2020.10.030.
[5] M. K. Naik, R. Panda, A. Wunnava, B. Jena, A. Abraham , *A leader Harris hawks optimization for 2-D Masi entropy-based multilevel image thresholding*, Multimedia Tools and Applications, **80**(28) (2021), 35543-35583, https://doi.org/10.1007/s11042-020-10467-7
[6] E. H.Houssein, M. R. Saad, F. A. Hashim, H. Shaban, M. Hassaballah, *Lévy flight distribution: A new metaheuristic algorithm for solving engineering optimization problems*, Engineering Applications of Artificial Intelligence, **94** (2020), doi:10.1016/j.engappai.2020.103731.
[7] A. Mohammadi-Balani, M. D. Nayeri, A. Azar, M. Taghizadeh-Yazdi, *Golden eagle optimizer: A nature-inspired metaheuristic algorithm*, Computers & Industrial Engineering, **152** (2021), doi.org/10.1016/j.cie.2020.107050.
[8] S. Yin, Q. Luo, Y. Zhou, , *EOSMA: an equilibrium optimizer slime mould algorithm for engineering design problems*, Arabian Journal for Science and Engineering, **47** (2022), 2) doi.org/10.1007/s13369-021-06513-7.
[9] Y. Wang, T. Du, *An improved squirrel search algorithm for global function optimization*,Algorithms, **12** (2019), doi.org/10.3390/a12040080.
[10] Y. Wang, T. Du, *A multi-objective improved squirrel search algorithm based on decomposition with external population and adaptive weight vectors adjustment*, Physica A: Statistical Mechanics and its Applications, **547** (2020), doi.org/10.1016/j.physa.2019.123526.
[11] M. Khishe, M. R. Mosavi, *Chimp optimization algorithm*, Expert systems with applications, **149** (2020), doi.org/10.1016/j.eswa.2020.113338.
[12] S. Abdulhameed, T. A. Rashid, *Child drawing development optimization algorithm based on child's cognitive development*, Arabian Journal for Science and Engineering, **47(2)** (2022),doi.org/10.1007/s13369-021-05928-6.
[13] A. Ramadan, S. Kamel, M. H. Hassan, T. Khurshaid, C. Rahmann, *An improved bald eagle search algorithm for parameter estimation of different photovoltaic models*, Processes, **9(7)** (2021), doi.org/10.3390/pr9071127.
[14] H. A. Alsattar, A. A. Zaidan, B. B. Zaidan , *Novel meta-heuristic bald eagle search optimisation algorithm*, Artificial Intelligence Review, **53(3)** (2020),doi.org/10.1007/s10462-019-09732-5.
[15] M. K. Naik, R. Panda, A. Abraham, *Adaptive opposition slime mould algorithm*, Soft Computing, **25**(22) (2021), doi.org/10.1007/s00500-021-06140-2, 14297–14313.
[16] S. Padhy, P. Sidhartha, *Application of a simplified Grey Wolf optimization technique for adaptive fuzzy PID controller design for frequency regulation of a distributed power generation system*, Protection and Control of Modern Power Systems, **6**(1) (2021), doi.org/10.1186/s41601-021-00180-4.
[17] H. Bayzidi, S. Talatahari, M. Saraee, C. P. Lamarche,*Social network search for solving engineering optimization problems*, Computational Intelligence and Neuroscience, **2021** (2021), Article ID 8548639 — https://doi.org/10.1155/2021/8548639.
[18] B. Abdollahzadeha, F. S. Gharehchopogha, S. Mirjalili, *African vultures optimization algorithm: A new nature-inspired metaheuristic algorithm for global optimization problems*, Computers, Industrial Engineering, **158** (2021), doi.org/10.1016/j.cie.2021.107408.
[19] M. Khishe, M. R. Mosavi,*Classification of underwater acoustical dataset using neural network trained by Chimp Optimization Algorithm*, Applied Acoustics, **157** (2020), doi.org/10.1016/j.apacoust.2019.107005.
[20] M. Khishe, A. Safari , *Classification of sonar targets using an MLP neural network trained by dragonfly algorithm*, Wireless Personal Communications, **108**(4) (2019), doi.org/10.1007/s11277-019-06520-w.
[21] W. Qiao, M. Khishe, S. Ravakhah, *Underwater targets classification using local wavelet acoustic pattern and Multi-Layer Perceptron neural network optimized by modified Whale Optimization Algorithm*, Ocean Engineering, **219** (2021), doi.org/10.1016/j.oceaneng.2020.108415.
[22] J. Wang, M. Khishe, M. Kaveh, H. Mohammadi, *Binary chimp optimization algorithm (BChOA): A new binary meta-heuristic for solving optimization problems*, Cognitive Computation, **13**(5) (2021), doi:10.1007/s12559-021-09933-7.
[23] M. Khishe, M. Nezhadshahbodaghi, M. R. Mosavi, D. Martín, *A weighted chimp optimization algorithm*, IEEE Access, **9** (2021), doi: 10.1109/ACCESS.2021.3130933.
[24] W. Kaidi, M. Khishe, M. Mohammadi, *Dynamic levy flight chimp optimization*, Knowledge-Based Systems, **235** (2011), doi.org/10.1016/j.knosys.2021.107625.
[25] A. Kumar, R. K. Misra, D. Singh, S. Mishra, S. Das, *The spherical search algorithm for bound-constrained global optimization problems*, Appl. Soft Comput., **85** (2019), doi.org/10.1016/j.asoc.2019.105734.
[26] A. Faramarzi, M. Heidarinejad, B. Stephens, S. Mirjalili,*Equilibrium optimizer: A novel optimization algorithm*, Knowledge-Based Systems, **191** (2020), doi.org/10.1016/j.knosys.2019.105190.
[27] G. Dhiman, V. Kumar,*Seagull optimization algorithm: Theory and its applications for large-scale industrial engineering problems*, Knowledge-based systems, **165** (2019), doi.org/10.1016/j.knosys.2018.11.024.
[28] L. zhendong, *Artificial Water Drop Algorithm (AWDA)*, MATLAB Central File Exchange, (2022),https://www.mathworks.com/matlabcentral/fileexchange/104480-artificial-water-drop-algorithm-awda.
[29] H. P. Peraza-Vázquez, A. F. Peña-Delgado, G. E. Castillo, A. B. Morales-Cepeda, J. Velasco-Álvarez, F. Ruiz-Perez, *A bio-inspired method for engineering design optimization inspired by dingoes hunting strategies*, Math. Probl. Eng., **2021** (2021), Article ID 9107547 — doi.org/10.1155/2021/9107547.
[30] A. S. Heidari, S. Mirjalili, H. Faris, I. Aljarah, M. Mafarja, H. Chen, *Harris hawks optimization: Algorithm and applications*, Future generation computer systems, **97** (2019), Article ID 2218594 — doi.org/10.1155/2022/2218594.
[31] M. K. Naik, R. Panda, A. Abraham,*Normalized square difference based multilevel thresholding technique for multispectral images using leader slime mould algorithm*, Journal of King Saud University-Computer and Information Sciences, **34** (2022), doi.org/10.1016/j.jksuci.2020.10.030.

[32] M. K. Naik, R. Panda,A. Abraham,*Adaptive opposition slime mould algorithm*, Soft Computing, **25(22)** (2021),doi.org/10.1007/s00500-021-06140-2.
[33] M. H. Qais, H. M. Hasanien, S. Alghuwainem, *Augmented grey wolf optimizer for grid-connected PMSG-based wind energy conversion systems*, Applied Soft Computing, **69** (2018), doi.org/10.1016/j.asoc.2018.05.006.
[34] S. Sharma, R. Kapoor, S. Dhiman, *A Novel Hybrid Metaheuristic Based on Augmented Grey Wolf Optimizer and Cuckoo Search for Global Optimization*, 2021 2nd International Conference on Secure Cyber Computing and Communications (ICSCCC), (2021), 376-381.
[35] A. Mohammadi-Balani, M. D.Nayeri, A. Azar, M. Taghizadeh-Yazdi, *Golden eagle optimizer: A nature-inspired metaheuristic algorithm*, Computers & Industrial Engineering, **152** (2021), doi.org/10.1016/j.cie.2020.107050.
[36] A. A. Heidari, S. Mirjalili, H. Faris, I. Aljarah, M. Mafarja, H. Chen, *Harris hawks optimization: Algorithm and applications*, Future generation computer systems, **97** (2019),doi.org/10.1016/j.future.2019.02.028.
[37] G. Dhiman, K. K. Singh, M. Soni, A. Nagar, M. Dehghani, A. Slowik, A. Kaur, A. Sharma, E. H. Houssein, K. Cengiz, *MOSOA: A new multi-objective seagull optimization algorithm*, Expert Systems with Applications, **167** (2021),doi.org/10.1016/j.eswa.2020.114150.
[38] A. Afroughinia, R. K. Moghaddam, *Competitive learning: a new meta-heuristic optimization algorithm*, International Journal on Artificial Intelligence Tools, **27(8)** (2018),doi.org/10.1142/S0218213018500355.
[39] M. Khishe, M. R. Mosavi, *Chimp optimization algorithm*, Expert Systems with Applications, **149** (2020), doi.org/10.1016/j.eswa.2020.113338.
[40] S. Mirjalilia, S. M. Mirjalili, A. Lewisa, *Grey Wolf Optimizer*, Advances in Engineering Software, **69** (2014),doi.org/10.1016/j.advengsoft.2013.12.007, 46-61.
[41] E. Rashedi, H. Nezamabadi-pour, S. Saryazdi, *GSA: A Gravitational Search Algorithm*, Information Sciences, **179(13)** (2009), doi.org/10.1016/j.ins.2009.03.004,2232-2248